THE MECHANISM OF COLLAGEN SELF-ASSEMBLY: HYDROPHOBIC AND ELECTROSTATIC INTERACTIONS

By

YUPING LI

A DISSERTATION PRESENTED TO THE GRADUATE SCHOOL
OF THE UNIVERSITY OF FLORIDA IN PARTIAL FULFILLMENT
OF THE REQUIREMENTS FOR THE DEGREE OF
DOCTOR OF PHILOSOPHY

UNIVERSITY OF FLORIDA

2009

To my grandma, the most influential person in my life

ACKNOWLEDGMENTS

I would like to thank Dr. Elliot P. Douglas, my advisor and committee chair sincerely for his guidance, understanding, patience, encouragement and support, most importantly, his conscientiousness during my graduate studies at University of Florida. I also thank my doctoral committee members: Dr. John Mecholsky, Dr. Christopher D. Batich and Dr. Richard Dickinson for their input, valuable discussion and accessibility. I want to thank all the members in Dr. Douglas's group: Chyh-Chyang Luo and Lewei Pu for helping me get through the hard times for the first two years at Gainesville; Andrew Stewart for his music; Sangwon Choi and Sangjun Lee for their humor and entertainment; Changhua Liu, Jie Li for listening and discussion; Amran Asadi, Margo R. Monroe, Chelsea E. Catania and Sasha L. Perkins for their collaboration. Especially, I want to thank Jennifer L.Wrighton for her assistance and help.

I would want to thank Dr. Laure Gower for her assistance and guidance in my graduate career. Besides, I am very grateful for the friendship with all of the members in her research group: Sangsoo Jee and Taili Thula, with whom I worked closely and figured out many of the research problems; Mark Bewernitz for training me on polarized optical microscopy and took my samples for testing; Chih-Wei Liao for providing suggestion and information on many technical problems.

Moreover, I thank the Department of Materials Science and Engineering, the University of Florida for providing me a great place for studying and living. Additionally, I thank the Major Analysis Instrumentation Center (MAIC), the Particle Engineering Research Center (PERC) and the staffs for their hard work, expertise and assistance.

Next, I want to acknowledge many friends I met at UF: Jianlin Li, Xiaobo Li and Hongxia Yan, Aijie Chen, Jessie Choi and Ying Zheng. Without you, I couldn't have such a joyful life in UF.

Finally, and most importantly, I would like to thank my parents and my brother for their support, encouragement, unselfish love and faith.

TABLE OF CONTENTS

page

LIST OF TABLES

LIST OF FIGURES

Abstract of Dissertation Presented to the Graduate School
of the University of Florida in Partial Fulfillment of the
Requirements for the Degree of Doctor of Philosophy

MECHANISM OF COLLAGEN SELF ASSEMBLY INTO FIBRILS: HYDROPHOBIC AND ELECTROSTATIC INTERACTIONS

By

Yuping Li

May 2009

Chair: Elliot P. Douglas
Major: Materials Science and Engineering

Collagen molecules assemble into fibrils with ordered structure is a spontaneous and thermally driving process which is favored by a large positive entropy contribution due to the displacement of structured water around collagen molecules. The underlying principle on forming fibrils with periodicity is still unclear. Our goal is to study the mechanism of collagen fibril formation by analyzing the intermolecular interactions during fibril formation. By introducing the anionic surfactant, we found those surfactants can accelerate the fibrillogenesis even though there are no remarkable interactions before fibril formation. The denaturation of collagen occurred with increasing concentration of surfactants. It is possible that the adsorption of surfactants on collagen through hydrophobic interactions destabilize the collagen triple helix when collagen molecules are dehydrated during incubation.

Collagen fibril formation is influenced by environmental factors especially the pH and electrolytes. We found collagen fibrils can be formed at pH from 6.6 to 9.2. Zeta potential measurements of soluble collagen indicate that the surface net charge of collagen is not only affected by the pH of medium but also by the presence of added salts. The acceleration of fibrillogenesis rate with increasing pH from 6.6 to 9.2 is consistent with a reduction of surface

net charge since the isoelectric point of soluble collagen is approaching. The native D-periodicity of 62 nm was found except at pH 7.1 where collagen molecules form short banding of 50-60 nm in the early stage of fibrillogenesis which might be caused by unusual alignment of collagen molecules in fibrils.

We also introduced different monovalent and divalent electrolytes into fibril formation instead of PBS buffer. It was found the fibril formation was facilitated by divalent ions. Divalent ions can shift the isoelectric point of collagen by adsorption. We proposed the adsorbed divalent ions form the salt bridges between collagen which facilitate fibril formation. The unusual periodicities along the collagen fibril were also found which might be come from altered alignment of molecules due to the change of surface charge.

These studies provide new insight on understanding the basis for collagen fibril formation and help for designing new biomaterials.

CHAPTER 1
INTRODUCTION

Collagen is the most abundant protein present in connective tissue. It is biodegradable, biocompatible, and can enhance cell attachment and cellular penetration[1]. The prevalence of collagen also makes it a natural choice as a polymer for biomedical materials and tissue-engineering matrices. The potential value of collagen as a biomaterial has led to research on use in scaffolds for wound repair, collagen hydrogel as drug delivery, and scaffolds of tissue engineering[2, 3]. Collagen is also a target for study in diseases involving extensive collagen remodeling, including aortic heart valve repair and bone repair[4, 5]. A better understanding of interactions between collagen allow for the more rational design and use of collagen scaffolds for biomedical application as well as understanding the biological system.

There are over 20 known types of collagen[6]. Type I collagen is the major fibril component in bone, skin, tendons, ligaments, cornea, and internal organs, accounting for 90% of body collagen; type II collagen comprising fibrillar cartilage, and vitreous humor of the eye; type III collagen comprising fibril skin, blood vessels, and internal organs. For all collagen types, each collagen molecule is composed of three left-handed α helix chains that twist together of form the right-handed triple helix. Each helix chain has about 1024 amino acids and each of collagen molecule is about 300 kDa, composed of about 10% each of proline and hydroxyproline, and has a glycine present at every third amino acid positions.

Collagen molecules can self assemble into fibrils with an ordered structure along the fibril *in vitro*. The mechanism of collagen self assembly has been studied a lot. However, it is still unclear. From a thermodynamic point of view, collagen self assembly is an entropy driving process. When temperature is increased, entropy of water is increased due to the dissociation of structured water around the collagen and entropy of collagen is decreased a little compared to the

water. Even though it is an endothermic process, the free energy of the whole process is negative which suggests collagen fibril formation is a spontaneous reaction. When structured water molecules are dissociated during heating, the exposed side groups of amino acids are attracted with each other. During the fibril formation, there exist many interactions, such as van der Waals attraction, electrostatic repulsion and hydrophobic attraction. Which interaction force play a major role during fibril formation? Why collagen molecules can align along the fibril to form ordered structure? Does collagen recognize the specific regions of nearby one to form the native fibrils? In this dissertation, I tried to comprehensively study the molecular interactions during fibril formation in order to provide insight into the mechanisms of collagen self-assembly into fibrils.

A literature review of the collagen molecules self assemble into fibrils is described in Chapter 2. It starts at the hierarchical structure of the collagen from the amino acids composition, triple helix structure to the collagen fibrils. The models of collagen fibrils from electron microscopy and XRD are also reported. The mechanisms of collagen fibrils formation studied from kinetics, and morphologies are also summarized.

In Chapter 3, the kinetics of collagen fibril formation was studied by turbidity measurement. The effects of collagen concentration, temperature, and ionic strength of phosphate buffer on fibril formation were investigated. The activation energy of collagen fibril formation was calculated. TEM was used to examine the morphologies of collagen fibrils in order to understand the fundamental mechanism about fibril formation.

By introducing anionic surfactants, sodium dodecylsulfate (SDS) or sodium dodecylbenzenesulfonate (SDBS), we hope to know if there are specific interactions between surfactants and collagen molecules as well as how those interactions influence the fibril

formation (Chapter 4). The anionic surfactants have both a hydrophobic hydrocarbon chain and negative charged head group. When collagen molecules are dehydrated during fibril formation, the exposed side groups of collagen interact with surfactants. The rate of collagen fibril formation was found to be accelerated remarkably in the presence of 0.1-0.5 mM SDS or SDBS while the unfolding of the collagen triple helix also occurred when up to 1 mM SDS was added or more than 0.35 mM SDBS was added. The morphology studies from SEM indicated partial unfolding occurred and non-fibrillar collagen gel formed within fibrils. The binding and denaturation effects of surfactants were also discussed.

In Chapter 5, Collagen self assembly *in vitro* was conducted in the pH range from 6.0 to 10.5 in order to investigate the electrostatic interactions that occurred during fibril formation. Collagen fibril morphologies imaged by TEM and SEM present bundling of fibrils with a small amount of non-fibrillar collagen. Even though the rate of fibrillogenesis accelerated with increasing pH in this range, the size distribution of fibrils didn't change significantly. We also found that the net surface charge of collagen molecules is not only affected by the pH of medium but also by the presence of added salts.

It was found that electrostatic interactions are important for fibril formation and the electrostatic interactions can be controlled through changing the pH of the medium. In Chapter 6 variant electrolytes instead of phosphate buffer is introduced in order to facilitate fibrillogenesis. In our studies, the facilitation of collagen aggregation through reducing surface net charge by divalent ions binding was observed. We also found the competition between unfolding and aggregation in collagen at high pH which inhibited the collagen fibril formation. The divalent ions binding to the collagen molecules not only change the surface charge but also create fibrils with native D-periodic banding pattern. It is possible that the binding divalent ions induce the

like-charge attraction during collagen self assembly into fibrils. The findings can help understanding the mechanism of fibrillgenesis.

In Chapter 7, a summary for the dissertation and the potential research work for the future were described.

CHAPTER 2
AN OVERVIEW OF COLLAGEN

Collagen and Its Applications

As one of the major components of connective tissue, collagens account for approximately 30% of all proteins in the human body[7, 8]. They are often found in every major tissue that requires strength and flexibility, such as tendon, skin, bone, and fascia. There are over 20 types of collagens (Table 2-1), with the most abundant type being type I collagen (more than 90% of all fibrous protein). The word ‘collagen’ describes a family of structurally related proteins that are located in the extracellular matrix of connective tissue.

Collagen has played a critical role in the evolution of large complex organisms, where it acts as an insoluble scaffold for providing shape and form, for attaching biopolymers, inorganic ions, and cells. They occur as supra-molecular assemblies that range in morphology from rope-like fibrils that provide the fibrous scaffold maintaining the integrity of tendons, ligaments and bone, to net-like sheets in the base discs that underlie epithelial and endothelial cells[9]. Type I collagen has become the biomaterial of choice for a number of important medical applications due to[10]:

- well developed technique for obtaining large quantities of medical grade collagen,
- a number of established collagen products, some of which are well known,
- a good safety profile as a biomaterial,
- easily used in minimally invasive procedures,
- the improved understanding of collagen’s role in wound healing, metabolism, catabolism, and the interaction between cells and collagen.

Table 2-1. List of the Collagen Types and Information on Chain Composition, Structure, Tissue Location and Related Information[42]

Types	Chain Composition	Structural Details	Localization	Notes
I	[a1(I)]2[a(I)]	300 nm, 67-nm banded fibrils	Skin, tendon, bone, etc.	90% of all collagen of the human body. Scar tissue-the end product when tissue heals by repair.
II	[a1(II)]3	300 nm, small 67-nm fibrils	Cartilage, vitreous humor	Articular cartilage
III	[a1(III)]3	300 nm, small 67-nm fibrils	Skin, muscle, frequently with type I	Collagen of granulation tissue, and produced quickly by young fibroblasts.
IV	[a1(IV)2[a2(IV)]	390 nm C-term globular domain, nonfibrillar	All basal lamina	Basal lamina
V	[a1(V)][a2(V)][a3(V)]	390 nm N-term globular domain, small fibers	Most interstitial tissue,assoc. with type I	Most interstitial tissue, assoc. with type I
VI	[a1(VI)][a2(VI)][a3(VI)]	150 nm, N1C term. globular domains, microfibrils, 100-nm banded fibrils	Most interstitial tissue, assoc. with type I	Most interstitial tissue, assoc.with type I
VII	[a1(VII)]3	450 nm, dimer	Epithelia	
VIII	[a1(VIII)]3	130 nm, N1C term. Globular domains	Some endothelial cells	
IX	[a1(IX)][a2(IX)][a3(IX)]	200 nm, N-term. Globular domain, bound proteoglycan	Cartilage, assoc. with type II	
X	[a1(X)]3	150 nm, C-term. Globular domain	Hypertrophic and mineralizing cartilage	
XI	[a1(XI)][a2(XI)][a3(XI)]	300 nm, small fibers	Cartilage	
XII	a1(XII)	75-nm triple helical tail, central globule, three 60-nm globule arms	Interacts with types I and III	

Mainly type I–IV have been utilized to varying degrees in tissue-engineering related biomaterials studies, with some efforts on the other types shown.

The potential value of collagen as a biomaterial has led to research on its use in scaffolds for ligament repair, collagen grafts for scar and burn repair, and the engineering of osterochondral tissue[2, 11-13]. The commercial applications of collagen are listed in Table 2-2.

Table 2-2. Commercially available collagen-based medical devices[10]

Medical Specialty	Application
General surgery	hemostastis
Dermatology	Soft tissue augmentation
Dentistry	Oral wounds; periodontal ligament attachment
Ophthalmology	Corneal shields
Cardiovascular	Anti-infectious catheter cuffs; Arterial puncture repair
Plastic and reconstructive surgery	Wound dressings; Artificial skin
Orthopedics	Bone repair
Urology	Bulking agent for incontinence
Drug delivery	Cancer therapeutics; growth factors

Structure of Collagen Triple-Helix

Type I collagen, the principal component of the organic matrix of bone, as well as other connective tissues, is a large fibrous protein with a highly repetitive amino acid sequence $[Gly\text{-}X\text{-}Y]_n$ where X and Y can be any amino acids but are frequently the imino acids proline and hydroxyproline, respectively(Figure 2-1). The three peptide subunits are two α1(1) and one α2(1) chains, which have similar amino acid compositions with each chain (Table 2-3), composed of about 1024 amino acid residues. They can fold into a unique triple-helical structure which consists of three domains: the $–NH_2$ terminated helical, the triple helical, and the –COOH terminated helical domains. It is also called telopeptide collagen or tropocollagen. When the helical domains are cleaved by pepsin digestion, the collagen is called atelopeptide collagen. The length of collagen molecule is about 300 nm, and the diameter is about 1.5nm[14].The single uninterrupted triple helical

domain represents more than 95% of the molecule. The triple-helical conformation based on high-angle X-ray diffraction patterns, consists of three polypeptide chains entwined into a left-handed helix with approximately 3.33 residues per turn and a unit twist of about 108°, in which adjacent chains are staggered by one residue. Successive units are translated by approximately 0.29 nm parallel to the helix axis (h) and chains are held together by two hydrogen bonds per triplet[15]. One hydrogen bond is formed between the NH group of the residue of the glycyl residue and the CO group of the residue in the second position of the triplet in the neighboring chains. Another one is formed via a water molecule participating in the formation of additional hydrogen bonds with the help of the hydroxyl group of 4-hydroxyproline in the third position of the triplet (Gly-X-Y)[16].

Table 2-3. Amino acid composition of type I collagen [6]

Amino acid	α1(I)	α2(I)
3-Hydroxyproline	1	1
4-Hydroxyproline	108	93
Aspartic acid	42	44
Threonine	16	19
Serine	34	30
Glutamic acid	73	68
Proline	124	113
Glycine	333	338
Alanine	115	102
Half-cystine	0	0
Valine	21	35
Methionine	7	5
Isoleucine	6	14
Leucine	19	30
Tyrosine	1	4
Phenylalanine	12	12
Hydroxylysine	9	12
Lysine	26	18
Histine	3	12
Arginine	50	50
All	1000	1000

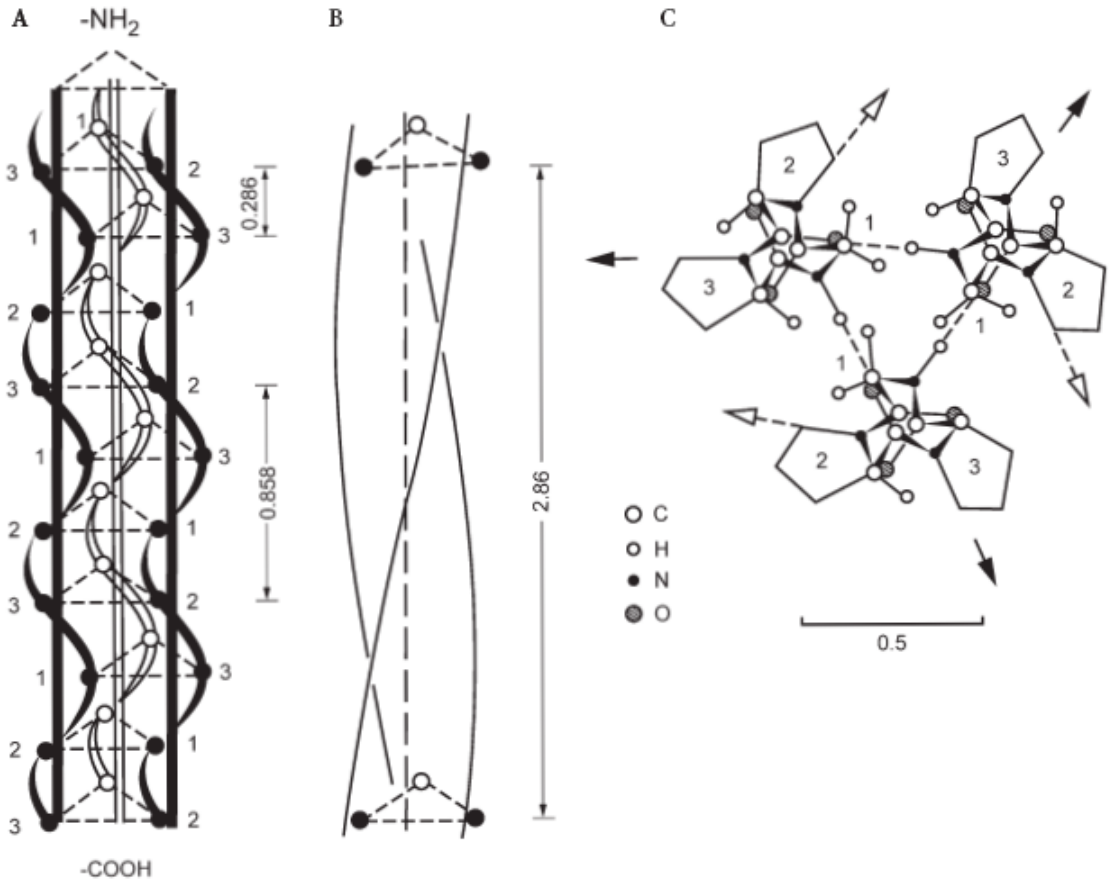

Figure 2-1. Model of the collagen triple helix. The structure is shown for (Gly-Pro-Pro)n in which glycine is designated by 1, proline in X-position by 2 and proline in Y-position by 3:A) and B) are side views. C) is top view in the direction of the helix axis. The three chains are connected by hydrogen bonds between the backbone NH of glycine and the backbone CO of proline in Y-position. Arrows indicate the directions in which side chains other than proline rings emerge from the helix. The residue-to-residue distances are indicated in nm.[43]

Stabilization of Collagen Fibrils by Covalent Cross-Linking

The assembly of type I, II and III collagen into fibrils is usually accompanied by formation of inter- and intra-molecular covalent cross-links between α-chains[17]. The cross-links in the fibrils provide the high tensile and mechanical strength needed for tissue integrity. These cross-links are based on aldehyde formation and condensation

involving specific peptidyl lysine and hydroxylysine residues[18] (Figure 2-2). The process is catalyzed by a single enzyme, lysyloxidase, which oxidatively deaminates the ε-amino group of certain lysine and hydroxylysine residues in the telopeptide regions of collagen molecules to form reactive allysyl and hydroxyallysyl aldehydes, respectively. These aldehyde groups then react with the ε-amino group of lysine and hydroxylysine residues and other aldehydes to form a variety of di-, tri- and tetrafunctional cross-links. Increasing the intermolecular cross-links can increase the biodegradation time by making collagen less susceptible to enzymatic degradation; decreasing the capacity of the collagen to absorb water; and increasing the tensile strength of the collagen fibers. For long-term biomimetic applications, the thermal and mechanical stability of collagen must be achieved by cross-linking. Over the years, a number of well-described physical or chemical techniques have been used such as de-hydrothermal treatment, UV-radiation and chemical cross-linking agents[1, 19, 20]. However, those methods might induce partial denaturation and substantially alter its *in vivo* degradation. Especially, some cross-linking reagents, such as aldehydes, polyepoxides, and isocyanates, are usually toxic and bio-incompatible.

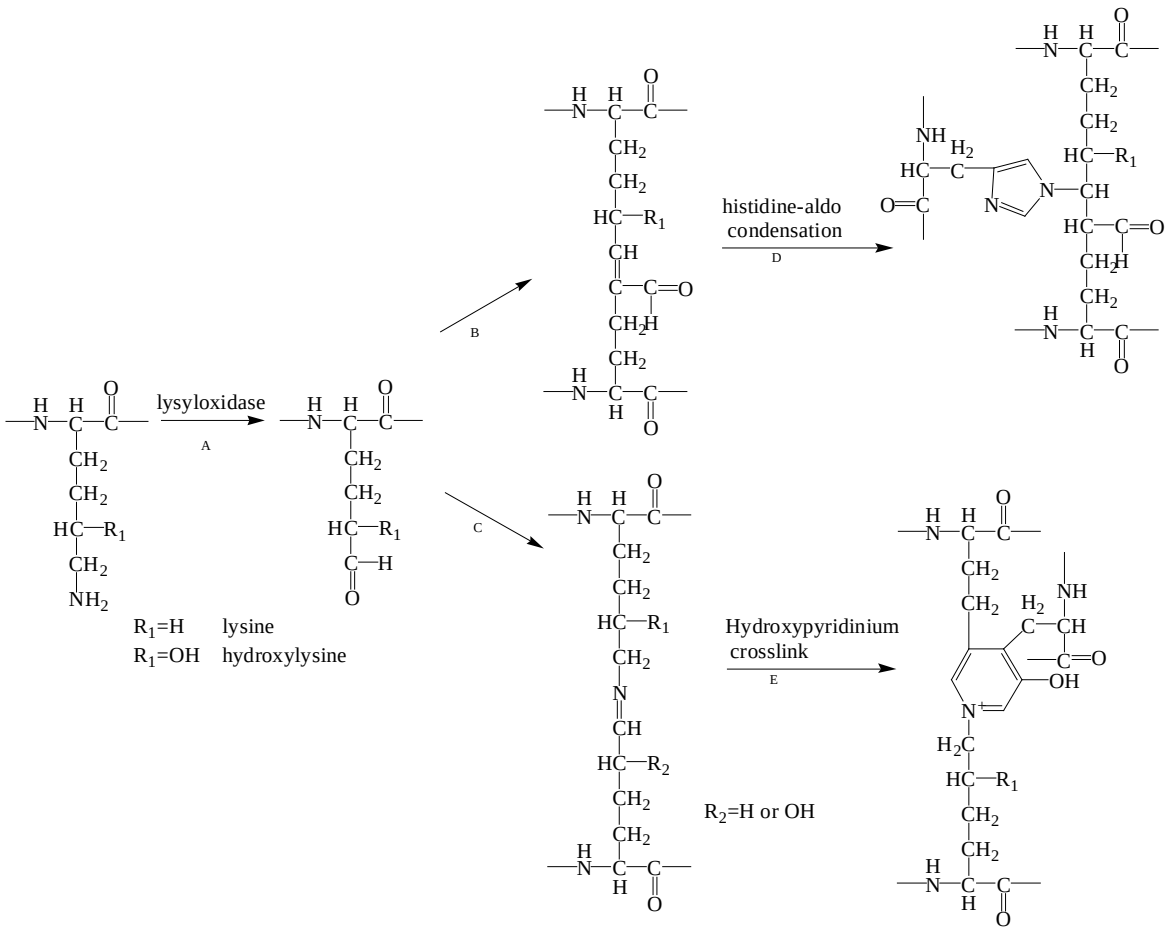

Figure 2-2. Chemical structures of collagen crosslinks in vivo. (A) oxidation of lysine and hydroxylysine via lysyloxidase, (B)intramolecular aldol condensation type of crosslink, (C) intermolecular aldimine type crosslink, (D) condensation of aldo condensation with hydroxyproline, (E) hydroxypyridinium type crosslink.

Fibril Structure Model of Collagen

X-ray scattering and electron microscopy are the principal techniques used to probe the structure of fibrils. The D-periodicity in collagen fibrils was observed by X-ray scattering and electron microscopy. An explanation of the D-periodicity in fibrils requires accurate determination of the molecular length of collagen and knowledge of the relationship between the collagen molecule and the fibril-banding pattern. Measurements

performed in collagen show that the molecular length, l, of type I collagen is approximately 4.4D. In the fibril, molecules are staggered with respect to one another. When they are regularly staggered by D (Figure 2-3), because of the nonintegral ratio of l/D, regions of gap and overlap are produced with the fibril; the overlap will be about 0.4D in axial extent and the gap will be approximately 0.6D[21, 22]. The D-periodicity of collagen fibrils is now known to an accuracy of one residue. Using a value of 234 residues for the 67-nm D-period length, the residue spacing, h, computes to 0.286 nm and is in good agreement with diffraction measurements of the axial translation of Gly-X-Y repeat units.

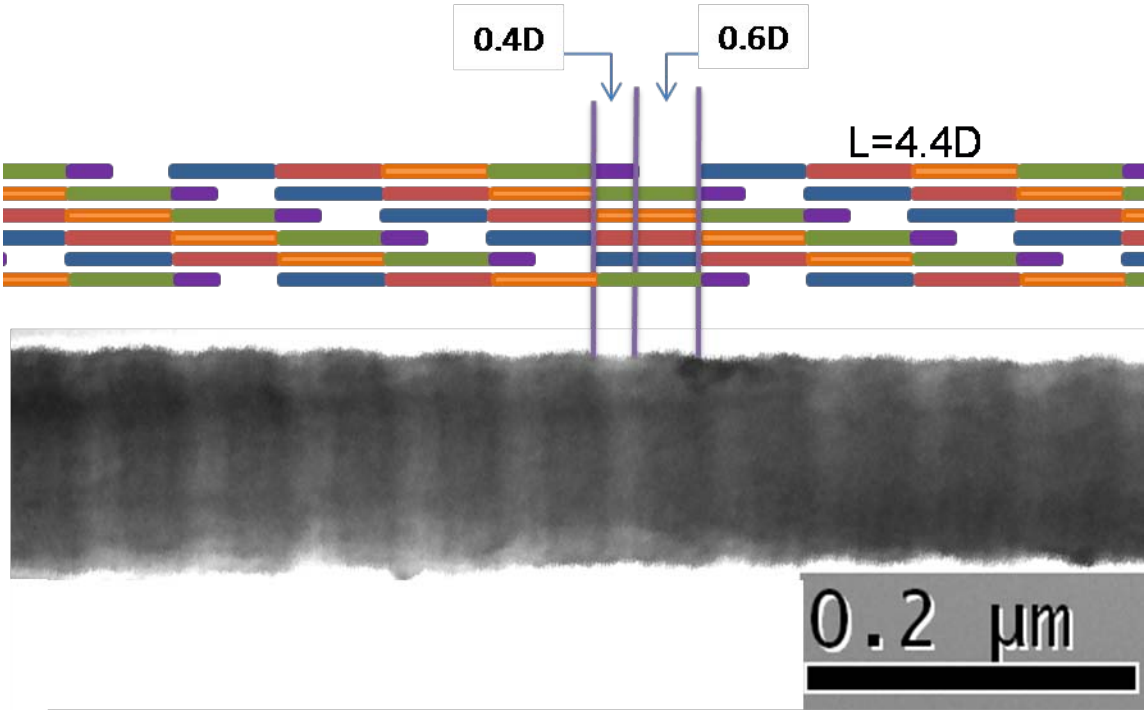

Figure 2-3. One dimensional packing arrangement model of molecules in a fibril. The lateral packing arrangement of collagen molecules shown here (collagen molecules mutually staggered by 1D 67-nm length) is only one of many possible arrangements. The gap overlap zones represent 0.6D and 0.4D, respectively. TEM image of a fibril negatively stained with phosphotungstic acid (1%, pH 7.4) is shown on the bottom.

Several models for the molecular packing of type I collagen fibrils have been proposed[23], either the tetragonal or hexagonal models. A better model is the quasi-hexagonal packing arrangement which fits with the X-ray diffraction data. This model is related with both the positions and intensities of the near-equatorial reflections and molecules tilted by 4° to the fibril axis to account for the reflections. In each unit, there are five molecules.

Structure and Mechanical Properties of the Collagen-Mineral Composite in Bone

Bone has a very complex hierarchical structure and is optimized to achieve remarkable mechanical performance[24]. The basic material of bone is the collagen-mineral composite, containing nano-sized mineral platelets (essentially carbonated hydroxyapatite), protein (predominantly collagen type I), and water. These components have different mechanical properties: the mineral is stiff and brittle while the protein is much softer but also more ductile than the mineral. Remarkably, the composite combines the optimal properties of the components, both the stiffness and the toughness. This rather unusual combination of material properties provides both rigidity and resistance against fracture.

A sketch of the most probable arrangement of the mineral particles with respect to the collagen molecules[25, 26] is shown in Figure 2-4. Bone mineral is a poorly crystalline hydroxyapatite phase. The reflections obtained by selected area diffraction (SAD) confirmed the hydroxyapatite nature of the mineral crystals. The strongest reflection comes from the 002 lattice planes indicating of the c-axis of the crystal which was preferentially oriented to the longitudinal axis of the fibrils [27]. Recent investigation on individual bone trabeculae revealed a predominant parallel orientation of the c-axis of

the mineral crystals with respect to the longitudinal axis of the trabeculae, whereby the crystals follow closely to the plane of the lamellae[27].

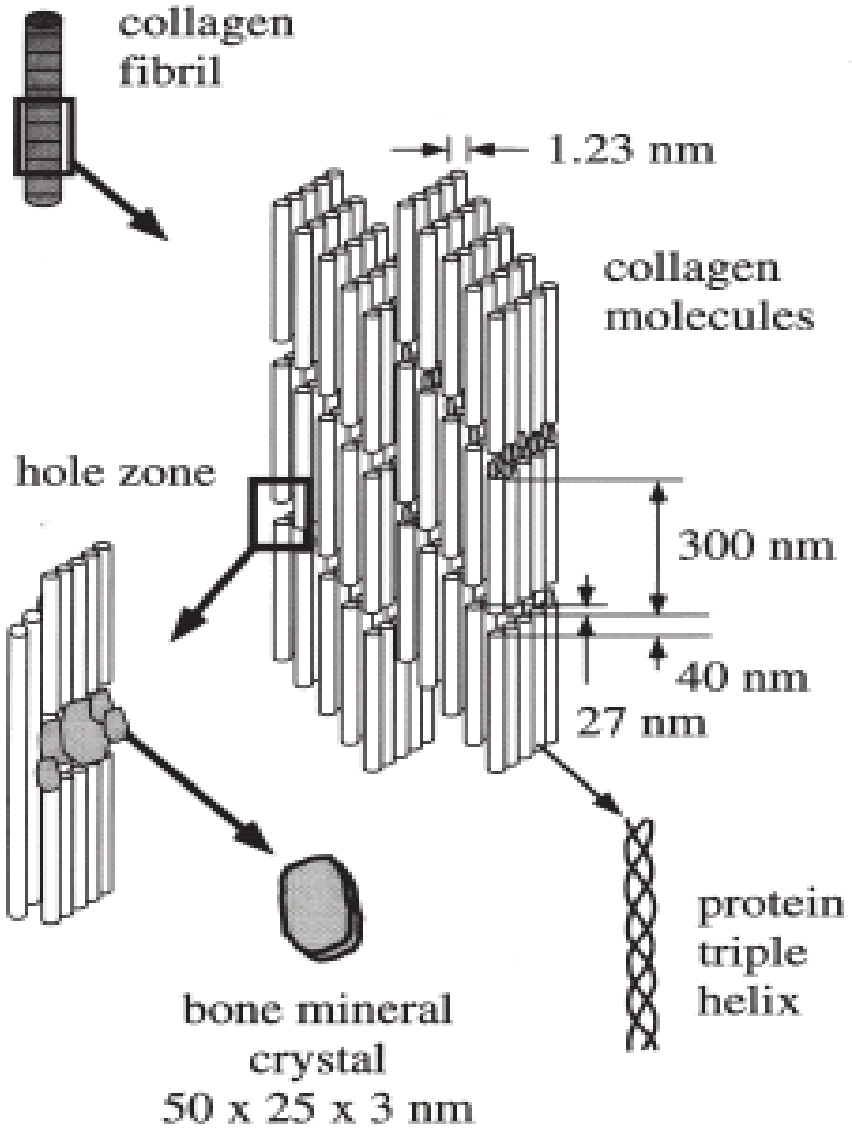

Figure 2-4. Sketch of the arrangement of collagen and hydroxyapatite composite. Hydroxyapatite is typically very thin crystals (2-4nm) and aligned with the collagen matrix. Hydroxyapatite is believed to be appeared within gap zone of fibrils. (Reproduced from Rho et al.[44])

Native type I collagen is hydrated moiety, greatly contributing to the viscoelastic properties of bone[28]. The mineralized collagen fibril about 100 nm in diameter is the

basic building block of the bone material. When the osteoblasts deposite the triple-helical collagen molecules into the extracellular space, they build fibrils by a self-assembly process. Adjacent molecules are staggered in their long axis by 67 nm in hydrated condition, generating a characteristic banding pattern of gap zones with 40 nm length and overlap zones with 27 nm length within the fibril[29]. There is evidence that the mineral particles start in the gap zones, growing initially in the gap zone and then further into the overlap zone, forming aggregates of staggered plate-like motifs[25, 26, 30, 31]. Thereby, the long axis (c-axis) of the mineral crystals is oriented parallel to the longitudinal axis of the fibrils.

Mechanism of Collagen Fibrillogenesis

Reconstituted collagen fibrils can also be self-assembled from purified collagen in vitro. The simplest system usually uses purified type I collagen extracted from skin or tendon. Typically, a solution of type I collagen in acidic solution is warmed and neutralized with buffer (pH 7.4, I 0.1) generating a gel of fibrils. The mechanism by which collagen molecules self-assemble into fibrils has been a topic of intense research since the 1950s. Early studies evaluated the kinetics of the transition of collagen from a soluble to a solid phase suggest that it was controlled by the addition of molecules at the fibril surface at temperatures above 16°C and limited by the rate of diffusion of collagen molecules at temperatures less than 16°C[32]. Thermodynamic studies indicated that native collagen fibril formation was an endothermic process that is thermodynamically favorable by the large increase in mobility of the water molecules as they are released. Early work using electron microscopy suggests that fibril growth proceeds via nucleation of monomers and growth to a fibril at a constant shape[33]. Further electron microscopic studies and examination from light-scattering techniques indicate, however, that

fibrillogenesis in vitro is a multi-step process in which the formation of linear aggregates precedes lateral growth[34]. Comparison of theoretically derived translational diffusion coefficients of the collagen monomer with those obtained experimentally from quasi-elastic light scattering studies of collagen solutions suggest that 4.4D staggered interactions occur in the early stages of assembly[35]. Electron microscopic observations on the early stages of assembly support the existence of 4.4D staggered dimers, but also show that the conditions under which fibril formation occurs influences the morphology of intermediate aggregates of the assembly process[36]. Telopeptide sequences at the N- and C-terminal of the triple-helical domains are important in stabilizing initial aggregates by formation of aldehyde adducts in vitro[37], whereby molecules in reconstituted fibrils have a memorial influence on the dissociation and reformation of fibrils[38].

Collagen Initial Aggregates in Lag Phase

Early turbidimetric studies of collagen self-assembly indicate that the lag period before fibril growth was important in determining the final fibril size. Factors such as pH, ionic strength, ion types, and temperature were found to influence the length of the lag period in manner that has only been explained phenomenologically. The mechanism of initiation, as well as a suitable explanation for lag phase and the influence of solution parameters should be important in understanding collagen self-assembly.

Inelastic light-scattering data indicate that the first-formed aggregates result from ‘linear’ rather that ‘lateral’ association of collagen molecules[39], i.e. molecules tend to associate with minimal overlap and hence maximal stagger. Gelman & Piez claim that this predominantly linear mode of assembly filaments is an intermediate step[34]. However, recent evidence does suggest that no unique assembly pathway exists[40].

Other methods used to initiate assembly can lead to the earlier onset of simultaneous linear and lateral association and the more rapid formation of native fibrils.

Lateral Arrangement of Collagen Molecules in Fibrils

Within a fibril, there is considerable long-range order in the axial direction, with neighboring collagen molecules staggered axially by integral multiples of D (i.e., nD, n=1, 2, 3, or 4, where D~67 nm, depending on tissue source). The lateral arrangement of molecules (i.e., in a plane perpendicular to the fibril axis) is less well established. In the fibrils from some tissues, x-ray diffraction indicates only liquid-like short-range order in the lateral packing, as shown by the diffuse equatorial scattering (i.e., perpendicular to the fibril axis) with a maximum in the region of the intermolecular interference function[41].

How size and form of collagen fibrils are regulated is not well understood. The regulation of fibril growth occurs in the growth step *in vivo*. Although collagen fibrils have broad diameter and length distribution, individual fibrils tend to be fairly uniform in diameter except at their ends. All the features of the fibrils observed *in vivo* have been observed in reconstituted fibrils, except the uniformity of diameter. Therefore, the components that regulate fibril size and length may be lost when collagen is extracted or when fibrils are generated from pure solutions[7]. However, studies on protease-damaged collagen that lacks the telopeptide sequences suggest that those short extrahelical sequences are critical for the formation of the uniform diameter.

Purpose of Our Study

It has been demonstrated that bone mineralization can be duplicated in Dr. Gower's group which involves the liquid-liquid phase separation of a fluidic amorphous precursor, induced by the presence of small amount of an acidic polymer in the crystallizing

solution. This process is termed the Polymer-Induced Liquid Precursor (PILP) process. It has been proposed that mineralization of collagen occurs by PILP process in which the liquid precursor phase is drawn into the collagen fibrils through capillary action. Therefore, the structure of collagen fibrils may influence the ability of the liquid precursor to be drawn into the fibrils.

The alignment of collagen molecules in fibrils results in hole and overlap zones where it is thought the liquid precursor may enter the hole zones. During collaboration on the project of mimicking bone, we found that forming collagen fibrils with native D periodicity is critical for the mineralization process.

In this dissertation, we hope to learn how collagen molecules self assemble into the fibrils and what are the major factors leading to native fibril formation. To answer the questions, we tried to examine the molecular interactions between collagen molecules during formation by introducing ionic surfactant, salts, or controlling the surface charges of collagen. We hope our studies can help in understanding the biological system, and furthermore, bring new clues on the design and development of new bio-mimetic materials.

The interactions between collagen during fibril formation have been studied a lot. However, due to the technique deficiency, there is no systematical observation on the fibril structure at nano-scale which casts a limitation on understanding the mechanism of fibril formation. In our studies, we focused on examining fibril structure by electron miscroscopy (TEM and SEM), especially measuring the banding length in the fibrils. We hope these examinations can bring new insight to understand the intermolecular interactions during fibril formation.

CHAPTER 3

KINETICS STUDIES OF COLLAGEN FIBRIL FORMATION

Introduction

It is well-known that collagen molecules form different types of aggregates in vitro, such as segment long-spacing type (SLS), fibrous long-spacing type (FLS), native-type fibrils, fibrils without periodic striation, under select conditions[45-47], as observed by electron microscopy, which might come from collagen specific intermolecular interactions. The factors affecting the interaction between collagen molecules are divided into three classes. The first class is concerned with the environment in the solution, such as the pH, ionic strength, ionic species, other substances, temperature and pressure. The second class is the molecular structure of the collagen itself, such as collagen sources, existence of non-helical regions, the formation of cross-links. The third class is the factors affecting collagen fibrillogenesis due to biological considerations, such as the concentration of collagen.

A number of studies have been carried on the effect of pH, ionic strength, and temperature on collagen fibril formation[40, 48, 49]. Turbidity-time examinations for type I collagen are commonly used to study the collagen fibril formation behavior. Turbidimetric curves are composed of lag and growth phases. During the lag phase, aggregation occurs primarily by linear addition of collagen molecules for forming end overlapped or 4.4D-staggered dimers and trimers[39, 50]. The time of the lag phase is dependent on both the presence of helical and non-helical ends [51, 52] and several studies suggest that charged and hydrophobic residues are important for aggregation. However, there are some disagreements on whether the aggregates that form during the lag phase are unstable “nuclei” that grow by monomer addition or subfibrillar components that grow in a multiple steps [50, 52]. It is clear from laser light scattering studies that physical changes can be measured during the lag phase[52]. Near the end

of the lag phase and during the growth phase lateral aggregation of elements is formed. Studies also suggest that lateral growth occurs via the formation of a subfibrillar unit composed of five trimers which can linearly and laterally associate with other subfibrillar components [39]. Linear and lateral aggregation of these units may be controlled by interactions between attractive charged pairs [35].

Since the experimental conditions and collagen source always influence fibrillogenesis kinetics and structure of fibrils, it is important to study the basic factors on fibril formation as well as the mechanism of self-assembly in order to design and fabricate collagen fibrillar matrices. In this chapter, the kinetics of fibril formation, the effects of collagen concentration, temperature, and ionic strength of phosphate buffer were investigated.

Materials and Methods

Materials

Purified type I collagen (99%) was purchased as a solution of pepsin-solubilized adult bovine dermal collagen dissolved in hydrochloric acid (0.012N) with the concentration of 2.9 mg/mL (Vitrogen; Cohesion Technologies, Inc., Palo Alto, CA).10-fold phosphate buffered saline, NaOH (0.1N) and HCl (0.1N) were purchased from Sigma.

Polyacrylamide Gel Electrophoresis In SDS (SDS-PAGE)

Collagen in 0.12N HCl with different concentrations was used for gel electrophoresis by dialyzing them overnight against a sample buffer containing 3 to 8% NuPAGE Tris-acetate Gels with Tris-acetate SDS buffer and stained with Coomassie blue. All samples were reduced and denatured before gel electrophoresis.

Turbidity-Time Measurement

Collagen fibrillogenesis in the range of 28°C to 34°C was studied by turbidity measurements. Chilled pepsin-solubilized collagen solution was mixed with 10-fold phosphate

buffered saline and 0.1 M NaOH in an 8:1:1 volume ratio in an ice bath to give a final composition of 10 mM phosphate and 168 mM of NaCl. The mixture was poured into spectrophotometer cells, which were sealed and transferred to the cell compartment of a UV/Vis spectrometer (Perkin-Elmer Lambda 800 UV/Vis spectrometer, Fremont, CA), equipped with a thermostated cell holder, and maintained at the desired temperature by water circulation. The process of fibrillogenesis was monitored by recording the light transmittance at 400 nm wavelength as a function of time.

The turbidity curves were plotted as follows: the absorbance at 400 nm was calculated by A=2-log (Transmittance), and the turbidity as an increase in absorbance was plotted versus time in minutes. Usually, absorbance was converted into turbidity by multiplying with 2.303[53]. In our study, the absorbance was taken as an indirect indication of turbidity. The curve consisted of an initial lag phase with no turbidity change, a growth phase during which there was an increase in turbidity and a plateau where no further change in turbidity was observed. The $t_{1/2}$ was defined as the time when half of turbidity change (ΔT) was attained. The reciprocal of $t_{1/2}$ was taken as an estimation of the apparent rate of collagen fibril formation in order to obtain the activation energy of the overall process.

Morphology Studies of Fibrils

Typical studies of the morphologies of collagen fibrils were conducted by TEM, in which image contrast is caused by the relative ability of regions of the fibril to scatter or transmitted electrons. Sample staining with heavy, electron scattering elements is often carried out in order to enhance the contrast within organic samples such as collagen. Within a fibril, the heavy metals which were deposited in the gap zone appear dark and the overlap zone, which has less metal deposition appear bright under the TEM examination. When preparing a sample, a small portion of collagen fibrils washed with MiliQ water were first placed on a cooper grid with mesh size of

300. After draining for 1 minute, it was negatively stained at room temperature for 15 second with 1% phosphotungstic acid at pH 7.4. Then, the grid was washed with water for 1 minute and air dried. The prepared specimens were examined in a Jeol TEM 200CX with acceleration voltage of 80 kV, and digital micrographs were taken at magnification of 37, 000X.

Mathematical Analysis of Kinetics of Fibril Formation

The turbidity of a macromolecule solution depends both on the size (molecular weight) as well as shape (particle dissipation factor). Therefore, turbidity increases result from size and shape changes which can be studied using a mathematical approach. Under ideal scattering conditions, the turbidity (T) is given by equation 3-1, where T is directly proportional to the weight concentration of macromolecules in solution, C; the molecular weight, M_r; and the particle dissipation factor, Q [54, 55]. The particle dissipation factor is inversely related to the largest macromolecular dimension and can be obtained for a given shape from tabulated values [54, 55]. As the particle gets bigger Q decreases and approaches zero. The constant of proportionality, H is a function of the index of refraction in solution n_0, the refractive index increment, dn/dc, Avgadro's number, N and the wavelength of light in solution, λ and is given by equation 2.

$$T=HM_rCQ \tag{3-1}$$

$$H=[32\pi^3 n_0^2(dn/dc)^2]/(3N\lambda^4) \tag{3-2}$$

As for a mixture of macromolecular species having different values of M and Q, the average turbidity (T) is proportional to the average molecular weight (Mr) and average Q (Q) were used for analysis [56].

By differentiating equation (3-1) with respect to time, the result of differentiation is given by equation 3-3.

$$\frac{d\bar{\tau}}{dt} = Hc\bar{Q}\left(\frac{d\bar{M}_r}{dt}\right) + Hc\bar{M}_r\left(\frac{d\bar{Q}}{dt}\right) + H\bar{Q}\bar{M}_r\left(\frac{dc}{dt}\right) \quad (3\text{-}3)$$

When dc/dt is isolated on the left hand side equation 3-3 becomes:

$$-\frac{dc}{dt} = \left(\frac{d\ln\bar{Q}}{dt} + \frac{d\ln\bar{M}_r}{dt}\right)c - \frac{d\bar{\tau}/dt}{H\bar{M}_r\bar{Q}} \quad (3\text{-}4)$$

When both sides of equation (3-4) are divided by the average molecular weight, equation (3-4) becomes a rate expression. Since the molecular weight increases as fibrils are formed, the left side of the equation (3-4) represents the decrease in the moles of collagen as fibrils are formed. A first order rate expression for the disappearance of moles of collagen would have the following form:

$$-\frac{d[c]}{dt} = k[c] \quad (3\text{-}5)$$

A plot of d[c]/dt versus [c] based on equation (3-5) is a straight line for a first order reaction and has a slope equal to k, the rate constant. By integrating equation (3-5), the equation of (3-6) can be given below:

$$\ln[c]/[c]_0 = -kt \quad (3\text{-}6)$$

As for the first order reaction, the reaction rate constant can be expressed by $t_{1/2}$, the time to reach the middle point of the final opacity

$$k = \ln 2/t_{1/2} \quad (3\text{-}7)$$

However, a more simplified equation has been proposed where the turbidity is proportional to the concentration. It turns out that $t_{1/2}$ in turbidity-time measurement can be used in studying the kinetics of fibril formation.

Activation Energies for Fibril Formation

Since the apparent rate constant can be treated as $t_{1/2}$ as discussed above, the activation energy, E_a, for the fibril formation can be determined. The activation energy is obtained from the temperature dependence of the apparent rate constant (k) using the Arrhenius relationship where

T is the absolute temperature in K, R is the gas constant and A is the rate constant as 1/T approaches 0.

$$k = Ae^{-E_a/RT}$$

(3-8)

A plot of ln(k) versus 1/T has a slope equal to the activation energy divided by the negative gas constant. Therefore, by plotting $\ln t_{1/2}$ versus 1/T, the activation energies for fibril formation can be obtained.

Results

Collagen Characterization

The SDS-PAGE analysis of collagen is shown in Figure 3-1. Line 1 is the protein markers. Lines 2 to 6 are the collagen content from 5 µg to 40 µg. A triple helix of type I collagen molecule is composed of two α1 chains and one α2 chain. Collagen molecules on SDS-PAGE show six distinct bands in line 2 which indicate the α1 and α2 trimers, α1 and α2 dimers, α1 monomer, and α2 monomer.[57] Thus, α1 and α2 have similar molecular weights of about 120 kDa and the type I collagen triple helix has a molecular weight about 360 kDa.

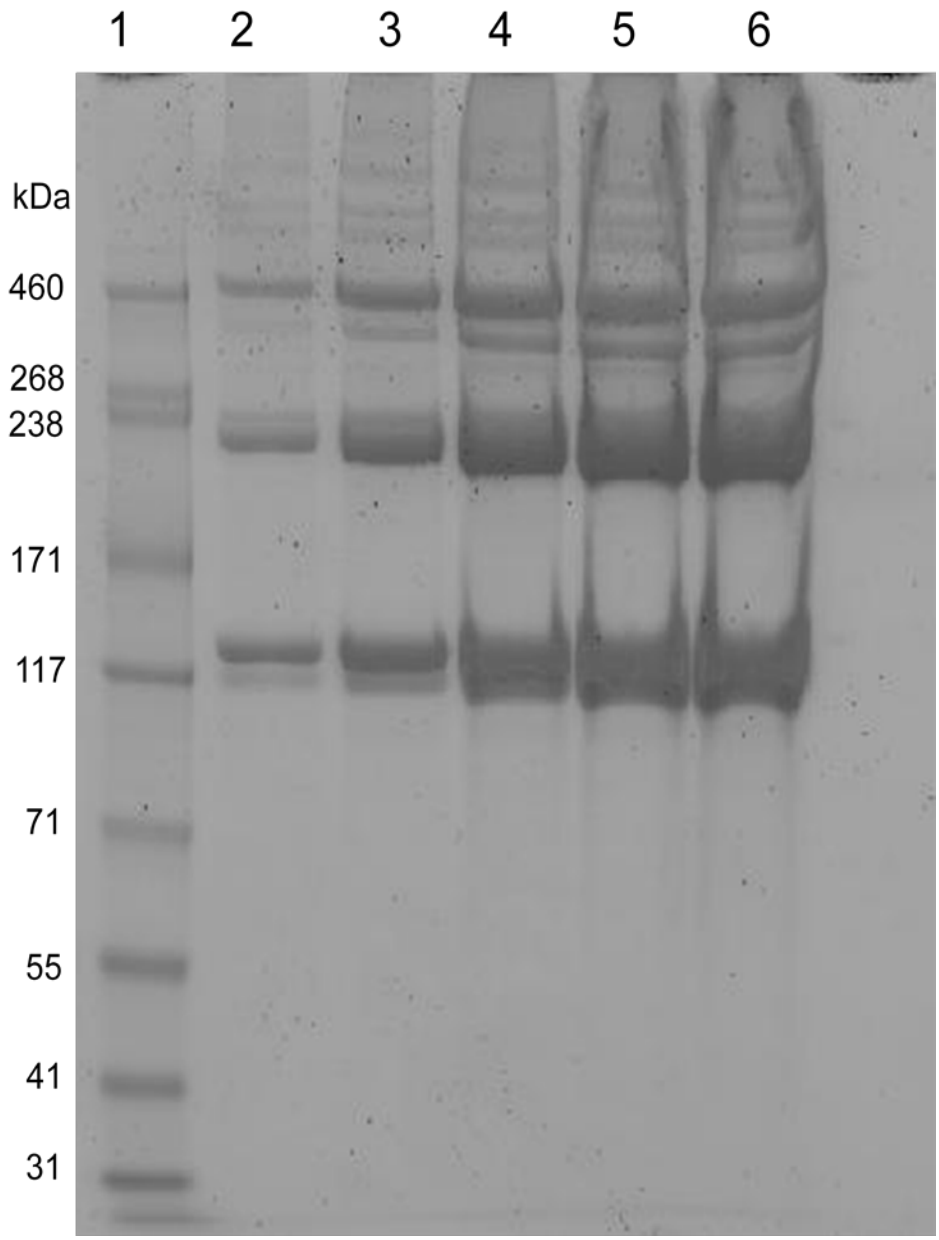

Figure 3-1. Coomassie blue stained SDS-PAGE of collagen. It was separated in 3 to 8% NuPAGE Tris-Acetate Gels with Tris Acetate SDS buffer. Lane 1, mass marker; Lane 2, 5 µg collagen; Lane 3, 10 µg; Lane 4, 20 µg; Lane 5, 30 µg; Lane 6, 40 µg.

Concentration Effects

Light scattering from collagen fibril formation is complex as described in the experimental section. It is proportional to the particle dissipation factor and concentration of fibrils. However,

it has been found that turbidity is proportional to the amount of precipitation and can be used for kinetics studies[58, 59]. A typical turbidity-time curve for type I collagen is shown in Figure 3-2. This curve is composed of three phases as described in the introduction part. In the lag phase, there is no detectable change in turbidity; in the growth phase, the turbidity changes rapidly, and at the plateau phase the turbidity remains constant again where the curve can be characterized by the total turbidity change ΔT and $t_{½}$ the time to reach the middle point of the final absorbance.

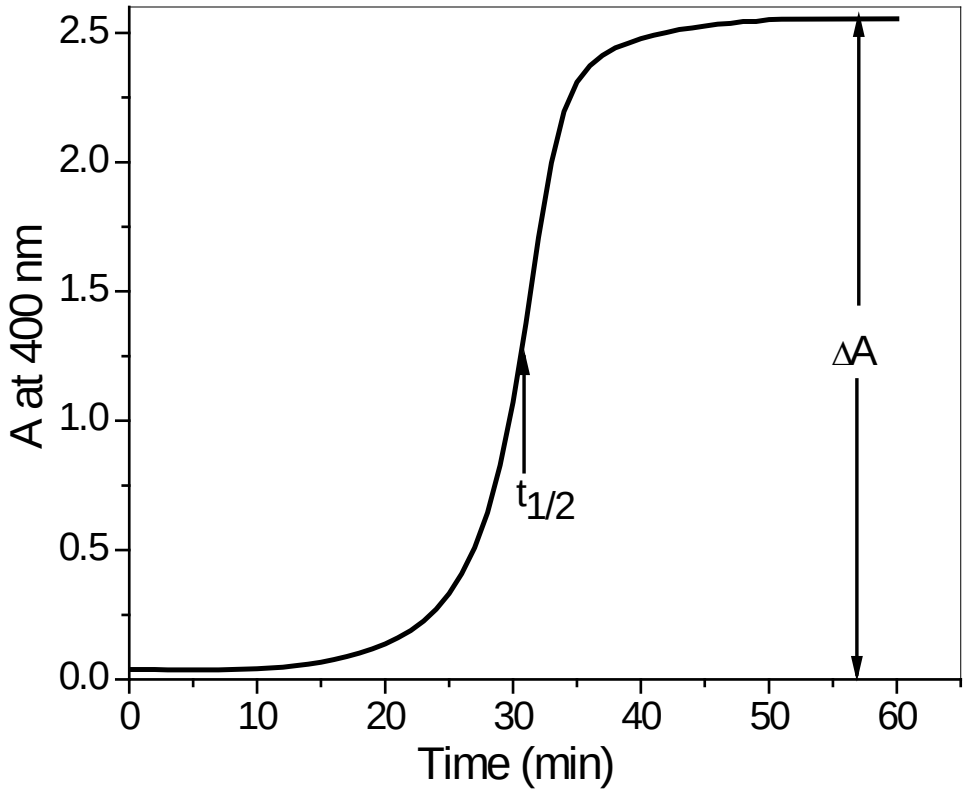

Figure 3-2. A typical turbidity curve presenting an increase in light absorbance as collagen fibrils are formed. The collagen concentration was 2.5 mg/mL and the temperature was 34°C.

The fibrillogenesis of collagen in different concentrations were conducted from 0.5 mg/mL to 2.5 mg/mL at 34°C (Figure 3-3). The rate of fibril formation and the final turbidity were

highly affected by the concentration. By increasing the concentration, the rate and the turbidity increased. A plot of the ΔA versus concentration (Figure 3-4) indicates that the final turbidity is proportional to the collagen concentration, which is consistent with previous reports [34, 49, 56]. The dependence of $t_{1/2}$ on concentration was plotted with the format of log ($1/t_{½}$) versus log concentration in Figure 3-5. The rate of fibril formation by measuring turbidity is proportional to collagen concentration on the first power which suggests the mechanism of fibril formation is the same at different concentrations of collagen, as reported before[58].

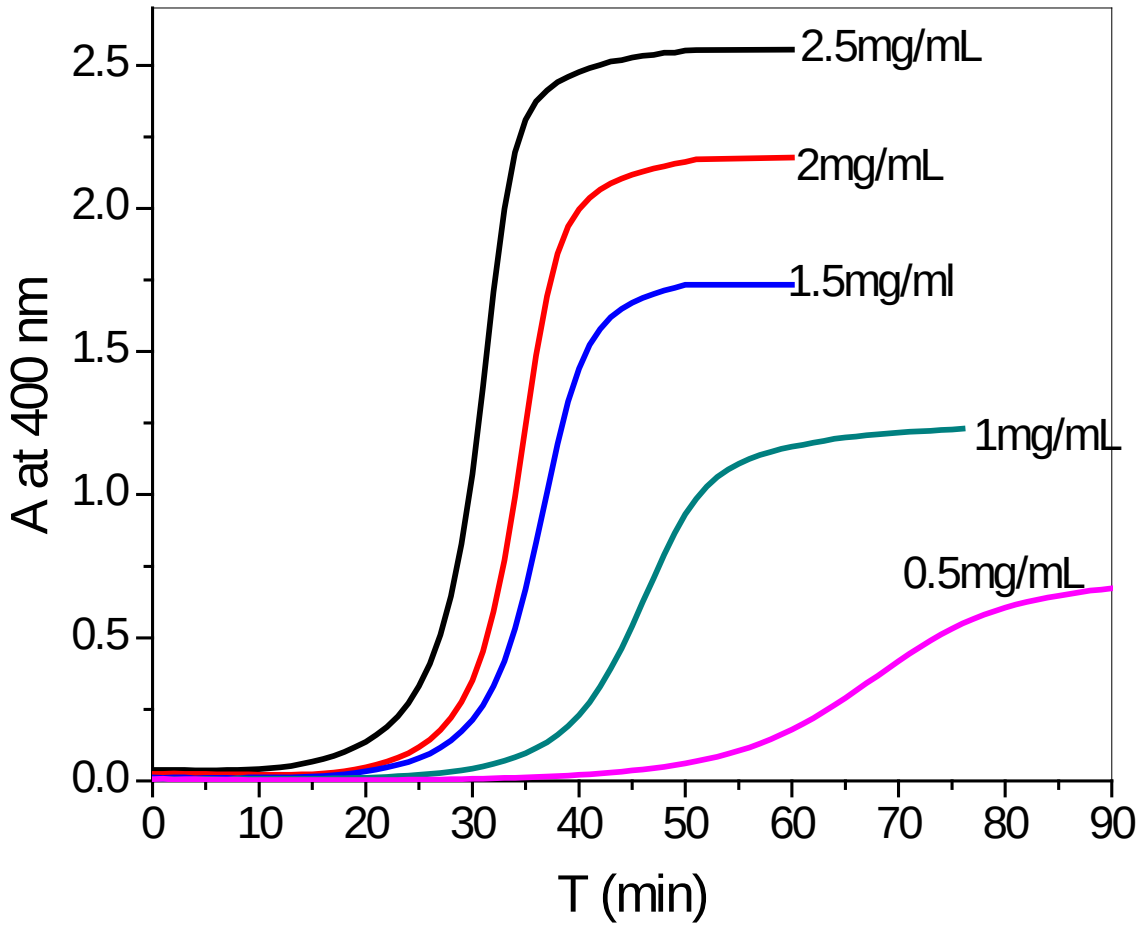

Figure 3-3. Effects of collagen concentration on collagen fibril formation. Condition: 34°C, pH 7.4; ionic strength 0.2; $Na_2HPO_4$0.02M, NaCl 0.14N.

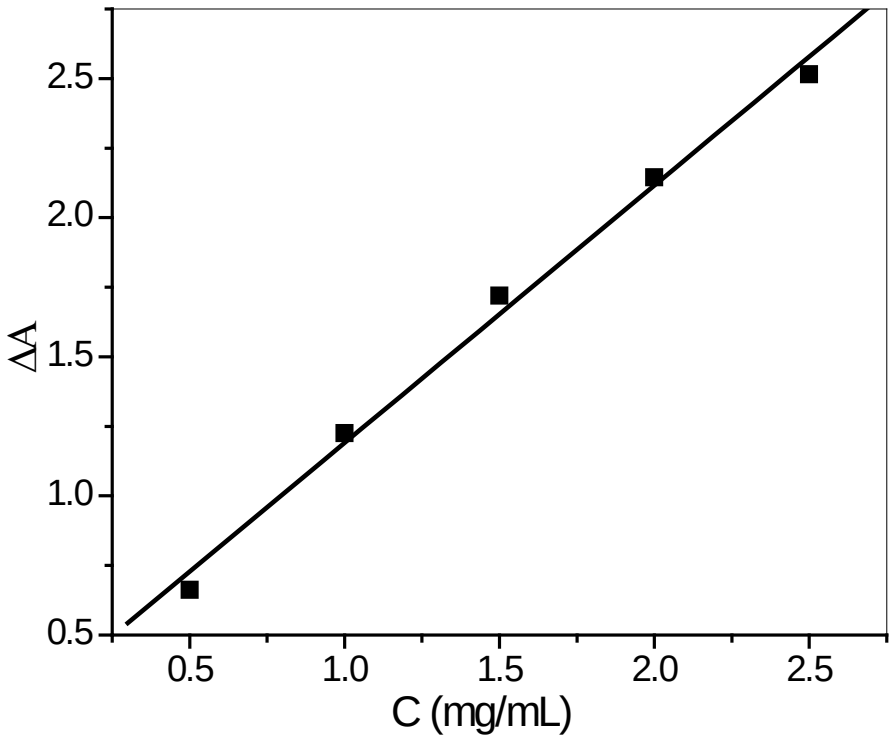

Figure 3-4. Linear dependence of ΔA on concentration of collagen type I. The relationship is consistent with the theoretical relationship in equation (3-1).

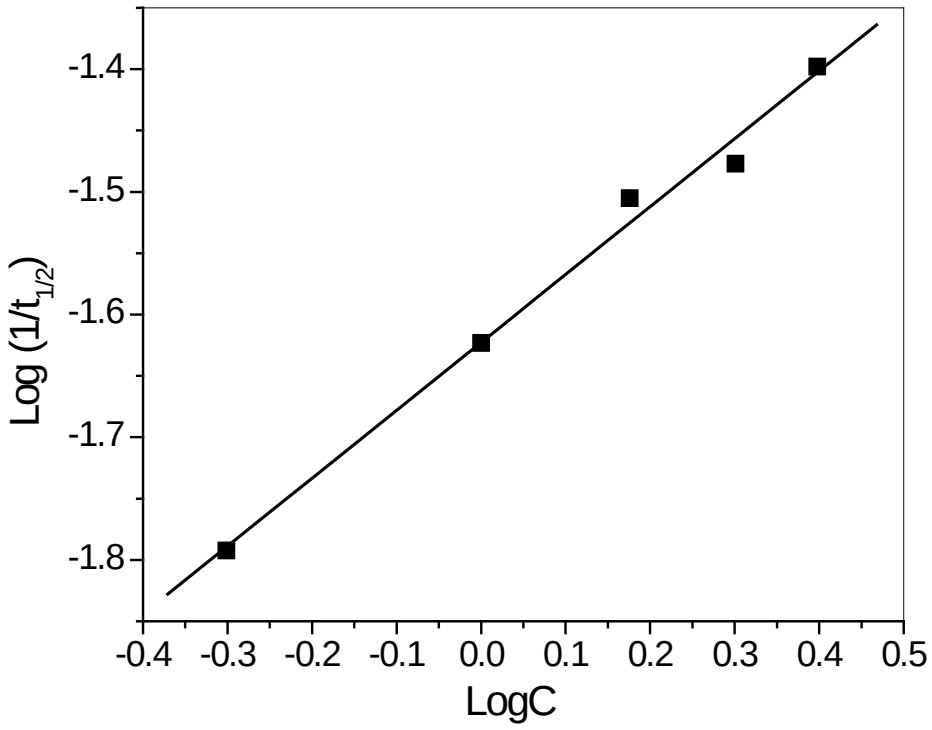

Figure 3-5. Effect of collagen concentration on rate of fibril formation. Condition: 34°C, pH 7.4, 10 mM phospate.168 mM NaCl.

Temperature Effects

It is well-known that temperature is of primary importance in collagen fibril formation. The results in Figure 3-6 indicate that the fibrillogenesis rate is influenced by the change of temperature. The higher the temperature, the faster the collagen fibrillogenesis proceeds. An Arrhenius plot for collagen fibril formation give an activation energy of 167.6 kJ/mol, which is similar to the result of fibrillogenesis from telopeptides collagen [53, 58]. It has been found that the removal of non-helical ends inhibited the initiation of the self-assembly of collagen molecules.[59] As for the atelopeptides which was used in studies here, it should have a high activation energy compared to telopeptides collagen in the same condition. However, the activation energy of fibrillogenesis can be also a result of the experimental conditions and

collagen source. Therefore, it is difficult to compare the activation energy to literature data directly.

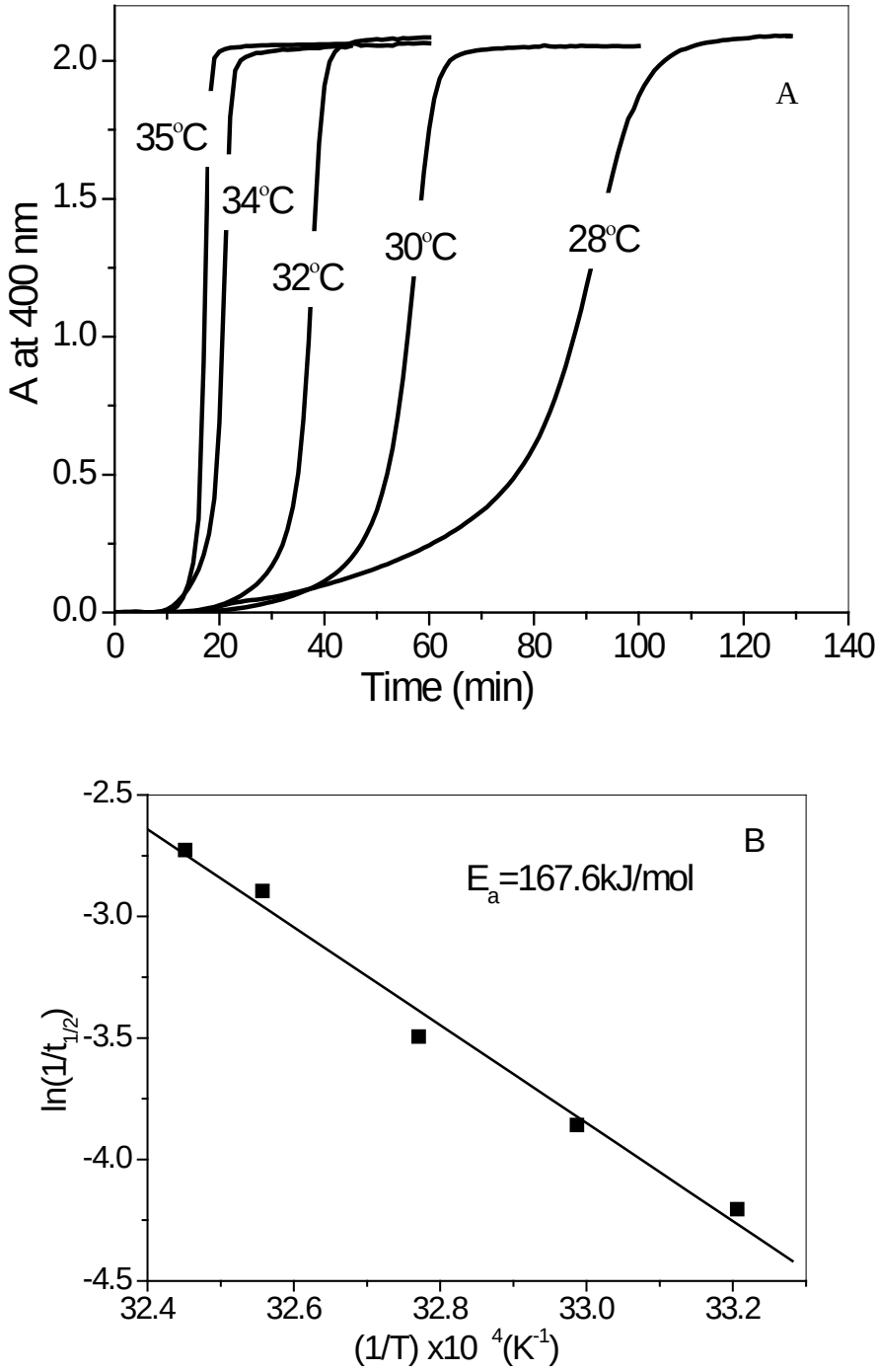

Figure 3-6. Turbidity measurements of temperature effects on collagen fibril formation. A) Turbidity-time measurements of fibril formation in different temperature. B) An Arrhenius plot for collagen fibril formation from A. Collagen 2.5 mg/mL, pH 7.4.

Temperature not only affects the fibrillogenesis rate, it also affects the final fibrils' morphology. As the temperature is decreased to less than 16°C, collagen molecular movements are inhibited, resulting in a reduced rate of fibril formation and most of the collagen appears as a mixture of filamentous aggregates with occasional thin fibrils. Moreover, at lower temperatures (e.g. room temperature), it is hard to form fibrils even after 10 days of storage while most of the collagen appears as a mixture of amorphous gel(data not show). Collagen thermal stability can also affect the fibril formation. When temperatures are higher than 37°C, the collagen molecules undergo helix-coil transition, and no fibrils are formed. In TEM measurements (Figure 3-7), with increasing temperature from 28°C to 37°C, the fibril size is decreased and the small fibrils with unclear D-periodicity appeared at 37°C.

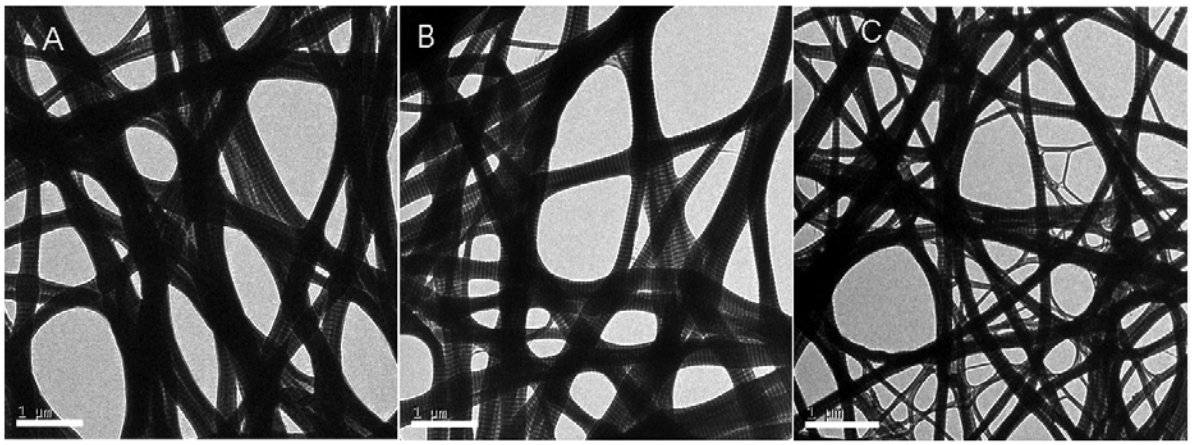

Figure 3-7. TEM images of collagen fibrils formed at different temperatures. A) Collagen fibrils are formed at 28°C. B) Fibrils are formed at 30°C. C) Fibrils are formed at 37°C. Collagen concentration is 2.5 mg/mL, scale bar 1 μm.

Effects of Phosphate and Ionic Strength

The effects of phosphate and ionic strength on collagen fibrillogenesis were also conducted at a constant pH, including 10mM phosphate with 168mM sodium chloride, 18mM phosphate

with 302mM sodium chloride, and 25mM phosphate with 421mM sodium chloride. At low phosphate concentrations, native fibrils were formed (Figure 3-8A). The fibrils showed the D-periodicity consisting of a fine polarized band pattern superimposed on alternate light and dark regions. The fibrils had diameters of about 130 to 200 nm and had a constant diameter along the fibril's direction but tended to bend and entangled with each other. At phosphate concentrations near 18 mM (Figure 3-8B), the native D-periodicity appeared clearly and fibrils had diameters of about 120 to 250 nm. At high phosphate concentrations, the fibrils had sizes of about 150 nm, which was smaller than in low phosphate concentrations and the D-periodicity was unclear (Figure 3-8C). Fibril formation in the absence of the PBS was also conducted (data not show), as a result, amorphous collagen gels with occasional fibrils were presented.

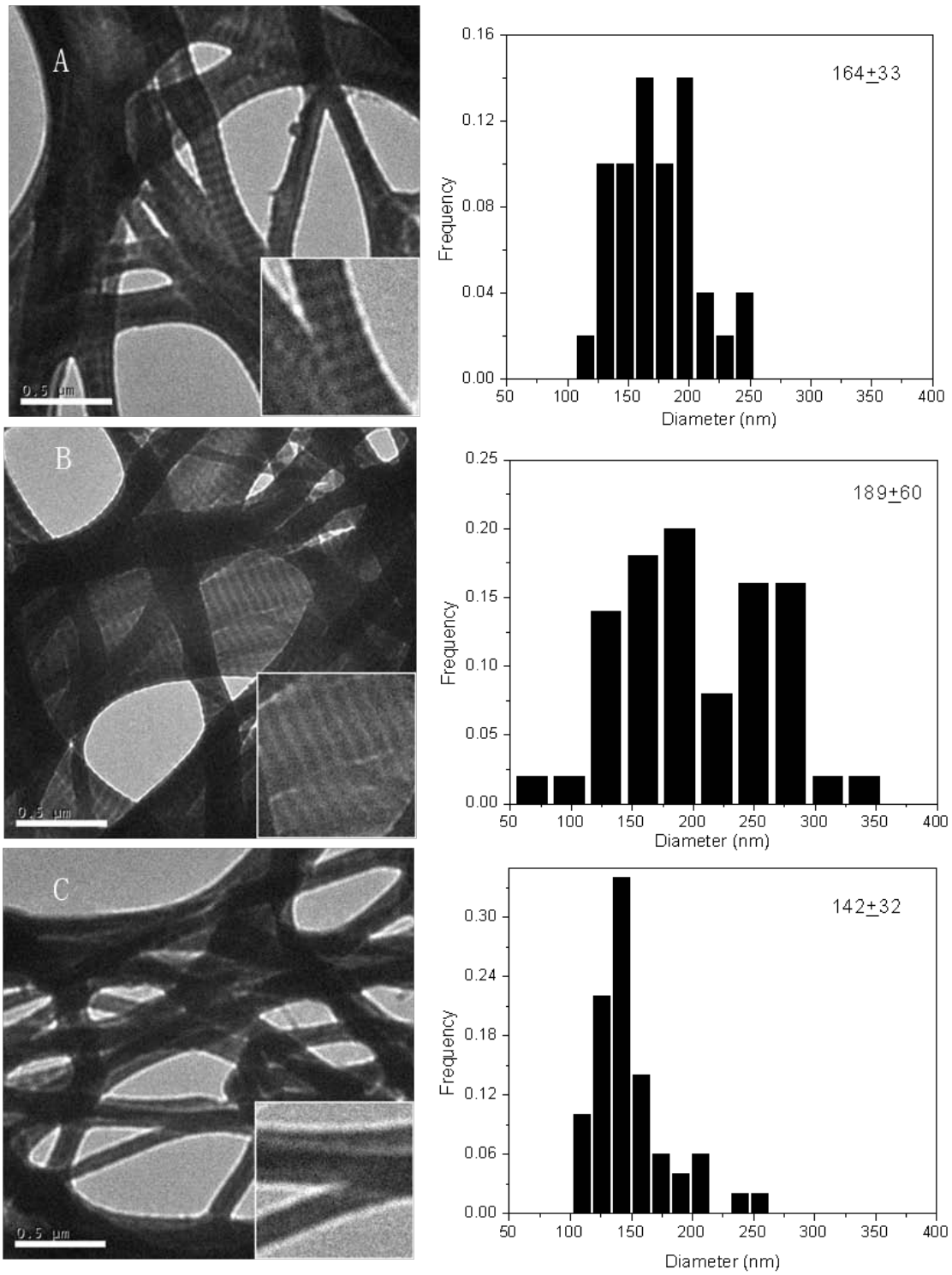

Figure 3-8. TEM images and corresponding fibril diameter distributions of collagen fibrils formed at various phosphate buffer concentrations and ionic strengths. A) 10mM phosphate and 168mM NaCl. B) 18mM phosphate and 296mM NaCl. C) 25mM phosphate and 402mM NaCl. Average fibril widths are in nm and standard deviations are shown. The number of fibrils measured was at least 50 for each sample. Scale bar is 0.5 µm.

Discussion

Turbidity-time studies of collagen fibrillogenesis have shown that collagen aggregation is a multiple step process which is composed of a lag phase, growth phase and plateau phase. It has been proposed that collagen fibril formation is a nucleation and growth process. But the power dependence of $t_{1/2}$ on collagen concentration of one indicates it is not the typical nucleation-growth process. Since the nucleation-growth process of keratin assembly has a power value of about 3[60] and hemoglobin S assembly is 30 to 40[61]. A power dependence of one suggests simple growth by accretion[58]. Time-lapse AFM studies on fibril formation by Cisneros, DA et al. suggest that collagen self assembly is a multi-step process: at the first step, the collagen molecules assemble with each other to form aggregates; at the second step, those aggregates turn into microfibrils which have diameters of about 4 nm, then these microfibrils self assemble into fibrils through longitudinal and lateral packing.[62] These multiple processes can't be directly examined by turbidity measurement since turbidity measurement can't measure the formation of microfibrils due to its small size. Based on the microfibril model of the collagen fibril, the lag phase may be dominated by forming intermediate and linear growth of microfibrils, which are too small to be detected by turbidity while the turbidity increase measures primarily lateral assembly of microfibrils to fibrils.

Self assembly of collagen type I molecules into fibrils is a temperature favored process which is thermodynamically favorable by a large positive entropy contribution, presumably arising from structural reorganization of the water during fibril formation[63, 64]. The importance of structured water in molecular interactions has been recognized and the interactions involving both polar and non-polar molecules in water can be stabilized by the large positive entropy contributions coming from releasing the structured water. Our studies on changing temperature for fibrillogenesis indicate low and high temperature inhibiting fibril formation. At

the low temperature, it is difficult to break the structured water and the repulsion between collagen molecules could not be overcome to form the fibrils. At the high temperature, partial denaturation of collagen triple helix also inhibits fibril formation. Temperature from 28 to 37°C is the suitable range for fibril formation without interrupting collagen's triple helix structure.

Phosphate appears to play a critical role in fibril formation beyond its capacity as a buffer[58]. Although phosphate inhibited the rate of fibril formation[65], its role cannot be only related to a rate effect, since 18mM is sufficient to produce well ordered native-banded fibrils. The nature of its interaction with collagen is not known, but it is necessary to add phosphate to trigger fibrils with native banding formation. Based on these results, phosphate at 18mM and 302mM sodium chloride was included in all further experiments. The specific role of phosphate on fibril formation will be studied in more detail in Chapter 5.

Conclusion

The collagen fibril formation in pepsin-digested collagen extracted from bovine dermis has been followed by turbidimetric examination under a range of experimental conditions. All fibrillogenesis curves showed a lag period, followed by a quick growth phase. Both phases were accelerated by increasing collagen concentration and temperature.

Collagen fibril formation is a temperature favored first order reaction and the activation energy is 167 kJ/mol. It is a multistep process which involves of nucleation, linear and lateral growth.

Phosphate ions play a key role on forming native banded fibrils which can not simply be explained by buffer solution. The specific effects of phosphates will be investigated in Chapter 5.

CHAPTER 4
INTERACTIONS BETWEEN IONIC SURFACTANT AND COLLAGEN ON FIBRIL FORMATION

Introduction

The surfactants, ionic or nonionic in nature, interact with protein which leads to significant changes in the bulk properties of protein solution. Sodium dodecyl sulfate (SDS), an ionic surfactant, has been generally used to denature protein for SDS-PAGE. SDS breaks up the two- and three-dimensional structure of the proteins by adding negative charge to the amino acids during heating. Through the like-charge repulsion, the proteins are more-or-less straightened out, immediately rendering them functionless. Alkyl sulphates, at concentrations below their critical micelle concentrations, (CMC) form complexes with human serum albumin and bovine serum albumin[66]. It is generally known that the formation of these complexes is accompanied by unfolding of the protein structure[66-68]. However, in some cases, the occurrence of the association between surfactants and bovine serum albumin has been observed without drastic conformational change[69].

It has been reported that ionic surfactants can accelerate the rate of collagen fibrillogenesis[70]. However, the acceleration effects and how surfactants can influence the morphologies of collagen fibrils are not well understood. The addition of anionic surfactants (e.g. SDS) stimulated the initial stage of aggregation and the growth, while non-ionic surfactants with oxyethylene groups stimulated all stages of fibril formation and formed the thinner collagen fibrils at low concentrations of surfactants[70, 71]. Investigations on the adsorption of anionic and nonionic surfactants to collagen suggest multiple adsorption occurred and the adsorption of nonionic surfactant on collagen through the hydrophobic interactions[72]. The systematic study of the role of SDS in conformational transitions of collagen suggest that under the non-isoelectric

conditions, both the electrostatic and hydrophobic interactions happen while at isoelectric conditions, hydrophobic interactions are dominant.[73]

Surface Tension Measurement

There are many methods which can be used to measure the surface tension. A simple one is the Wilhelmy plate method[74]. The basic mechanism of Wilhelmy plate method is that a thin plate, such as a microscope cover glass or platinum foil, will support a meniscus whose weight is measured by detachment given very accurately by the "ideal" equation (assuming zero contact angle):

$$\gamma \cos\theta = \frac{W_{total} - (W_{plate} - b)}{2l} \quad (4\text{-}1)$$

Where γ is the surface tension, θ is the contact angle, W_{total} is the total weight to be measured, W_{plate} is the weight of platinum plate, b is the buoyance force, l is the length of plate (Figure 4-1). Normally, a platinum plate is used and contact angle is very small (θ→0), and the plate just touches liquid so the buoyancy is small which can be ignored.

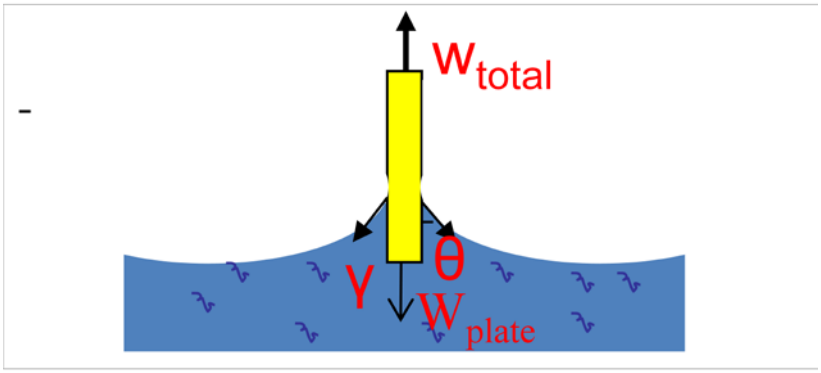

Figure 4-1 Illustration of surface tension measurement by Wilhelmy plate method.

In this chapter, sodium dodecylsulfate (SDS) or sodium dodecylbenzenesulfonate (SDBS) were used to study the effects of ionic surfactants on collagen fibril formation. The interactions between surfactant and collagen were observed by turbidity and surface tension measurements.

The denaturation effect of surfactants on collagen and the specific interactions between surfactant and collagen were discussed.

Materials and Methods

Materials

Purified type I collagen (97%) with the remainder being comprised of type III collagen was purchased as a solution of pepsin-solubilized adult bovine dermal collagen dissolved in hydrochloride acid with a concentration of 3.0 mg/mL (PureCol®, INAMED, Inc., Fremont, CA). 10x concentrate phosphate buffered saline (PBS) pH 7.4, sodium dodecylsulfate (SDS) and sodium dodecylbenzenesulfonate (SDBS) were purchased from Sigma.

Surface Tension Measurement of Surfactants

Surface tension was measured using the Wilhelmy platinum plate method (~5 cm perimeter) at 17±1°C. The Wilhelmy plate was washed by de-ionized water, methanol, acetone and water, then burned for 15 second to remove impurities. All aqueous surfactant solutions were kept at room temperature for at least 30 minutes before measurement in order to obtain stable data. Critical micelle concentrations (CMCs) were determined from the inflection points of the respective surface tension curves. The standard deviation for the experimental surface tension was less than 0.02mN/m. Surface tensions of surfactant in collagen solution were also measured in the same process.

Turbidity Measurement

To produce collagen fibrils, the chilled type I collagen solution was mixed with PBS at the ratio of 8:1 v/v and self-assembled with incubation at 30ºC for 2 hours. The pH of the solutions was mediated by adding 0.1M NaOH. The degree of the fibrillar assembly with the incubation time was recorded by measuring the transmittance at 400nm using a UV-Vis spectrometer

(Perkin-Elmer Lambda 800 UV/Vis spectrometer, Fremont, CA), equipped with a thermostat cell holder, and maintained at the desired temperature by water circulation.

SEM Measurements of Collagen Fibrils

The morphology of collagen gel was examined by scanning electron microscopy (SEM, Jeol, JSM-6335F). The freeze dried collagen samples were mounted on a stub and carbon coated. The morphologies were observed at an accelerating voltage of 15kV.

Results

Surface Tension Measurements

In order to investigate the interactions bewteen surfactant and collagen molecules, the surface tensions of surfactants solution with/without collagen at room temperature were measured. It is known that surfactants can reduce the surface tension of water by absorbing at the air/water interface. They can also assemble into aggregates in the bulk solution that are known as micelles. The concentration at which surfactants begin to form micelles is known as the critical micelle concentration (CMC). As reported in the literature, the CMC value of surfactants decreases as the concentration of electrolyte increased since the electrolytes neutralize the charge around the micelle surface and reduces the thickness of the ionic atmosphere around the surfactant ionic heads and the electrostatic repulsions between them[75]. The decrease in the CMC of an ionic surfactant due to the effects of the electrolyte counter-ion can be quantified through the following empirical expression, developed by Corrin and Harkins[76]:

$$\log CMC = a + b \log c_i \qquad (4\text{-}2)$$

where a and b are constants that mainly depend on the surfactant species and the temperature, and c_i is the total counter-ion concentration. For SDS, Corrin et al. gave the following equation at 25°C based on the results determined by a spectrophotometric method[76]:

$$\log CMC = -3.249 - 0.458 \log c_i \quad (4\text{-}3)$$

Fuguet et al. obtained a similar equation using a different method (conductometric measurements) [77]. They found that this equation can accurately predict the CMC of SDS obtained from experimental measurements:

$$\log CMC = -3.230 - 0.486 \log c_i \quad (4\text{-}4)$$

The surface tensions of SDS in MilliQ water and PBS were measured at room temperature (Figure 4-2). It displays the typical surfactant behavior in aqueous solution that lowers the surface tension of water by absorbing at the air-water interface. The reduction of the surface tension of SDS after the addition of PBS was observed. In order to check the accuracy of the measurements, the CMC values of SDS, which was calculated from inflection points in the figure, are listed in Table 1. Compared to the literature data, the CMC value is matched well with that of the literature: the CMC of SDS in MilliQ water is 10.5mM and in PBS is 1.1mM. The surface tensions of collagen solutions in PBS were 72.4mN/m (0.5mg/mL), 72.12mN/m (1.0mg/mL) and 69.43mN/m (2.5mg/mL) respectively, which is close to MilliQ water (72.88mN/m at 20°C). After adding collagen with concentration of 0.5, 1.0 and 2.5mg/mL respectively, a small reduction in the surface tension of SDS in collagen was observed without changing the CMC value. The surface tension of SDBS in water was also conducted and the critical micelle concentration of SDBS in PBS was found at 0.1mM.

Table 4-1. CMC values of SDS determined in salt solution.

Electrolyte concentration (mM)	CMC (mM)				
	SDS[a]	SDS[b]	SDS[c]	SDS[d]	SDS[e]
0	8.08	8.13	10.5		
5	6.09			6.38	7.73
10	4.61			4.65	5.52
15	3.84			3.86	4.53
20	3.27			3.38	3.94
30	2.73	3.12		2.81	3.24
40	2.30			2.46	2.81
50	1.99			2.22	2.53
100		1.33		1.62	1.8
168			1.1	1.28	1.4
200		0.90		1.18	1.29
400		0.55		0.86	0.92
500		0.52		0.77	8.25

a All values of CMC are from data in ref.[77], SDS in phosphate buffer (pH 7.0).
b Value of CMC is from data in ref. [86], SDS in the presence of NaCl . The micelles in these solutions exist in the presence of monomeric detergent ions of concentration equal to the added electrolyte concentration plus the CMC. This only has an appreciable effect on the results for the solution containing no added salt.
c Value of CMC is from our data measured by surface tension.
d Calculated by equation (4-3)
e Calculated by equation (4-4)

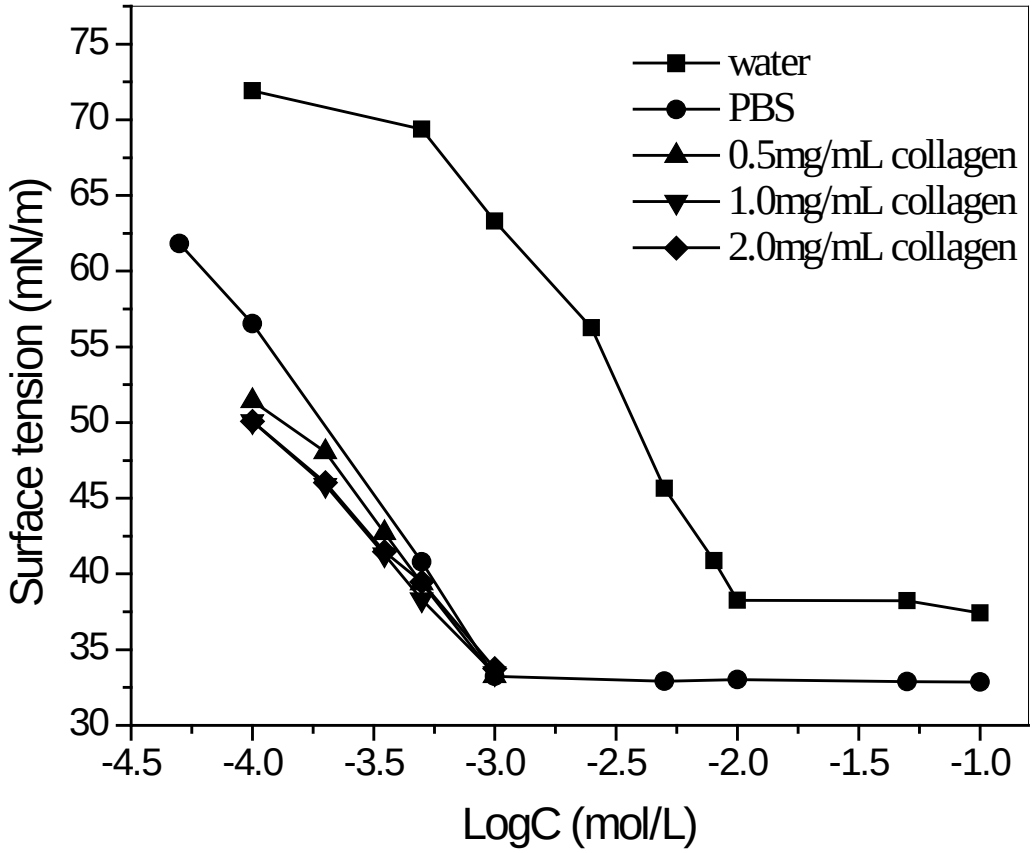

Figure 4-2. Surface tension of SDS in water, SDS in PBS and SDS in PBS mixed with collagen as a function of the concentration.

Turbidity Measurements

The effects of surfactants on the collagen fibril formation measured by turbidimetric method are shown from Figure 4-3 to Figure 4-6. In high concentration of collagen (2.5 mg/mL), the fibrillogenesis rate was accelerated by SDS from 0.1 to 0.5 mM(Figure 4-3). By increasing the concentration of SDS, the fibrillogenesis was significantly promoted and the final turbidity did not change with surfactant concentration. Moreover, the acceleration occurred in both lag and growth phases. Compare to the SDS on accelerating collagen fibril formation, SDBS also promoted the fibrillogenesis rate with increasing concentration from 0.1 to 0.5mM. (Figure 4-4) The early precipitation was also observed before incubation when the concentration of SDBS was higher than 0.1 mM. Since SDBS is more hydrophobic than SDS and has the CMC at 0.1

mM in PBS buffer, it is reasonable that precipitation results from the formation of SDBS micelles. During incubation, collagen fibrillogenesis occurred and the turbidity increased again in the presence of SDBS. Lower final turbidity was observed in high concentration of SDBS which might be resulted from collagen denatuation.

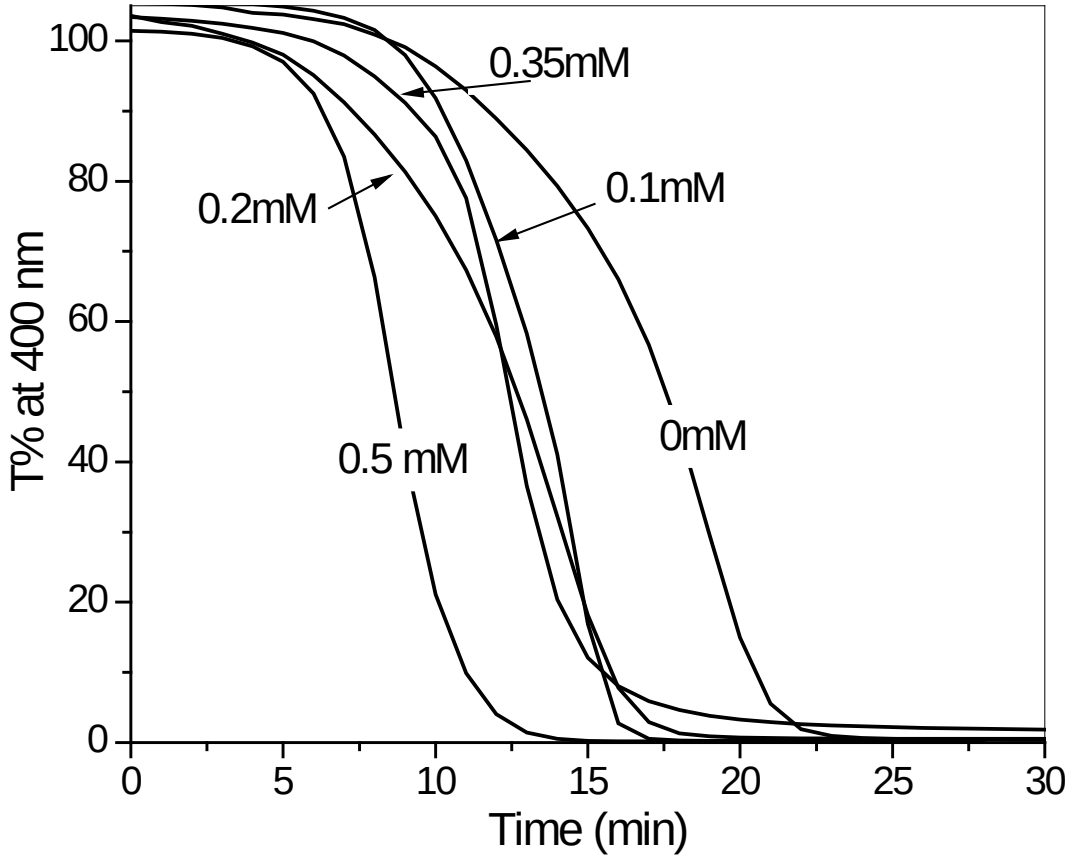

Figure 4-3. Turbidity measurements of collagen gelation (2.5mg/mL) in sodium dodecylsulfonate at the different concentrations. Thermometer temperature was 34°C.

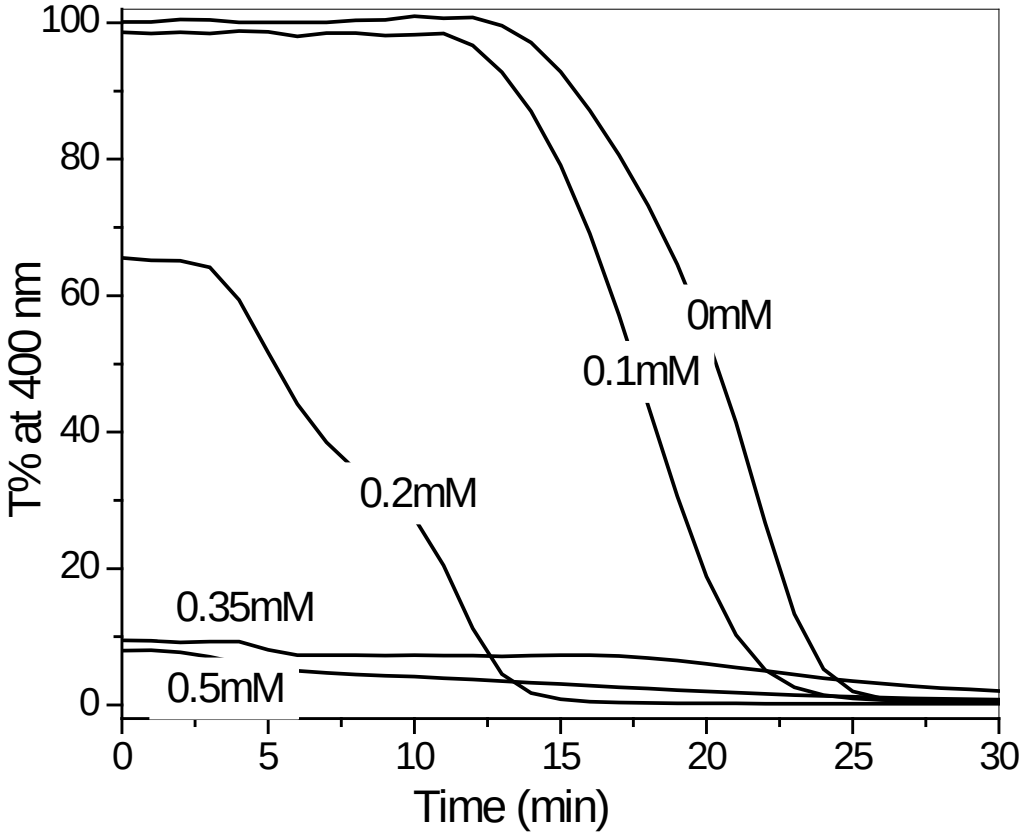

Figure 4-4. Turbidity measurements of collagen gelation (2.5 mg/mL) in sodium dodecylbenzenesulfonate at the different concentrations. Thermometer temperature was 34°C.

The effects of surfactant on collagen fibril formation at collagen concentration of 0.5 mg/mL were also investigated. It was found that SDS accelerated the collagen fibril formation with increasing surfactant concentration from 0.1 mM to 1 mM but the final turbidity was appreciably decreased at high surfactant concentrations. (Figure 4-5) In 1 mM SDS, where the molal ratio of SDS to collagen is 600 considering the molecular weight of collagen of about 300,000 g/mol, the collagen fibril formation occurred at the beginning of 15 minutes and then dissolved. These results indicate that the high concentration of SDS inhibits fibril formation by unfolding the collagen triple helix, even though the incubation temperature, 30°C, was below the body temperature. In the presence of SDBS, the stronger denaturation effect on collagen was observed (Figure 4-6) and collagen molecules could not form fibrils when the molal ratio of

SDBS to collagen was up to 200. At ratios below 200, a decrease on final turbidity was also observed even though acceleration on fibrillogenesis rate occurred. When in the high concentration of collagen (2.5 mg/mL) where the ratio of surfactant to collagen was in the range from 13 to 63, the final turbidity was not noticeably changed. As the molal ratio of surfactant to collagen increased, the inhibition on final turbidity significantly appeared. This inhibition effect on turbidity was also stronger in the presence of more hydrophobic surfactant. Hayashi and Nagai have observed similar results that 1.7 mM SDS inhibited the collagen fibril formation in the concentration of 1.2 mg/mL by denaturing collagen molecules while 0.14 mM SDS promoted fibril formation[71].

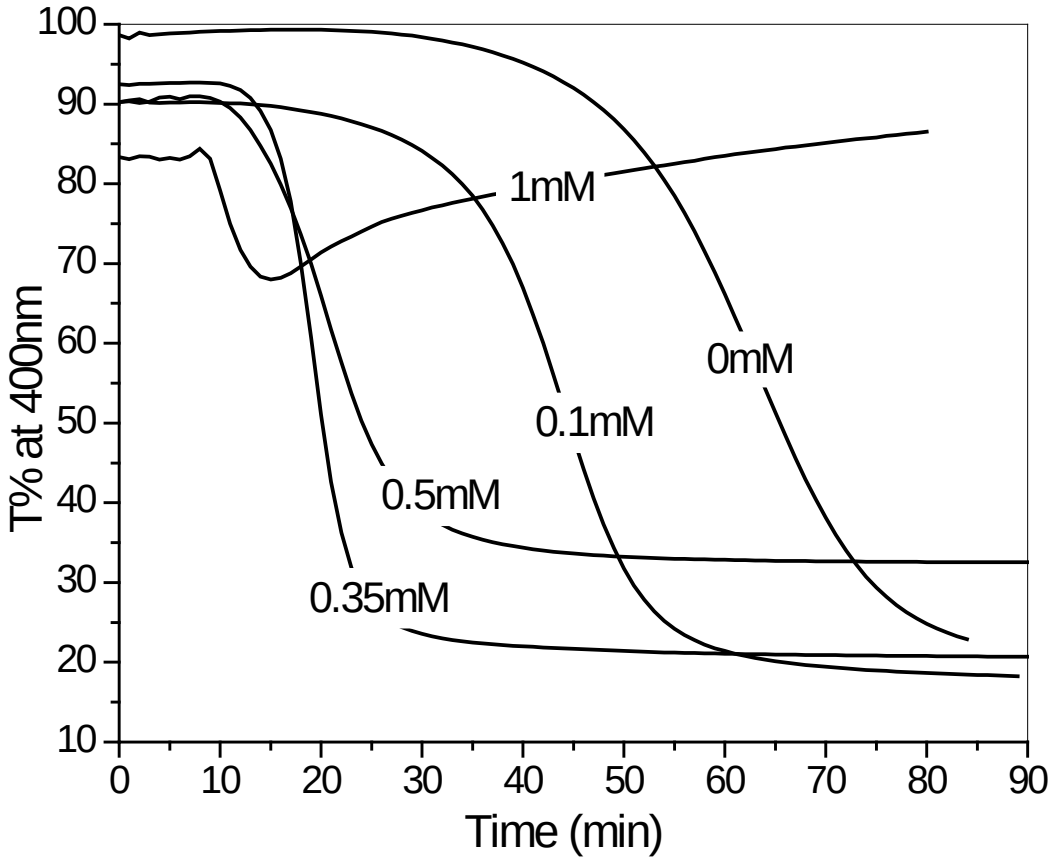

Figure 4-5. Turbidity measurements of collagen gelation in the presence of sodium dodecylsulfonate (SDS). Collagen concentration was 0.5mg/ml, thermometer temperature was 34 °C.

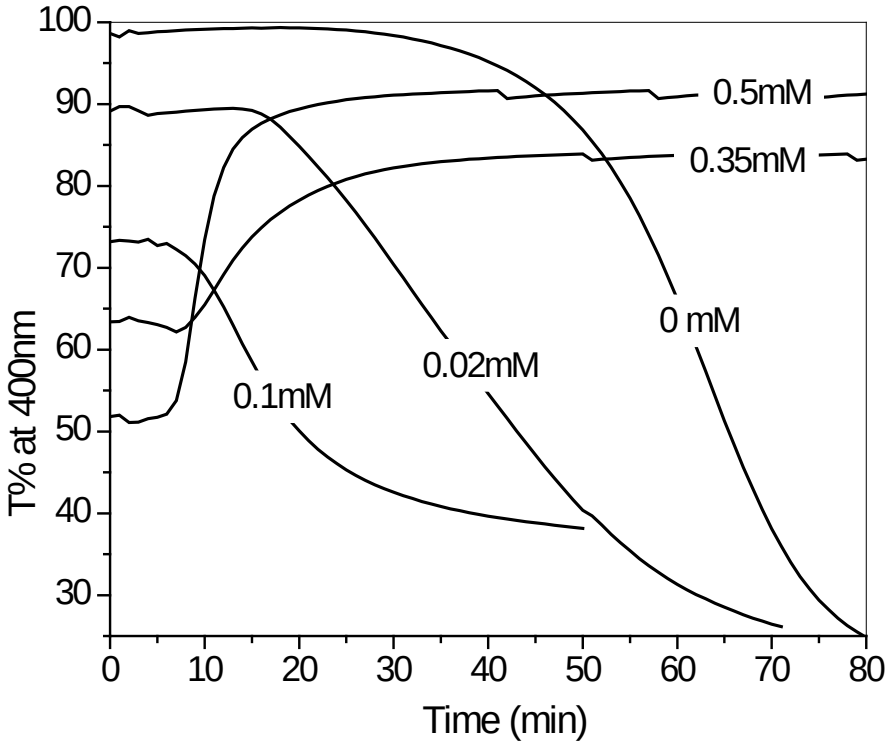

Figure 4-6. Turbidity measurements of collagen gelation (0.5mg/mL) in sodium dodecylbenzenesulfonate (SDBS) at the different concentrations. Thermometer temperature was 34°C.

The Effect of Temperature and Activation Energy

The effects of surfactant on collagen fibrillogenesis under different temperatures were conducted and plotted in Figure 4-7 and 4-8. The increase of temperature accelerated the collagen fibrillogenesis which is consistent with data in Chapter 3, since collagen fibril formation is an endothermic process which is made thermodynamically favorable by large positive entropy of precipitation associated with structural changes. The final turbidity of fibrils did not change with increasing temperature, indicating no inhibition of fibril content was detected. The Arrehenius equation for the effect of temperature on the rate of fibril formation under the surfactants of SDS and SDBS was plotted and activation energies were calculated from the slopes. Without surfactant, the activation energy of fibril formation of type I collagen is 167.6

kJ/mol. By adding 0.1 mM SDS or SDBS, the activation energies are reduced to 153.6 and 114.7 kJ/mol respectively.

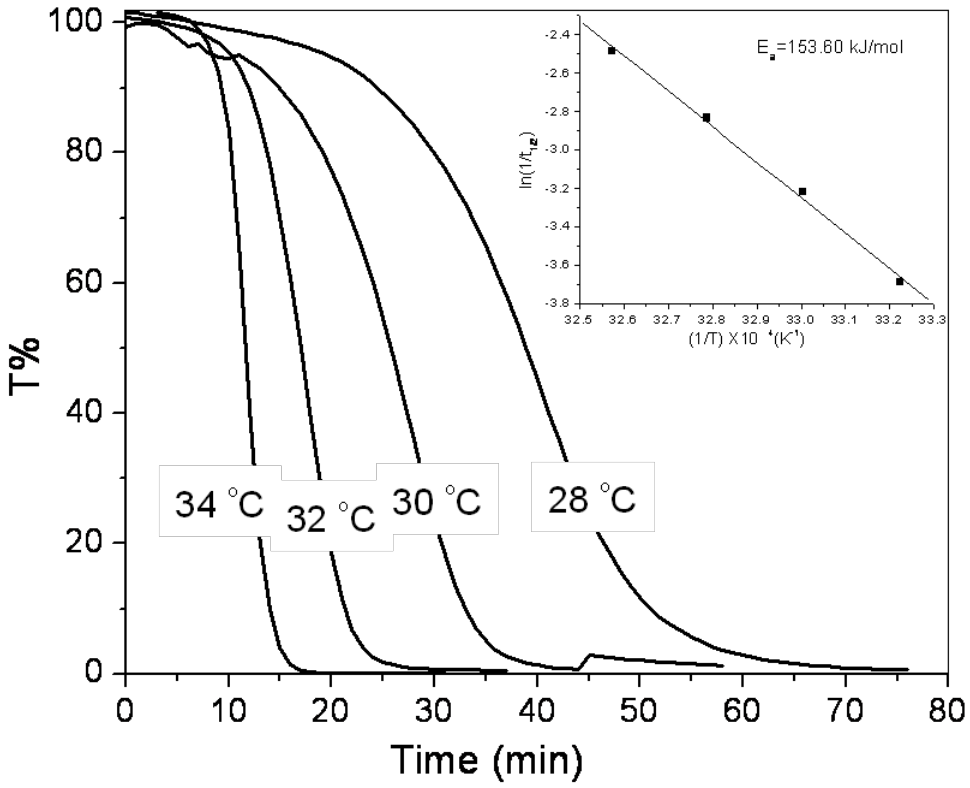

Figure 4-7. Temperature effects on collagen fibril formation in SDS. The concentration of SDS is 0.1 mM, Collagen is 2.5 mg/mL, pH7.4

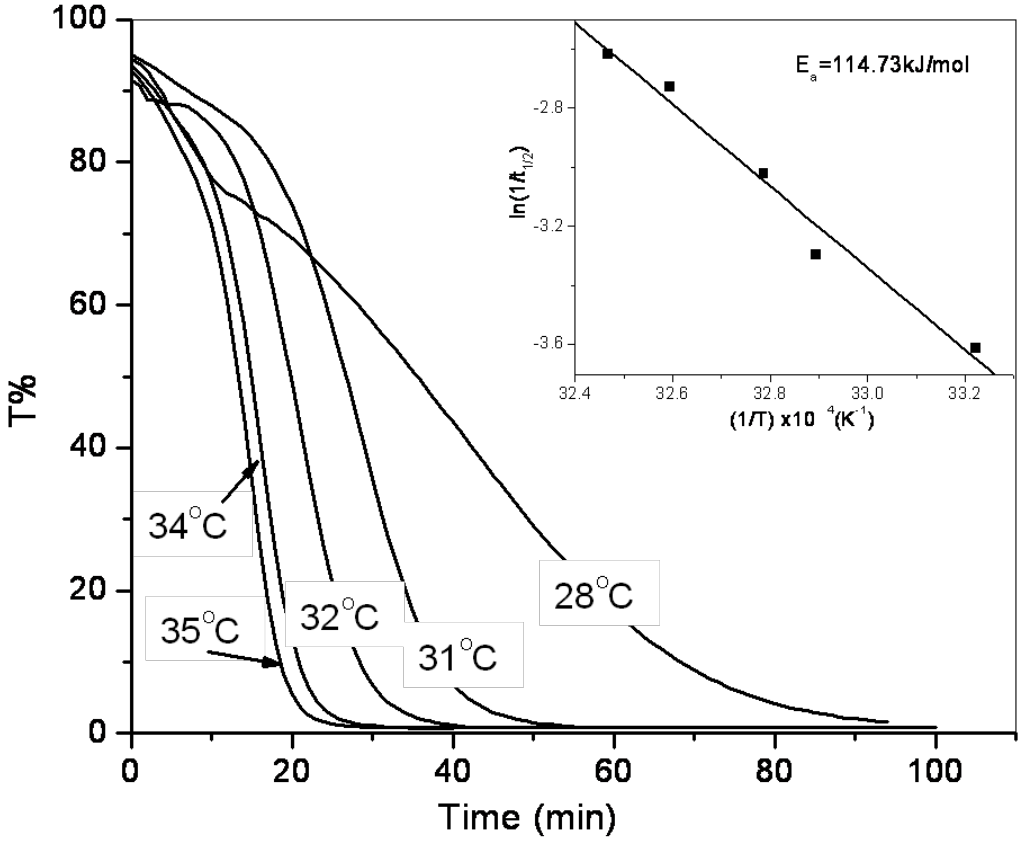

Figure 4-8. Temperature effects on collagen fibril formation in SDBS. The concentration of SDBS is 0.1 mM, Collagen is 2.5 mg/mL. pH 7.4

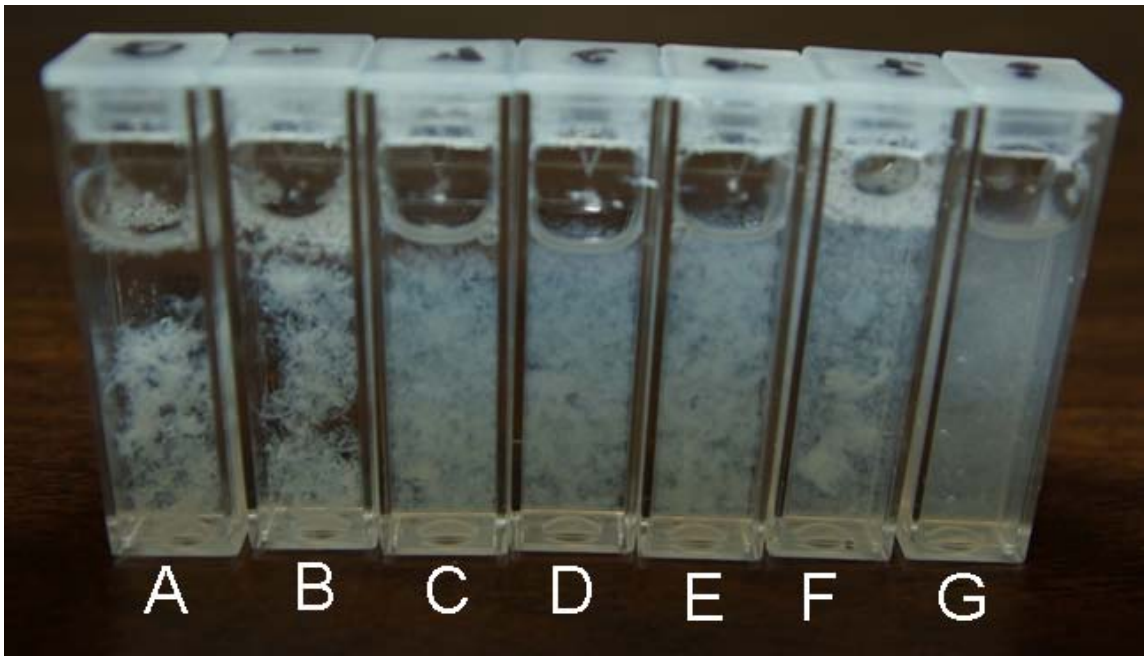

Figure 4-9. Photograph of shaked collagen gels formed in surfactants. A) Collagen fibril bundles formed without surfactant. B) Collagen fibril bundles formed in 0.1 mM SDS. C) Collagen gel clots formed in 0.35 mM SDS. D) Collagen gel clots formed in 0.5 mM of SDS. E) Collagen gel clots formed in 0.1 mM SDBS. F) Collagen gel clots formed in 0.35 mM SDBS. G) Collagen gel clots formed in 0.5 mM SDBS.

Morphology of Collagen Fibrils

Reconstituted collagen fibrils are generally composed of a random mesh of collagen fibrils and more than 95% of excess fluid. It has been observed that the fluid was a result of the casting, and can be expelled out by plastic compression[78]. Except for the fibrils and fluid, insoluble collagen, insoluble random coiled network and the soluble random coiled collagen can also appear depending on the incubation temperature and stability of collagen[73]. In the conditions where collagen was destabilized, the increase of temperature led to fibrils re-dissolving, collagen unfolding and partial denaturation. The appearance of non-fibrillar collagen influences the mechanical properties of collagen gel. In our experiments, we got the similar collagen gels when surfactants were added before fibril formation. However, when the gels were shook, the broke collagen gels presented the different macro-scale morphologies as showed in Figure 4-9. The bundles of fibrils can be directly visualized when no surfactant was added, as well as in the

presence of 0.1mM SDS. However, with increasing concentrations of surfactant SDS and SDBS, the collagen gel clots appeared instead of the fibrils bundles. The difference of shaken gels in the presence of surfactant might be the result of non-fibrillar collagen. The ultrastructure of collagen fibrils with different surfactants were also analyzed by SEM (Figure 4-10). Native fibrils were present in all the samples and non-fibrillar collagen was also observed. The addition of the surfactants made the collagen fibrils more compact due to the appearance of non-fibrillar collagen. In the magnified collagen fibrils in Figure 4-10H, the characteristic D-periodicity was well observed which suggests that surfactants do not change the mechanism of collagen self-assembly into native fibrils.

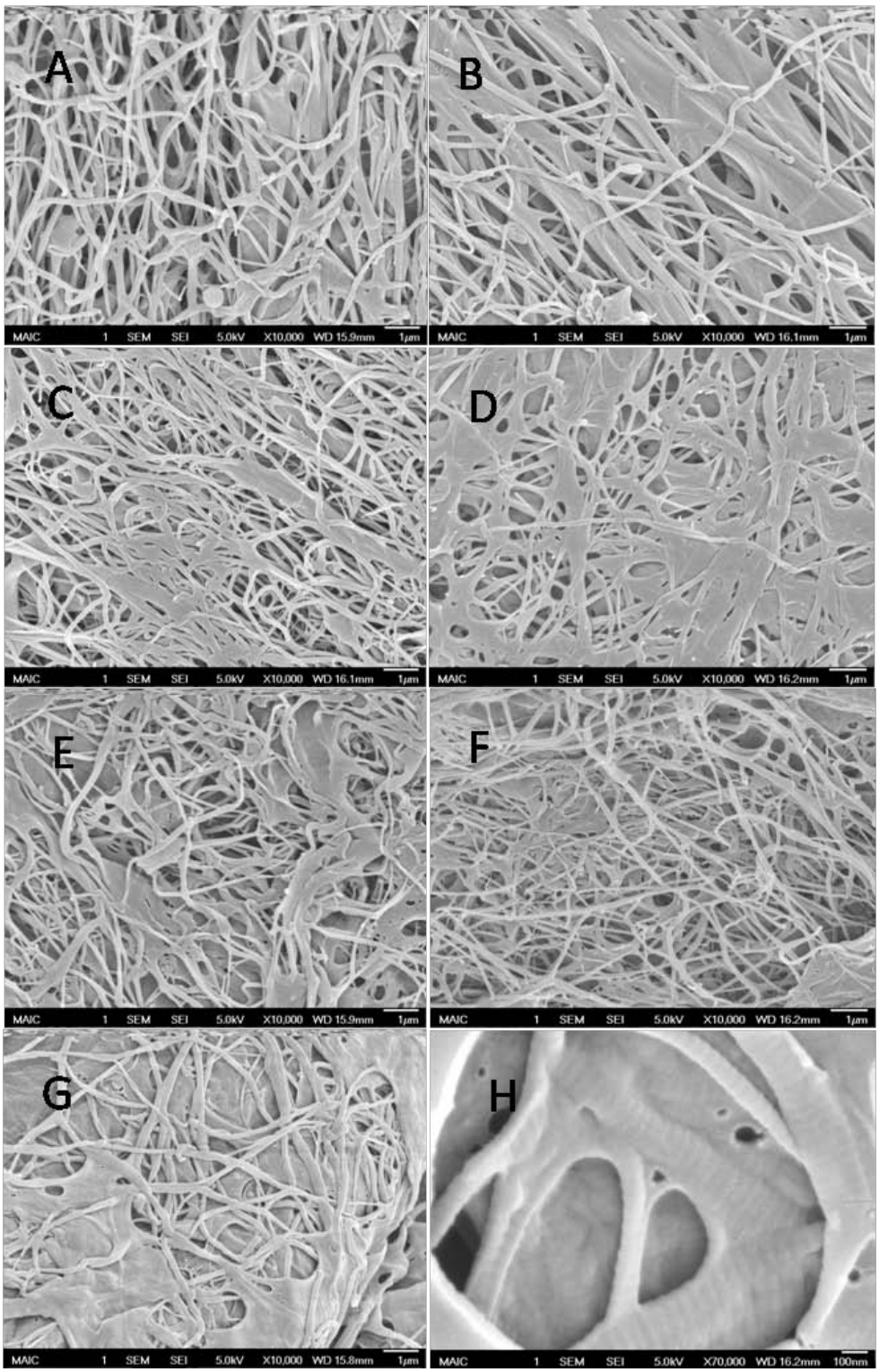

Figure 4-10. SEM images of collagen fibrils formed in the presence of surfactants. A) Fibrils formed in PBS buffer without surfactant. B), D) and F) Collagen fibrils formed in 0.1mM, 0.35mM and 0.5 mM SDS respectively. C), E) and G) Fibrils formed in 0.1mM, 0.35 mM and 0.5 mM SDBS respectively. H)The magnified collagen fibrils formed in 0.5 mM SDS. Scale bars in H 100 nm, others are 1 μm.

Discussion

Interactions between Collagen and Surfactants

The effect of the presence of various electrostatic and hydrophobic surfactants on collagen fibrillogenesis has already been extensively studied in literature[65, 70, 71, 73, 79]. However, how could the interactions influence the collagen fibrils formation is not well understood. It has been reported that the rate of collagen fibril formation was accelerated remarkably in the presence of 0.1 mM SDS or 1-10 mM non-ionic surfactants with polyoxyethylene groups[70]. The acceleration on the lag phase of fibril formation and subsequent acceleration of the growth of collagen fibrils, and fibrillogenesis rate with more hydrophilic polyoxyethene chains suggests the occurrence of interactions between the hydrophilic chains of the non-ionic materials and collagen molecules[70, 80]. The electrostatic and hydrophobic interactions between ionic surfactants and collagen have been reported[70, 72].The interactions between ionic surfactant and collagen depend on the charges of collagen[81]. In high or low pH solution when collagen molecules are highly ionized, the interactions between collagen and ionic surfactant molecules are attributed primarily to the electrostatic attraction between head groups of surfactant and lysine and arginine residues of the collagen molecules. In the condition where collagen molecules are neutralized, e.g. at its isoelectric point, the major interactions between collagen and ionic surfactants are the hydrophobic interactions between hydrocarbon chains of surfactant and hydrophobic amino acid residues of collagen.

In our studies, collagen molecules were dissolved at pH7.4 in PBS, the hydrophobic interactions between surfactants and collagen molecules might be the major one during fibril formation. The existence of variant amino acid side groups on collagen molecules suggests the possibility of interactions between them and small molecules containing hydrocarbon chains or hydrophilic groups. That binding effect regulates the collagen fibril formation and fibrils

structure. Through the study of surface tension of SDS, only weak interactions between the surfactant and the collagen were seen before fibrillogenesis, despite the fact that the SDS/collagen molal ratio from the solution concentrations is relatively high (12 or greater). These results are consistent with results from the literature which observed no interaction between collagen and nonylphenol poly(oxyethylene) in aqueous solution[72] or between collagen and pluronic PE 6800 in PBS solution[82]. Before collagen fibrillogenesis, collagen molecules are hydrated, the helical structure of collagen around H_2O can not be interrupted by the surfactant. However, during collagen fibril formation where the structured water molecules around collagen are broken, the exposed amino acid side groups interact with nearby surfactants or collagen. The turbidity measurements in 2.5 mg/mL collagen indicate that the interaction was more related to the hydrophobic property since SDBS has a stronger acceleration effect than SDS.

Even though surfactants accelerated the fibrillogenesis rate both in the lag and growth phase in the high concentration of collagen (2.5mg/mL), the denaturation effects of surfactants on low concentration of collagen have also been observed. The adsorption of surfactants on collagen destabilizes the collagen triple helix. Collagen molecules within the fibril are substantially more thermally stable than the same molecules in diluted solution[83, 84]. Collagen molecules in solution also undergo unfolding close to the body temperature of the species from which the molecules are extracted[85]. It is possible that denaturation of collagen molecules in the presence of surfactant occurred which influences the kinetics of fibril formation. In fact, the remarkable acceleration effect of surfactants on collagen fibril formation suggests there are some specific interactions between surfactants and collagen molecules. Since a very small amount of surfactant can greatly affect collagen fibril formation, surfactant molecules may bind strongly to

collagen molecules during fibril formation as in the case of most globular proteins[69]. The morphology studies indicate the non-fibrillar collagen appeared and increased with increasing surfactant concentration. Moreover, collagen molecules are completely denatured at a high ratio of surfactants, where no fibrils were formed. It is possible collagen molecules which are bound by ionic surfactants are more easily denatured and the denatured collagen molecules do not take part in forming native fibrils.

Conclusion

Self assembly of Collagen molecules into fibrils is an endothermic process and it has been thought that hydrophobic interactions play the dominant role. We intended to introduce ionic surfactant to collagen fibril formation. At room temperature, there was no significant appearance of interactions between surfactants and collagen since collagen molecules were fully hydrated and neutralized. As the temperature increased, we propose that surfactant molecules bind to collagen which accelerated the fibril formation. The strong binding occurred through hydrophobic interactions between surfactants and collagen molecules by forming collagen-surfactant complexes. Those collagen molecules bound by surfactants are possibly denatured and do not form the native fibrils.

CHAPTER 5
PH EFFECTS ON COLLAGEN FIBRILLOGENESIS IN VITRO: ELECTROSTATIC INTERACTIONS AND PHOSPHATE BINDING

Introduction

As the primary structural protein in connective tissues, type I collagen is a major component of tendon, cartilage, ligament, skin, cornea and bone. It forms insoluble networks of fibrous bundles which act as scaffolding, providing shape and support in the body. Moreover, it is capable of being mineralized in vertebrate tissues, offering mechanical support and strain energy storage in bone[44, 87, 88]. As a potential biomimetic material, design and mimicry of mineralized collagen has attracted much attention[89-92]. Comprehensive information about the mechanism of collagen fibrillogenesis is required with respect to improving the design of collagen-based materials, as well as exploring their functional properties in biological systems.

Type I collagen is a triple helix consisting of three left-handed polyproline peptide chains intertwined in a right-handed manner. Self assembly of soluble collagen into fibrils with characteristic D-periodicity in vitro was observed more than 50 years ago[93]. The D-periodicity is described as consecutive domains consisting of 234 amino acid residues, and can be observed via electron microscopy[94] and X-ray diffraction[95, 96]. It has been found that the conditions for the formation of native type fibrils are in the pH range of 5.0-8.5, ionic strength between 0.1 and 0.8, and temperatures between 15 and 37°C[40, 49, 97, 98]. Subsequent studies also indicate pH, temperature, ionic strength, ion species, surfactants, saccharides, and the removal of the nonhelical ends of collagen have a strong influence on modifying collagen fibril formation[49, 65, 99, 100]. Mechanisms of forming D-periodicity during fibril formation are still not well understood. Collagen fibrillogenesis is a thermally driven process which is favored by a large positive entropy contribution due to the displacement of structured water around collagen molecules[64]. Hydrophobic interactions between non-polar regions of adjacent molecules are

the predominant effect governing collagen fibril formation due to the negative temperature coefficient of collagen solubility and the endothermic nature of in vitro fibrillogenesis[64, 101]. It has also been reported that the collagen fibrillogenesis is driven by hydrogen bonding between polar residues through direct measurement of forces between collagen molecules[102]. Early electron microscopic investigations and theoretical models indicate the highest polar and hydrophobic contact is achieved when molecules were shifted against each other by the distance of 234 amino acid residues[103]. In fact, the ionized residues along collagen regulate the stability of the collagen triple-helix; the pH of the medium affects the stability of collagen fibrils, as well as the diameter and the D-periodicity of fibrils[65, 104-108]. However, the effect of electrostatic interactions on collagen self-assembly is still unclear. It has been reported that divalent phosphate ions binding on collagen molecules appear to form salt bridges within regions of high excess positive charge in collagen fibrils[109]. Charges on ionizable groups whose charging is pH-dependent take part in electrostatic interactions. The salts which bind to the collagen might also affect the electrostatic interactions. The occurrence of salt bridges indicates that the effect of pH on fibrillogenesis is not due to electrostatic interactions alone.

Therefore, in order to choose proper conditions to create the desired morphology of collagen fibrils and study the underlying mechanism of collagen fibrillogenesis, the kinetics of fibril formation and the subsequent morphologies of fibrils were examined under the different pH conditions of the medium. Further, the surface charge of soluble collagen as a function of pH was measured and correlated with the fibrillogenesis process. The results were analyzed in relation to the possible intermolecular interactions.

Zeta Potential and Electrical Double Layer

Electrical Double Layer

It is well known that most solid surfaces in aqueous are electrostatic charged, i.e., an electrical surface potential. When the liquid contains a certain amount of ions, the electrostatic charges on the solid surface will attract the counterions in the liquid. Thus, an electrical double layer is formed in the region of the solid-liquid interface. As illustrated in Figure 5-1, this double layer consists of two layers: a stern layer that includes counter-ions bound relatively tightly to the surface, normally about several angstroms thick. Because of the electrostatic attraction, the counter-ion concentration near the solid surface is higher than that in the bulk liquid far away from the solid surface. The concentration of co-ions is lower than that in the bulk liquid due to the electrical repulsion. So there is a net charge in the region close to the surface. From the stern layer to the uniform bulk liquid, the net charge density gradually reduces to zero. Ions in this region are less affected by electrostatic interactions and are mobile. This layer is called the diffuse layer. The thickness of the diffuse layer depends on the concentration of bulk ions and the electrical properties of the liquid and usually ranging from several nano meters to several micrometers. The boundary between the compact layer and diffuse layer is called as shear plane. The electrical potential at the shear plane is called the zeta potential, ζ and can be measured experimentally since the electrical potential at the solid-liquid interface is difficult to measure directly.

The electric potential Ψ(X) in the diffuse layer decays over the distance of the order of the Debye length 1/κ from the shear plane. For a general electrolyte condition, κ is defined by

$$\kappa = \left(\frac{N_A e^2}{\varepsilon_0 \varepsilon_r k_B T} \sum_{i=1}^{n} C_i Z_i^2\right)^{1/2} \quad (5\text{-}1)$$

where ε_r is the relative permittivity (dielectric constant) of the solution, ε_0 is the permittivity of free space, k_B is the Boltzmann constant, T is the absolute temperature, e is the elementary charge, NA is Avogadro's number, C_i is the molar concentration of the i-th ion (mol/L), and Z_i is the charge number of the i-th ion.

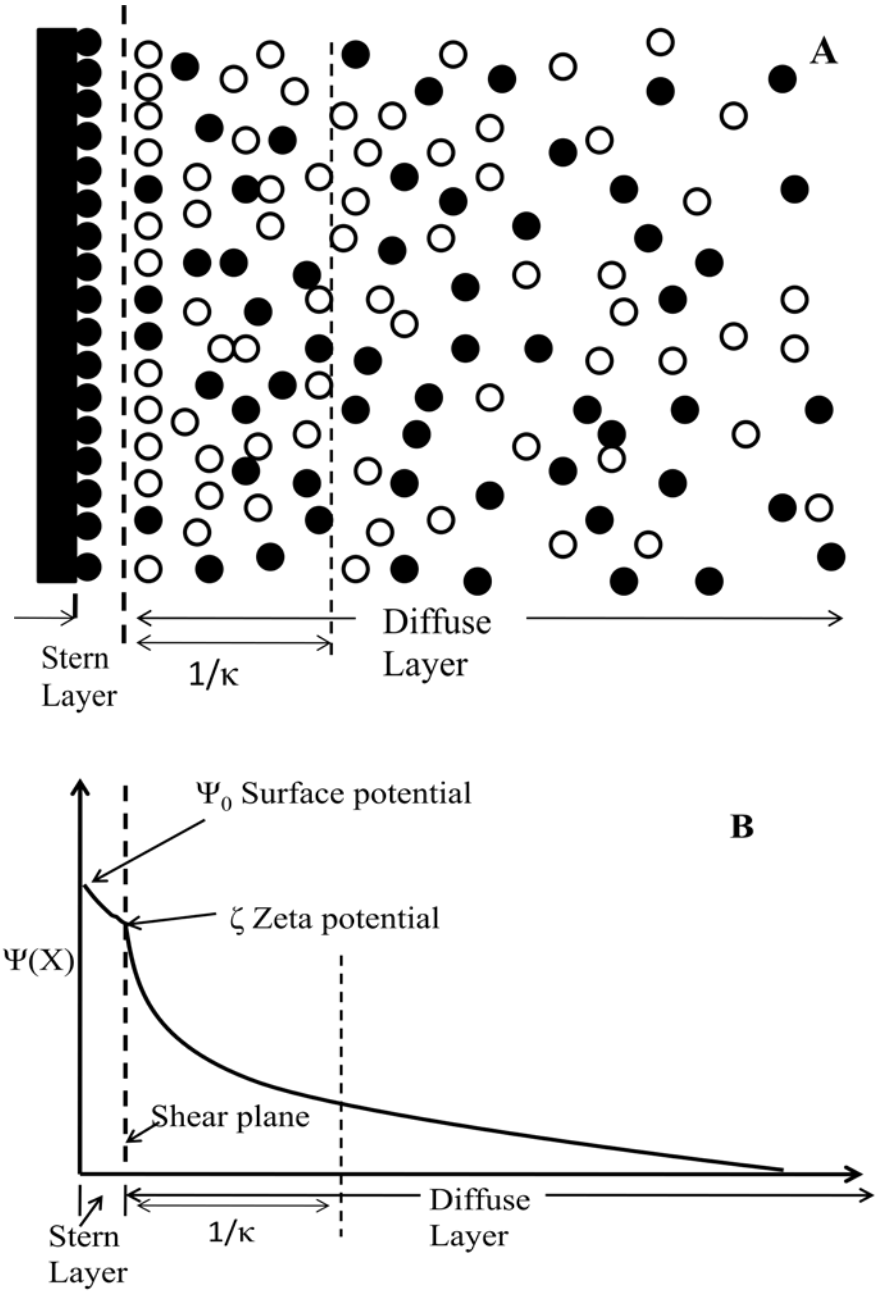

Figure 5-1. Illustration of an electrical double layer at a solid-liquid interface. A) ion distribution; B) electrical potential distribution

In an electric field, such as in microelectrophoresis, each particle and its most closely associated ions move through the solution as a unit, and the potential at the surface of shear plane between this unit and the surrounding medium is known as the zeta potential. Zeta potential is therefore a function of the surface charge of the particle, any adsorbed layer at the interface, and the nature and composition of the surrounding suspension medium. It can be experimentally determined and, because it reflects the effective charge on the particles and is therefore related to the electrostatic repulsion between them, the zeta potential has proven to be extremely relevant to the practical study and control of colloidal stability and flocculation processes.

Zeta Potential

Zeta Potential is the electrical potential that exists at the "shear plane" of a particle, which is some small distance from its surface. Zeta Potential is derived from measuring the mobility distribution of a dispersion of charged particles as they are subjected to an electric field. Mobility is defined as the velocity of a particle per electric field unit and is measured by applying an electric field to the dispersion of particles and measuring their average velocity. Depending on the concentration of ions in the solution, either the Smoluchowski (for high ionic strengths) or Huckel (for low ionic strengths) equations are used to obtain the Zeta potential from the measured mobility.

Smoluchowski's Equation

The electrophoretic mobility μ of a particle moving with a velocity U in an electrolyte solution in an applied electric field E is given by the ratio U/E. The most widely employed formula relating the electrophoretic mobility μ of a particle to its zeta potential ζ is Smoluchowski's formula,

$$\mu = \frac{\epsilon_r \varepsilon_0}{\eta} \zeta \qquad (5\text{-}2)$$

Here, ε_r and η are the relative permittivity and the viscosity of the electrolyte solution, respectively, and ε_0 is the permittivity of a vacuum. The zeta potential ζ is defined as the potential at the plane where the liquid velocity μ relative to the particle is zero. This plane is called the slipping plane or shear plane. The slipping plane does not necessarily coincide with the particle surface. Only if the slipping plane is located at the particle surface, does the zeta potential ζ become equal to the surface potential Ψ_0 which happens at low concentration of electrolytes. In the studies, we treated $\zeta = \Psi_0$.

Smoluchowski's equation was derived on the basis of approximations. This equation is valid for large particles irrespective of their shape and the dimension of the particle is much larger than the Debye length $1/\kappa$, and the surface of the particle can be considered to be locally planar. For a sphere with radius α, this condition is expressed by $\kappa\alpha >> 1$.

Hückel's Equation

The electrosphoretic mobility of very small sphere ($\kappa\alpha << 1$) is given by Hückel's equation:

$$\mu = \frac{2\varepsilon_r \varepsilon_0}{3\eta}\zeta \tag{5-3}$$

The difference between Smoluchowski's equation and Hückel's equation is by a factor of 2/3. Most electrolyte ions in the double layer experience an undistorted original field for the thick double layers ($\kappa\alpha << 1$). However, for the thin double layers ($\kappa\alpha >> 1$), most electrolyte ions in the double layers experience a distorted field. This is the reason why Smoluchowski's equation differs from the Hückel equation by 2/3.

For a cylindrical particle, the electrophoretic mobility is related to the orientation of the particle with respect to the applied electric field. When the cylinder is oriented parallel to the applied electric field, its electrophoretic mobility μ is given by Smoluchowski's equation (5-1). When the cylinder is oriented perpendicularly to the applied field, then the mobility depends not

only on ζ but also on the value of κα. It has been showed that f(κα) for a cylindrical particle of radius α oriented perpendicularly to the applied field is given below:

$$\mu_{\perp} = \frac{\varepsilon_r \varepsilon_0}{\eta} \zeta f(\kappa\alpha) \tag{5-4}$$

With

$$f(\kappa a) = \frac{1}{2}\left[1 + \frac{2}{\left[1+\frac{2.55}{\kappa\alpha\,(1+\exp\,(-\kappa\alpha))}\right]^2}\right] \tag{5-5}$$

As κα→∞, f(κα)→1 and equation 5-4 gives Smoluchowski's equation, while κα→0, f(κα)→1/2. Even though, the collagen molecule has cylinder shape which is about 300 nm long and 1.5nm in diameter as reported, the collagen in aqueous solution are relatively flexible[110] and we are going to treat as particle and use Smoluchowski's equation for the measurements.

Materials and Methods

Materials

Purified type I pepsin-treated adult bovine dermal collagen (97%, with the remainder comprised of type III collagen) dissolved in 0.012N hydrochloric acid was purchased as a solution with concentration of 2.9 mg/ml (PureCol®, INAMED, Inc., Fremont, CA). 10-fold concentrated phosphate buffered saline (PBS) pH 7.4 was purchased from Sigma.

Turbidity Measurements of Fibrillogenesis

To produce collagen fibrils, the chilled type I collagen solution was mixed with 10-fold PBS at the ratio of 4:1 v/v on ice. The pH of each solution was adjusted by adding enough 0.1 M NaOH to reach the desired pH, resulting in a final concentration of 2.1 mg/ml collagen in buffer solution with 18 mM sodium phosphate and 283 mM sodium chloride. The samples were then sealed in 1.5 ml vials and thermostated at 30 °C. The degree of fibril formation with incubation time was recorded by measuring the absorbance at 400 nm using a UV-Vis spectrometer (Perkin-

Elmer Lambda 800 UV/Vis spectrometer, Fremont, CA), equipped with a thermostat cell holder, and maintained at the desired temperature by water circulation.

Electron Microscopy of Collagen Fibrils

The collagen fibrils with D-periodicity were viewed by transmission electron microscopy (TEM; TEM 200CX, JEOL) using an accelerating voltage of 80 kV. TEM samples were prepared by placing the collagen suspensions on copper grids with 200 mesh size and removing excess water by placing a piece of filter paper at the edge of the grid. Then, the fibrils were negatively stained with 1% phosphotungstic acid solution at pH 7.4 for 15 seconds. The stained grids were rinsed with MilliQ water (deionized water, R=18 MΩ cm; Millipore Billerica, MA) and air dried. The collagen fibrils were also examined by scanning electron microscopy (SEM, JEOL, JSM 6400). The freeze dried collagen samples were mounted on stub and carbon coated. The morphologies ware observed at an accelerating voltage of 15 kV.

Image Analysis of Fibrils from TEM

Image analysis of collagen fibrils was performed using NIH ImageJ software version 1.38 developed at the National Institutes of Health (Bethesda, MD). For each sample, at least five TEM images were randomly captured with magnification of 20,000 and at least 30 different fibrils were selected from each image. The fibril size was measured to generate histograms of fibril frequency vs. fibril diameter with x-axis representing the fibril diameter and y-axis representing the number of fibrils in each interval. The D-periodicity of fibrils was also estimated from the TEM images. To obtain average D-periodicities, 150 measurements were taken for each fibrillogenesis condition and averaged. Each measurement consisted of averaging 5 periodicities on a fibril.

Zeta Potential Measurement of Collagen Solution

The determination of zeta (ζ) potential was performed using a Brookhaven ZetaPlus. A solution of type I collagen was diluted to 0.5 mg/ml in 12 mM HCl with MilliQ water and sonicated for 5 min. The pH of the solution was measured with pH paper and adjusted to the desired value within the range of 3 to 11 by adding 0.1 M NaOH. The zeta potential measurement was carried out at 17 ºC immediately after pouring 2 mL of freshly prepared solution into a plastic cuvette in order to avoid gel formation. Zeta potential was calculated using the Smoluchowski's equation.

Results

Turbidity Measurement at Different pH

The kinetics of type I collagen fibrillogenesis was determined by turbidity measurement. As shown in Figure 5-2 the turbidity vs. time curves of collagen fibrillogenesis were sigmoidal curves with a lag phase before the onset of the turbidity increase and a plateau phase after the growth phase. In our study, it takes more than one day to achieve completion of fibrillogenesis due to the relatively high concentration of ions while a short time is needed in one fold PBS[49, 56]. An apparent retardation in growth phase, as evidenced by an intermediate plateau, was found from pH 6.9 to pH 9.2 and the highest fibrillogenesis rate and optical density was achieved at pH 9.2. At low pH (pH 6.5) and high pH (pH10.5), where fibril formation was strongly inhibited, the fibrillar gel was of relatively weak strength.

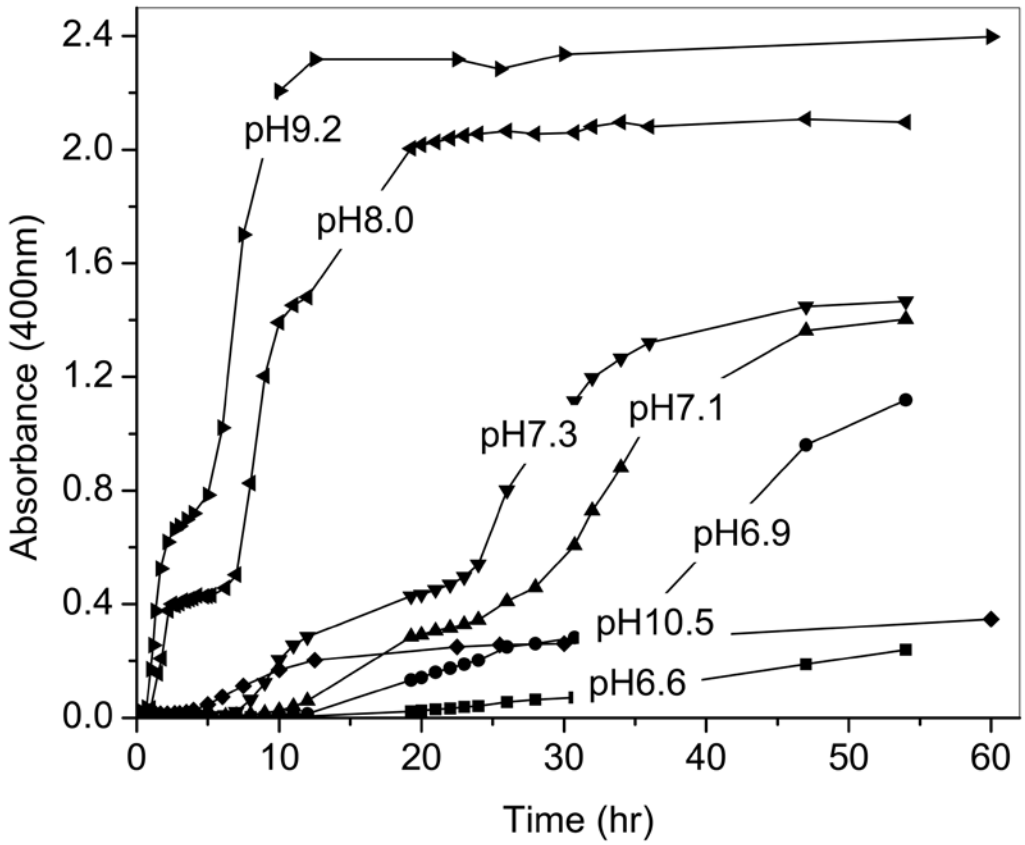

Figure 5-2. Turbidity measurements of collagen fibrillogenesis at different pH. Collagen concentration is 2.1 mg/ml in 18mM phosphate, 283 mM sodium chloride.

Fibril Morphologies

The morphologies of collagen fibrils varied widely depending on the pH condition. Fibrils with characteristic D-periodicity were present in TEM images (Figure 5-3). Fibrils with variable size were formed at low pHs, where in the presence of the large fibrils, many small fibrils with no D-periodicity were detected. With increasing pH, the fibrils were more uniform and interwoven into a network. SEM data were consistent with TEM images (Figure 5-4). When fibrillogenesis was highly inhibited, in the range from pH 6.0 to pH 6.9, the gels were composed of more nonfibrillar collagen. The more highly fibrillogenesis was inhibited, the greater the amount of nonfibrillar collagen. From pH 7.1 to pH 10.0, no apparent difference was found in SEM results.

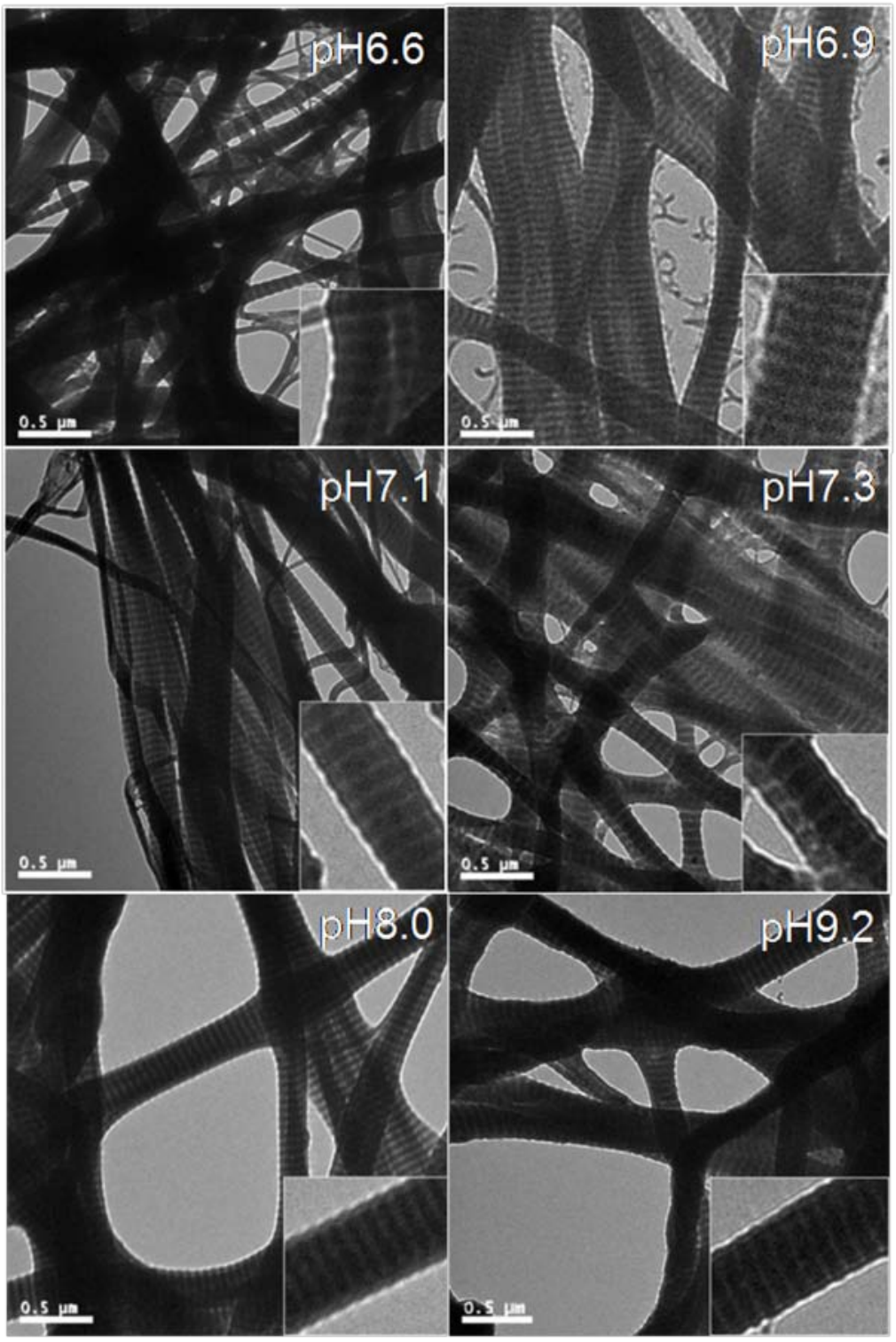

Figure 5-3. TEM images of self-assemble collagen fibrils after three days of fibrillogenesis. The inserts in the lower right hand corner of each image show a magnified view of a single fibril to highlight the banding pattern. Scale bar 500 nm.

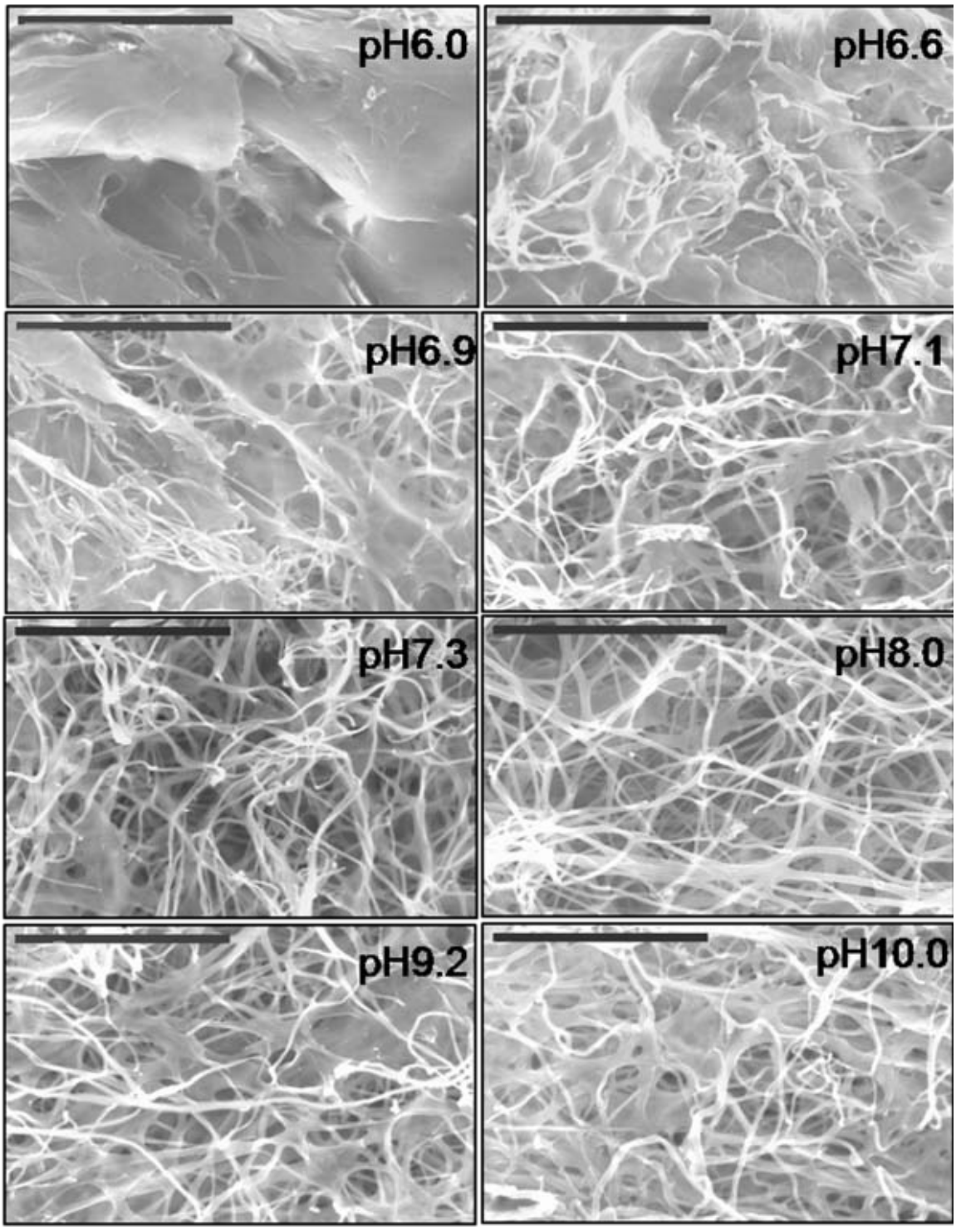

Figure 5-4. SEM images of collagen fibrils obtained in different pH conditions. The fibrils form branched networks with non-fibrillar collagen. Scale bar is 10μm for all the images.

Fibril diameter distributions measured from TEM images are summarized in Figure 5-5 and only fibrils with size larger than 45 nm are counted. No data were collected at pH 6.0 for one day since the fibrils can not be visualized. Small fibrils with diameter approximately 85 nm were obtained at pH 6.6 after three days of fibrillogenesis. The final fibrils have a constant diameter of approximately 200 nm at pHs between 6.9 and pH 8.0 in spite of the remarkable difference in the fibrillogenesis rate. An increase of diameter as a function of time was found at pHs between 6.9 and 7.3 while no obvious change in fibril size was found at pH 8.0 since the fibrillogenesis was finished within one day.

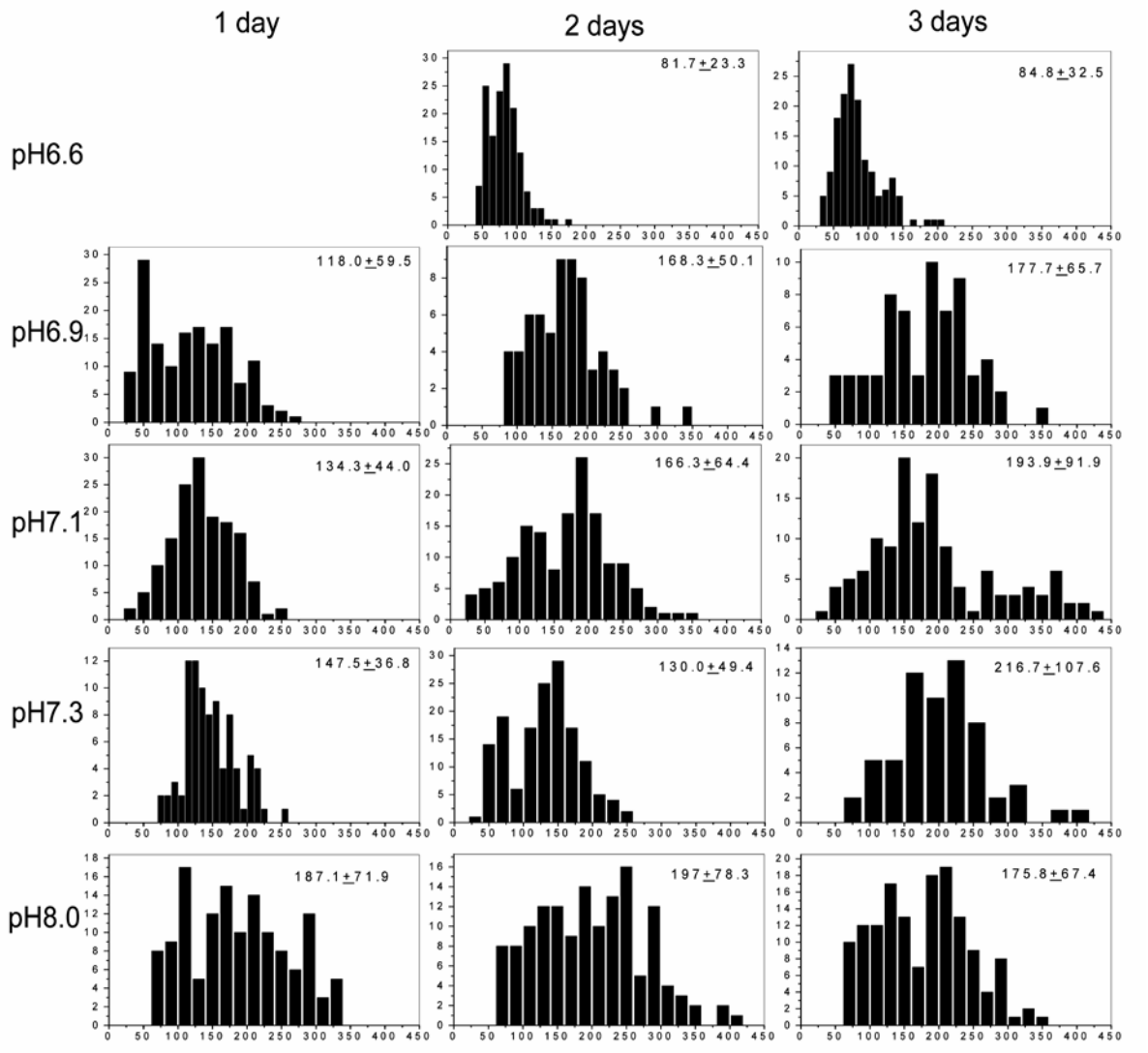

Figure 5-5. Histograms of diameter distribution from pH 6.6 to 8.0. X-axis is diameter in nm, Y-axis is the frequency. Average diameters and standard deviations are in unit of nm.

D-Periodicity Measurements

It is worth measuring D-periodicity of reconstituted fibrils since the presence of native D-periodicity is believed to be important for the mechanical and biological functions of collagenous matrix[111, 112]. Fibrils with native D-periodicity also play an important role in mineralization[112]. The reported D-periodicity is near 67.0 nm for wet tissues and 64.0 nm for air dried samples[113]. Skin tissues have a banding length of 65 nm in the wet state[114]. As summarized in Table 5-1, the average D-periodicity after three days of fibrillogenesis was

approximately 62 nm which matches well with native D-periodic banding length since our samples are dehydrated collagen fibrils reconstituted from calf skin. Two unusual D-periodicities appeared at pH 7.1 after one and two days, which had an average D-periodicity of 50 nm and 54 nm, respectively.

Table 5-1 D-periodicity of collagen fibrils at various pHs and fibrillogenesis times.

pH	**D-periodicity (nm)**		
	One day	Two days	Three days
6.9	60.4±7.8	64.9±3.8	62.1±5.7
7.1	50.5±4.5	54.3±9.1	62.3±6.0
7.3	65.8±7.6	64.0±6.7	62.2±3.6
8.0	62.4±5.3	62.5±5.1	61.6±4.4

Electron micrographs were taken at a constant magnification of 37,000. Each value in the table is the mean ± standard deviation for 150 D-periodicity measurements.

Surface Charge Measurement

To study the electrostatic interactions of collagen during fibrillogenesis, we measured the zeta potential of collagen molecules in aqueous solution. Collagen molecules are less soluble at the isoelectric point (pI) and therefore favor fibril formation. Collagen is reported to have an isoelectric point (pI) of pH 9.3, which was determined in the absence of other electrolytes[115]. However, it has been found that the pI was affected by adsorption of ions. Jackson and Neuberger observed the shift of the isoelectric point to lower pH with increasing ionic strength due to the preferential binding of the anions of aldolase in gelatin[116]. Freudenberg et al. [117]found a shift from pH 7.5 to 5.3 with increasing ionic strength of KCl while, in the presence of $CaCl_2$, the isoelectric point shifts to more basic pH. The shift of pI in different electrolyte conditions indicates it is difficult to quantify the surface net charge directly. As shown in Figure 5-6, the pH corresponding to the pI of soluble collagen was 9.2 in 12 mM of NaCl which is consistent with the pI in the absence of salts[116]. However, when 10 mM Na_2HPO_4 was added, the pI shifted to pH 7.5. Since in zeta potential measurement the surface charge is measured at

the slip plane, the shift of pI with added salts might be due to the preferential adsorption of phosphate ions to the surface of collagen.

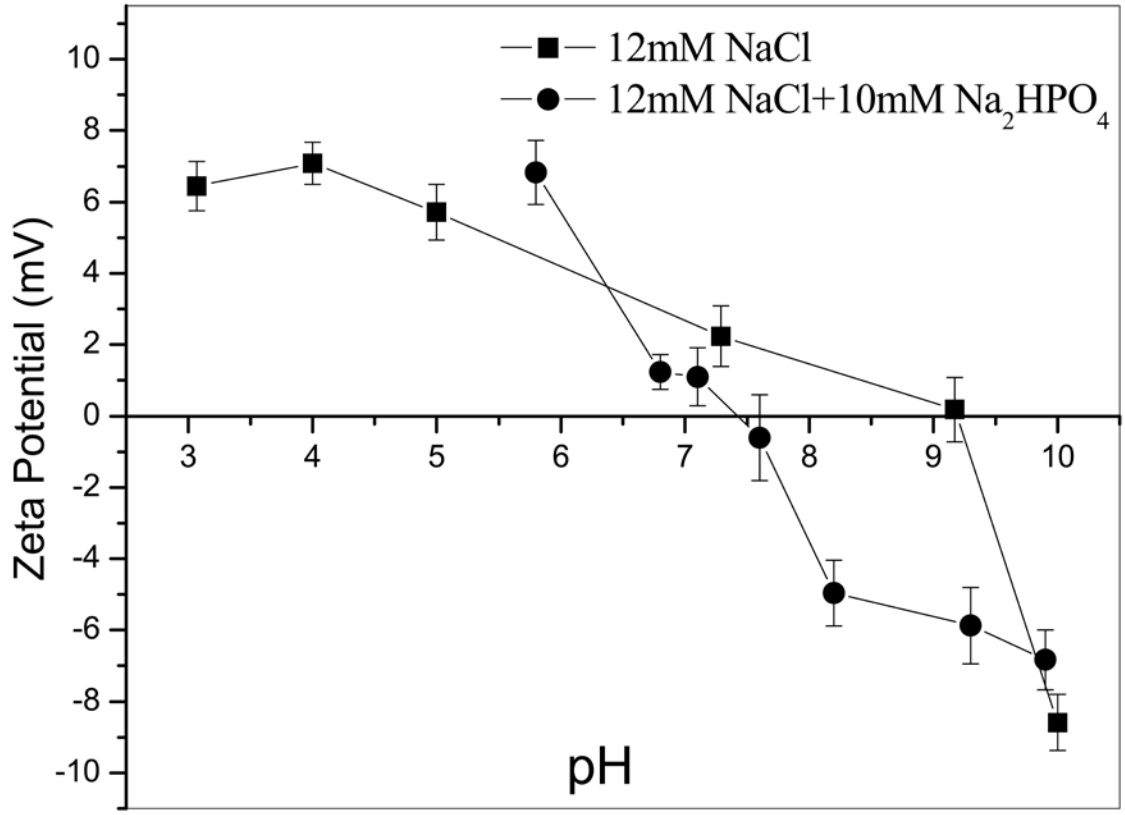

Figure 5-6. Zeta potential measurement of surface charge of soluble collagen as a function of pH.

Discussion

Collagen Fibrillogenesis

The growth of collagen fibrils in vitro is a time-dependent process. When monitored by changes in turbidity, it consists of three major phases: a lag phase, in which there is no change in turbidity; a growth phase, when turbidity rapidly increases; and a plateau phase where turbidity stops increasing. Ultrastructural studies of the lag and early-growth phase using laser light scattering and atomic force microscopy have revealed the fibril formation is a multistep process[52, 62], where a number of different intermediates are formed during the early-growth

phase. These ultrastructural studies have further suggested that addition of these intermediate to the ends of microfibrils results in linear growth, while lateral growth occurs through fusion of microfibrils. These two processes appear to occur simultaneously. In our study, the process of how collagen molecules self-assemble into fibrils was well observed by the combination of turbidity measurement and morphology examination. In the turbidity measurement, lag, growth and plateau phases are observed from pH 6.6 to pH 9.2. Further examination of fibril size indicated that obvious lateral growth occurred during the growth phase, as evidenced by either the increase in average diameter with time or a shift in the distribution of diameters. Surprisingly, an inhibition in the growth phase was observed as an intermediate plateau during growth for some fibrillogenesis conditions. A similar phenomenon has also been reported where no difference before and after the intermediate plateau was found in AFM examination[118]. Collagen fibril formation is a multistep process which involves molecular packing into an ordered structure. Type I collagen is unstable and partial denatured within a couple of days at body temperature[119]. The occurrence of denaturation during fibrillogenesis seems to inhibit fibril growth in all our case since a longer fibrillogenesis time was used. In addition, our TEM and SEM images show the presence of amorphous collagen which further indicates some inhibition of fibrillogenesis.

Electrostatic Effects

A number of studies have been carried out on the mechanism of collagen fibril formation in vivo and in vitro[49, 104, 108, 120-122]. The aggregation of collagen monomers is controlled to a significant degree by electrostatic interactions. To discuss the effect of electrostatic interactions, the length scale over which electrostatic interactions occur (Debye screening length κ^{-1}) is taken into account. The Debye length is the characteristic distance over which the electrostatic potential near a charged entity decays. Using Equation 5-1, the Debye length κ^{-1} of

soluble collagen is reduced from a theoretical maximum of ~970 nm in pure water to less than 0.6 nm under our electrolyte condition. The distance between the surfaces of two collagen monomers in fully-hydrated reconstituted collagen fibrils is approximately 0.5 nm[123], and so the electrostatic interactions only become important when the monomers are aggregated to form fibrils.

Fibrillogenesis is a thermally driven process which is favored by hydrophobic interactions. When the pH approaches the pI, the surface charge of the collagen monomers is reduced, which would minimize the electrostatic repulsion and favor collagen molecule aggregation. A strong influence of the ion species on the surface charge on collagen was found in our zeta potential measurement. This shift might be the result of preferential adsorption of phosphate ions. Weinstock et al observed binding of ~6 phosphates per collagen molecule at 100 mM NaCl and ~20 phosphates at low NaCl concentration[124]. In our system, the pI of collagen is pH 9.2 in 12 mM NaCl while it is at pH 7.4 in 12 mM NaCl and 10 mM Na_2HPO_4. Correspondingly, in the presence of 18 mM phosphate and 283 mM NaCl, which we used for fibril formation, it is reasonable that the pI of collagen is around pH 9.2 due to less phosphate binding in the presence of high concentration of NaCl, as shown by Weinstock et al[124]. Unfortunately, zeta potential measurements could not be conducted under the conditions used for fibrillogenesis because the high ion concentration interferes with the measurement. The fibrillogenesis rate accelerated by increasing pH from 6.0 to 9.2 and then decreased, which is consistent with a reduction in the net charge on the collagen molecules as the pI is approached.

When fibril formation was accelerated by increasing pH from pH 6.9 to 8.0, there is no difference in the final fibril diameter. This phenomenon suggests that fibril size has no direct relationship with the rate of fibrillogenesis. Even though there is a difference in pH conditions

from pH 6.9 to pH 9.2, it does not appear that the resulting change in surface charge affects the size of the fibrils.

D-periodicity

The presence of a periodic banding pattern along a fibril is the distinguishing feature of collagen fibrils from other structures in connective tissues. The observed D-periodicity after fibrillogenesis in our results is in agreement with that of native collagen fibrils, which typically have a D-periodicity ranging from 62 to 67 nm depending on the source of collagen and sample preparation[125, 126].

Smaller D-periodicity was observed at pH 7.1 at one and two days. Less than 56 nm banding was also reported from tendon, cornea, skin, liver, and reconstituted fibrils[127-131]. The presence of a small amount (15%) of type III collagen in skin was proposed to account for the unusual periodicity, since type III is associated with type I collagen in skin while bone consists of almost 100% type I collagen[113, 114]. However, the presence of short D-periodicity reported in the early growth of tendon and reconstituted fibrils[127, 129] cast doubt on this proposal since tendon consists of 100% of type I collagen while reconstituted collagen consists of 97% type I collagen. The binding of chondroitin sulfate associated with rat tail tendon[132], the binding of dermatan sulfate associated with skin,[114] and the cleavage of nonhelical telopeptide by pepsin treatment of reconstituted fibrils[127] have also been proposed to account for the unusual D-periodicity. Since pepsin treated collagen molecules have a shorter length than native collagen due to partial cleavage of non-helical telopeptides, the specific binding of phosphate in a similar manner as chondroitin sulfate and dermatan sulfate may alter the charge distributions and water binding, permitting a somewhat shorter length for the molecule leading to a shorter banding. Our data also shows that normal banding was found at the final stage of fibril formation, suggesting that native D-periodicity is the most stable state and that the shorter D-

periodicity is a transient structure that occurs during the growth process. However, we can not yet provide a specific structural model to explain the short banding.

Conclusion

The rate of collagen fibrillogenesis is affected to a significant degree by electrostatic interactions and its optimal fibrillogenesis was achieved when pI of soluble collagen was approached. However, those electrostatic interactions have a weak effect on fibril size and morphology. The surface charge measurement indicates that phosphate binding has a great effect on electrostatic interactions. The average D-periodicity was 62 nm with two notable exceptions at pH 7.1. We propose that the unusual D-periodicity (50 and 54 nm) might come from altered alignment of molecules due to the change of surface charge.

CHAPTER 6
THE FORMATION OF NATIVE FIBRILS INDUCED BY DIVALENT IONS

Introduction

For more than 50 years, the fibrillogenesis of type I collagen has been intensively studied in vitro[49, 97, 133]. This has lead to the reproducible procedures for the production of collagen fibrils with the essential native banding pattern found in biological tissues. Collagen fibril formation is a thermally driven process which is favored by a large positive entropy contribution due to the release of structured water molecules[64]. Non-covalent forces including Coulombic, van der Waals and hydrophobic forces play important roles in fibril formation. Although a neutral pH and a physiological condition are generally used for collagen fibril formation, the underlying effects of salts on fibril formation are not completely understood. Our surfactant studies on collagen self assembly into fibrils indicate that the introduction of hydrophobic interaction could not facilitate fibril formation. The pH and phosphate studies have indicated that pH and phosphate play a significant role on forming native fibrils. The question is whether the phosphate can be replaced by another buffer or salt? What is the critical factor on forming the native fibrils?

Salts can modulate the conformation of collagen molecules and the electrostatic interactions[117, 134]. The importance of pH and ionic strength for the thermal stability of collagen has been demonstrated by several authors. The stability of collagen in solution correlates with both the type of salt and the pH[135-137]. For $CaCl_2$ a decrease in thermal stability of soluble collagen with increasing salt concentration was observed in the physiological pH range while the thermal stability was reported to increase with increasing ionic strength at pH 2.3. In the case of KCl at pH 6, a slight decrease of the thermal stability was found with increasing salt at low concentration. Arktas reported an increase of the thermal stability with

increasing the ionic strength of NaCl at pH 3.7 and pH 5.7, but a decrease for an addition of the $CaCl_2$ at pH 5.7[135]. By changing the solution pH in invariant electrolyte, a maximum thermal stability of the collagen type I molecules was determined in the physiological pH range[137].

The surface charge which is related with salts and the pH of the solution is an important parameter for collagen self assembly into fibrils. To facilitate the collagen self-assembly, the triple helix of collagen should be stable long enough to begin assembly. Moreover, the surface charge of collagen should be screened in order to reduce the electrostatic repulsion. Collagen has the IEP at 9.3 as we determined in Chapter 5. It is expected to accelerate fibrillogenesis with increasing the pH to isoelectric point. However, Wood et al. found the fibrillogenesis rate to increase with decreasing pH from 7.4 to 6 while to decrease with increasing pH from 7.4 to 8[49]. This might come from the binding of salt which can change the surface charge of collagen and intermolecular interaction. It has been reported that preferential adsorption of ions can shift the IEP and influence the conformational stability of the collagen[117]. These binding ions should also affect the surface charges of collagen molecules and change the fibrillogenesis rate. However, due to the affinity of ions and the difficulty in surface charge measurement, there are no systematic studies of salts on collagen fibrillogenesis related to surface charge.

Salts influence the stability of collagen, conformation and intermolecular interactions through salting-in, salting-out and binding[134, 138]. It has been proposed that divalent phosphate and sulfate ions binding to collagen molecules appear to form salt bridges within regions of high excess positive charges in fibrils [109]. During fibril formation, the attraction between the hydrophobic side groups as well as opposite charges groups is thought to be the major interactions. The electrostatic interactions between charged amino residues strongly contribute to the molecular organization of D-staggered array model of collagen fibrils.

Electrostatic interactions in aqueous media are commonly understood in terms of screening Coulomb interactions, where like-charged objects, such as polyelectrolytes, always repel in the Poisson-Boltzmann theory (PB theory). However, a series of experiments on charged biopolymers, including DNA, F-actin fibers, microtubules and aggregating viruses indicate that in the presence of small amounts of polyvalent salts, attractive forces of different origins (e.g., hydrophobic or hydration interactions) overwhelm electrostatic repulsion[139-141].

Protein-Salt Interactions

Salting-out/Salting-in Theory

The protein solubility can be expressed in terms of the solvation free energy of the protein molecule in the equilibrated fluid phase[142]. When the solubility is small, fluid-phase protein-protein interactions can be neglected. The phase-equilibrium criterion (the chemical potential of the protein in the crystal is equal to that in the fluid) at a given salt concentration reduces to:

$$\boldsymbol{\mu_2^s - \mu_2^0 = RTln\frac{S_2}{S_2^0}} \quad (6\text{-}1)$$

Where μ_2^s and μ_2^0 are the chemical potential of the protein in the solid phase and the infinite-dilution standard-state chemical potential of the protein, respectively, and $\boldsymbol{S_2/S_2^0}$ is protein solubility relative to a standard state solubility. The major assumption of the salting-out theory is that the protein is a pure phase and the salting-out behavior is determined from the dependence of the standard-state chemical potential on salt concentration.

Protein-salt interactions can be divided into three main groups: 1) effect of salt on charged groups, 2) effect of salt on exposed peptide groups, and 3) effect of salt on nonpolar groups[143, 144]. At low salt concentrations there is a salting-in effect due to the favorable interaction between the protein and the surrounding ion atmosphere. At higher salt concentrations, protein solubility is determined by the balance of unfavorable interactions between the salt and the

nonpolar surface of the protein and favorable weak ion-binding interactions between the salt and the protein. In most cases, because the unfavorable hydrophobic interactions are greater than the attractive weak ion-binding interactions, salting-out is observed.

Surface-Tension-Increment Effect

The surface free energy of a nonpolar group of the protein in contact with water is related to the surface tension of the water. Because all salts increase the surface tension of water, similarly, they increase the surface free energy of nonpolar groups. As a result, the magnitude of the salt-protein interaction is related to the molal surface tension increment of the salt. The molal surface tension increment of the salt is correlated with the ion's position in the lyotropic series that was originally developed to describe the salting-out effectiveness of various ions for globular proteins. For anions, the series in decreasing order of the molal surface-tension increment is $\boldsymbol{SO_4^{2-}}$>HPO_4^{2-}>$\boldsymbol{Cl^-}$>$\boldsymbol{Br^- > I^- > NO_3^- > SCN^-}$; the corresponding series for cations is $\boldsymbol{Mg^{2+} > Ca^{2+} > Na^+ > K^+ > NH_4^+ > Cs^+}$. High lyotropic-series salts (kosmotropes) are good salting-out agents because they interact strongly with water; water molecules surrounding the salt ions are more structured relative to bulk water. Low lyotropic-series salts (chaotropes) break the structure of water of the surrounding water molecules. Chaotropes are weak salting-out agents due to weak interaction with water[145].

Preferential Ion-Binding Interactions

Studies on the solubility of proteins in salt solutions have shown that there is salting-in effect due to the electrostatic interaction between the salt ions and the peptide group[146, 147] which is attributed to the large dipole moment of the peptide group. Since amino groups of protein carry a partial positive charge and the carbonyl oxygen groups carry a partial negative charge, it is possible that anions bind at or near the nitrogen atoms and cations bind at or near the oxygen atoms. In addition, divalent cations have stronger binding affinities to the peptide group,

as indicated by measurements of the retention times of salt on columns containing a stationary phase of polyacrylamide[143]. In these studies, chaotropic anions or divalent cations were retarded due to interaction with the peptide group, whereas kosmotropic anions were not retarded due to unfavorable interaction with the nonpolar backbone of polyacrylamide.

Anion binding to the positively charged groups of protein molecules has been observed in studies concerning stabilization of folded structures of protein molecules at low pH. The strength of this interaction is related to the ion's position in the electroselectivity series[148], as measured by the affinity of the ion in an anion-exchange resin. The series adsorption dependendence on the resin was exploited, and the general trend is in the order of $\boldsymbol{SO_4^{2-}}$>$\boldsymbol{SCN^-} > I^-$>$\boldsymbol{Br^-}$>$\boldsymbol{Cl^-}$. For monovalent anions, the electroselectivity series is the inverse of the lyotropic series. It is likely that higher binding affinities of the chaotropic anions reflect weaker unfavorable interactions with the nonpolar backbones of the resins. However, a divalent charge interacts more strongly with the charged resin than the monovalent charge, as is observed with $\boldsymbol{SO_4^{2-}}$. In fact, the intensity of anion binding to positively charged surfaces is the reverse of lyotropic-series dependence of the solubility of basic proteins for monovalent anions[149]. This reverse solubility dependence is attributed to the formation of insoluble protein-anion complexes. It was commonly thought favorable protein-salt interactions should favor solubilization of the protein molecule. However, in addition to protein-salt interactions, changes in protein-protein interactions must also be considered; a decline in solubility occurs if there is an increase in the net attraction between the proteins.

In the present study, we found that polyvalent electrolytes adsorb on collagen molecules which shift collagen's isoelectric point. There is a competition between fibrillogenesis and denaturation at pH condition. We also found that collagen fibril formation is not solely a salting-

out process which is regulated by screening surface charge. The likely charge attraction originated by divalent ions bridging play a critical role on forming native fibrils.

Materials and Methods

Materials

Purified type I pepsin-solubilized adult bovine dermal collagen (97%, with the remainder comprised of type III collagen) dissolved in hydrochloride acid was purchased as a solution with a concentration of 2.9 mg/ml (PureCol®, INAMED, Inc., Fremont, CA). $CaCl_2$, NaCl, KCl, Na_2HPO_4, Na_2SO_4, K_2HPO_4, $MgCl_2$, ethylenediaminetetraacetic acid (EDTA) and 0.1M NaOH were purchased from Fischer Scientific.

Zeta Potential Measurement

The determination of zeta (ζ) potential was performed using a Brookhaven ZetaPlus. A solution of type I collagen was diluted to 0.5 mg/ml in 12 mM HCl with desired salts and sonicated for 5 minutes. The pH of the initial solution was measured with pH paper and adjusted within the range of 3 to 11 by 0.1 M NaOH. Fresh solutions were used for zeta potential measurements at each pH.

Turbidity Measurements

The turbidity was recorded by measuring the transmittance at 400 nm using a UV-Vis spectrometer (Beckman DU-640 Spectrophotometer). In a typical experiment, 1.2 ml collagen was mixed with 0.1M NaOH to desired pH. After adding the desired salt, the mixture was incubated at 30°C for 20 hours before turbidity measurement.

Electron Microscopy Measurement

In order to verify collagen fibril formation, electron microscopy of the final collagen gel was taken. The collagen fibrils with native banding were viewed by transmission electron microscopy (TEM; TEM 200CX, JEOL) using an accelerating voltage of 80 kV. TEM samples

were prepared by placing the collagen clot on a 200 mesh copper grid and staining with phosphotungstic acid (1%, pH7.4).

Small Angle X-ray Scattering (SAXS)

SAXS measurements at a wavelength of λ=0.154 nm were carried out using a laboratory pinhole instrument (NanoStar from Bruker AXS, Karlsruhe, Germany) in Dr. Peter Fratzl's lab in Germany. Radial averaging of the two-dimensional scattering data gave the intensity I as a function of the modulus of the scattering vector, which is defined as

$$Q = 4\pi \sin\theta/\lambda \quad (6\text{-}2)$$

Where 2θ is the scattering angle.

Circular Dichroism Measurement

After turbidity measurement, samples of collagen with low turbidity were used for CD measurement in order to determine the thermal stability of the triple helix in specific salts condition. Collagen samples in 350 mM $CaCl_2$, $MgCl_2$ and NaCl at pH 7.4 were diluted with DI-water to give a concentration of about 0.27 mg/ml. The samples then were placed in a jacketed cell at 25°C with a 1-mm light path and the CD spectra were obtained by using a Circular Dichroism Spectrometer (Model 400, Biomedical, Inc. Lakewood, NJ, USA) in Dr. Joanna Long's Lab.

For comparison, the CD spectra of helical and random coil form of collagen were also obtained. The random coil form was obtained after raising the temperature of solution to 50 °C where melting is completed. Samples were scanned at 25°C from 250 nm to 180 nm in 1-nm steps using 1-sec time constant. The results were calculated as the molecular ellipticity, [θ], using the relationship: $[\theta]=10^{-3}\theta M/LC$ (deg cm^2 $dmol^{-1}$), where θ is the measured ellipticity in degree, L is the path length in millimeters, C is the concentration in milligrams per milliliter, and M is the average residue molecular weight of collagen and its value is 91.2.

Results

Surface Charges Measurement

To investigate the influence of salt type on the thermally driven self-assembly of collagen, the surface net charge of collagen molecules were measured by Zeta potential in different salt type (Figure 6-1). It can be seen that not only the surface charge of proteins but also the isoelectric point can be affected by salt specificity. In the control solution, the pH corresponding to the isoelectric point of collagen was found to be approximately 8.9, which is the approximate isoionic point[116]. After adding 10 mM Na_2HPO_4, the isoelectric point of collagen shifted to 7.5. Similarly, adding Na_2SO_4 causes the IEP shift to acid side. On the other side, by adding $CaCl_2$, the IEP of collagen shifted to 9.4. In other words, at the fixed pH, the surface of collagen is more positive charged with multivalent cations than with monovalent ions; collagen is more negatively charged with multivalent anions than with monovalent ions.

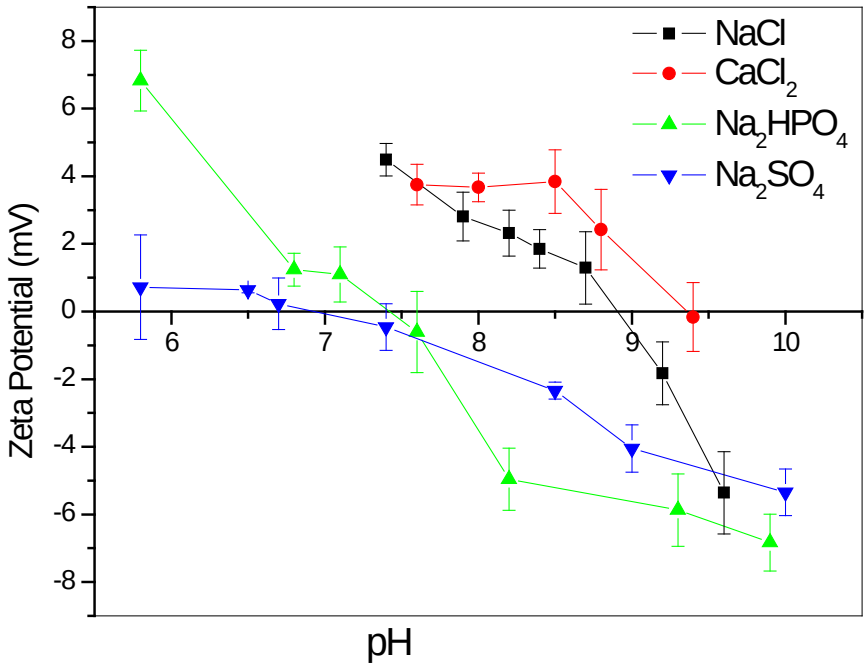

Figure 6-1. Zeta potential measurement of surface charges of collagen affected by salts.

Turbidity Measurements

Collagen fibril formation was conducted at physiological pH and salt condition in order to generate native collagen fibrils. To manipulate surface net charge of collagen, the specific salt, ionic strength and pH were used in our studies. Based on the surface charge results described above, it is expected collagen monomers are less surface charged at physiological pH in multivalent anions than monovalent ions, while more positively charged in multivalent cations than monovalent ions.

Figure 6-2 and 6-3 compare turbidity of collagen fibrils data for various salts at pH 7.4 and 9.0, respectively. The trends are different at both pH conditions. At pH 7.4, with increasing ionic strength, the difference in gelation degree increases in divalent anions of Na_2SO_4, Na_2HPO_4 and K_2HPO_4. In divalent cations of $MgCl_2$ and $CaCl_2$, the gelation degree is highly reduced when ionic strength increases to 250 mM. For the monovalent ions of NaCl and KCl, the gelation degree is reduced at ionic strength of 250 mM. The specific nature of the ion is less important at an ionic strength less than 250 mM since there is no remarkable difference in gelation degree. The difference in gelation degree becomes significant for different salt types above ionic strength 250 mM. At pH 7.4, the surface charges of collagen in divalent anions are very low from the zeta potential measurement while highly positively charged in monovalent ions and divalent cations condition.

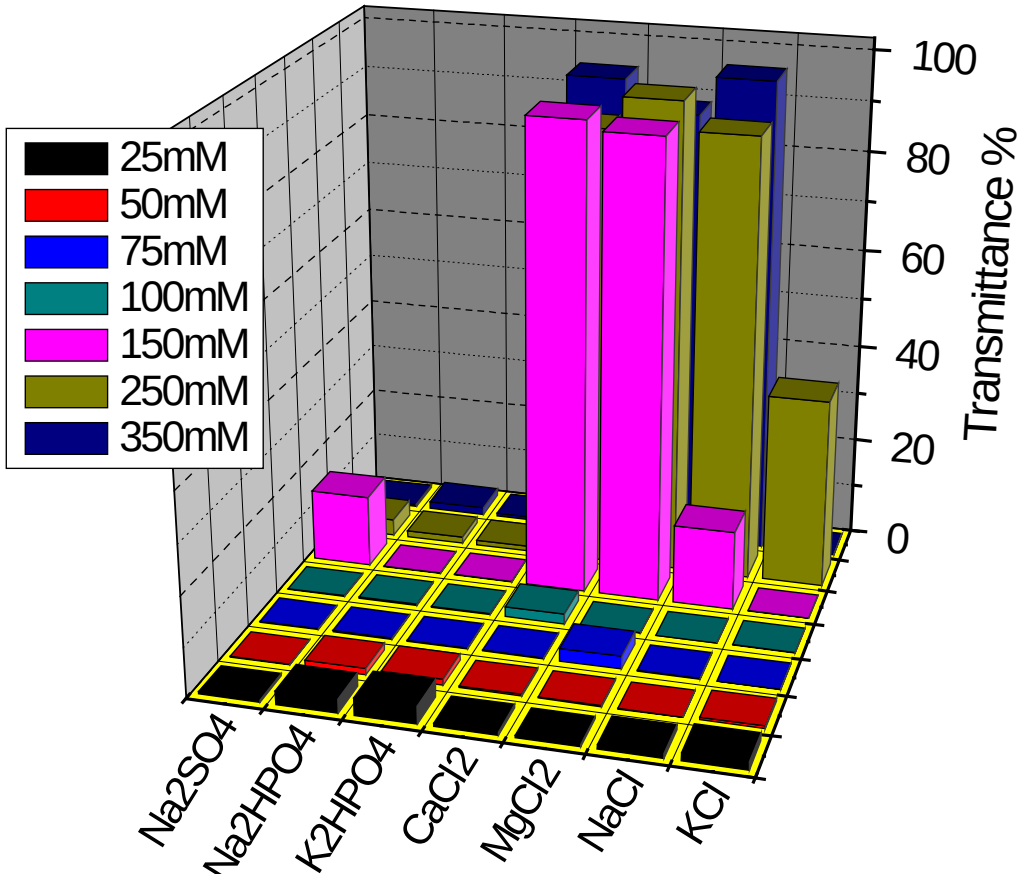

Figure 6-2. Effects of salt type and ionic strength on the collagen gelationat pH 7.4. The gelation degree is increased with increasing ionic strength while gelation is inhibited in $CaCl_2$, $MgCl_2$, KCl and NaCl when ionic strength is about 250 mM.

Figure 6-3 shows gelation data for salts and ionic strength at pH 9.0. Compared to results at pH 7.4, gelation is highly inhibited at pH 9.0 in the range of ionic strength investigated since low turbidities were measured. However, in the divalent cations of $MgCl_2$ and $CaCl_2$, a high degree of gelation was obtained at ionic strength from 50mM to 150mM. In the divalent anions of K_2HPO_4 and Na_2HPO_4, a medium degree of gelation was obtained by increasing the ionic strength which might result from the buffer effect of HPO_4^{2-}.

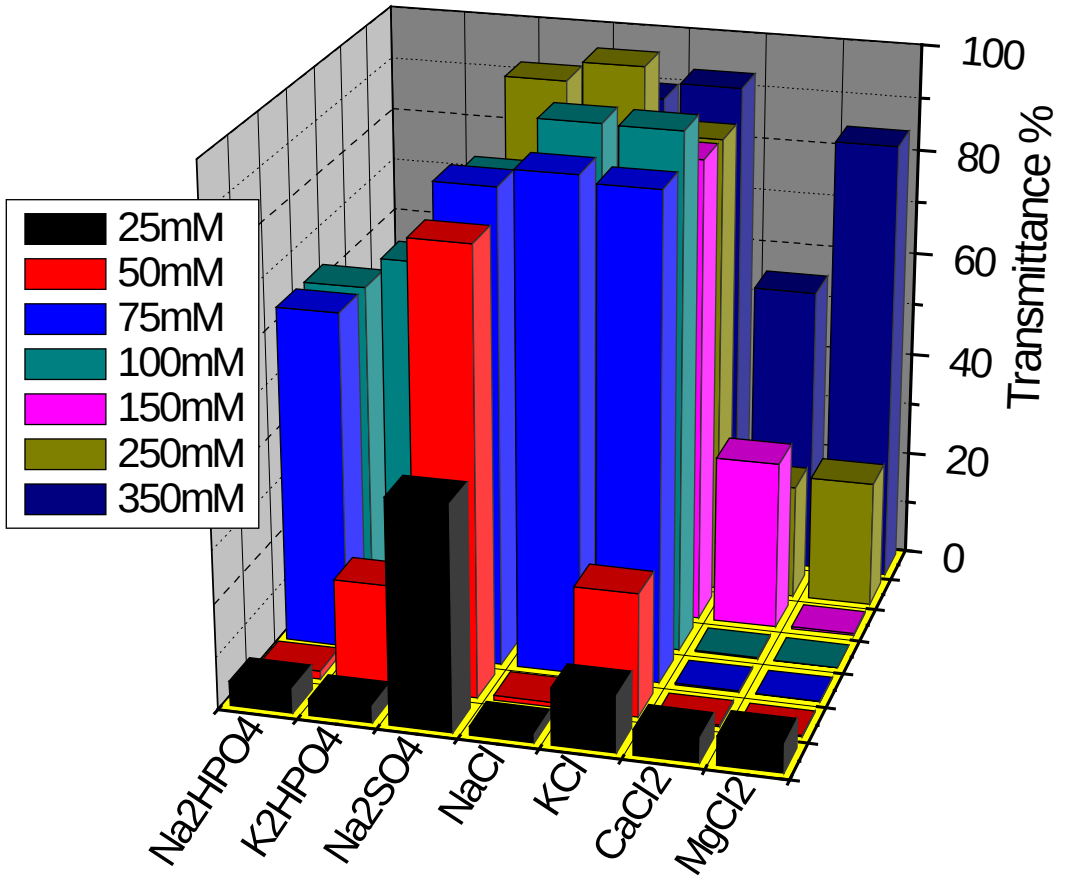

Figure 6-3. Effects of salt type and ionic strength on the collagen gelation degree at pH 9.0. Low gelation is obtained in all salt type except in divalent cations of $CaCl_2$ and $MgCl_2$.

Circular Dichroism Spectroscopy

Turbidity measurements indicated gelation was inhibited by the salts concentration and pH. It has been found that high ionic strength destabilizes collagen's triple helix structure[143] which might inhibit the gelation. It is necessary to determine the helical structure of collagen after incubation. The CD of collagen was performed in 350 mM of $CaCl_2$, $MgCl_2$ and NaCl at pH 7.4 where there is no gel formed at all (Figure 6-4). The helical and random coil forms of collagen were also conducted for comparison. It can be observed that the helical form of collagen has a characteristic positive band at 221 nm and a large negative band at 197 nm while the

random coil form, the positive and negative bands have almost disappeared. The spectra of collagen in the presence of $CaCl_2$, $MgCl_2$ or NaCl have a similar profile with respect to the spectrum of helical form of collagen but the intensity of the bands decreased which might be attributed to partial loss of helical form.

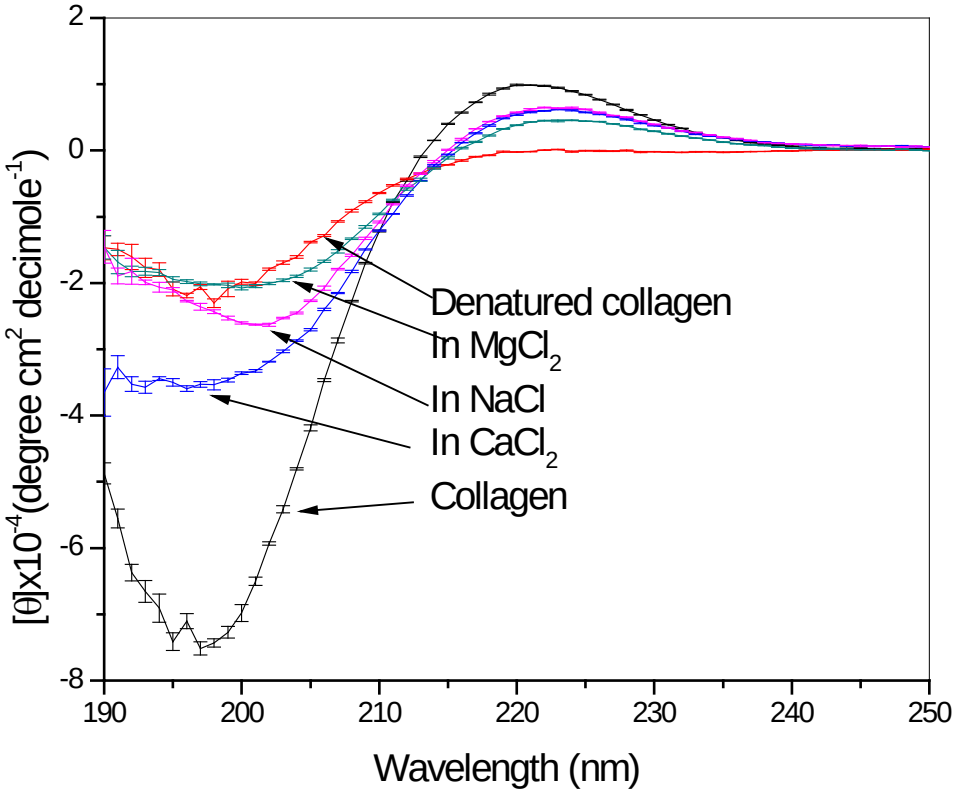

Figure 6-4 Circular dichroism spectra of collagen. The concentration of collagen was 0.27mg/ml. Collagen (native) has characteristic bands at 197 nm and 212 nm. The bands disappeared after denaturation. In 350 mM salts of $CaCl_2$, $MgCl_2$ and NaCl, two bands are decreased due to the partial denaturation.

TEM Morphologies Of Fibrils Formed In Salts

Electron microscopy images were obtained for the collagen gelation after incubation at 30°C for 20 hours in 100 mM and 200 mM ionic strength of salt, pH 7.4. In 100 mM NaCl and KCl, collagen monomers tend to associate into microfibrils (Figure 6-5). No banding pattern can

be observed within these loosely formed microfibrils while non-fibrillar collagen monomers coexist with fibrils. However, when ionic strength is increased to 200 mM, the collagen monomers form more highly-ordered fibrils. Alongside the microfibrils, larger fibrils with D-periodic banding pattern are also found. When in the presence of divalent anions of Na_2SO_4 and Na_2HPO_4, the lateral alignment of the fibrils is clear and the characteristic D-banding pattern of collagen fibrils across the whole collagen fibrils bundle (Figure 6-6) is well demonstrated. Even in 100 mM of Na_2HPO_4, small fibrils also displayed the characteristic D-periodic banding pattern. Compared to the fibrils formed with monovalent ions, the collagen fibrils with divalent anions have more highly-ordered structure. In the presence of $CaCl_2$ and $MgCl_2$ at ionic strength of 200 mM and pH 9.0, the TEM images of collagen fibrils in divalent cations at 100 mM are showed in Figure 6-7. Large and bundled fibrils with D-periodicity appeared in the whole image. Since the lateral growth of fibrils is a diffusion control process, we though the slow rate of gelation in divalent cations might be the reason for large fibrils and decided to study the kinetics of fibrillogenesis in salts.

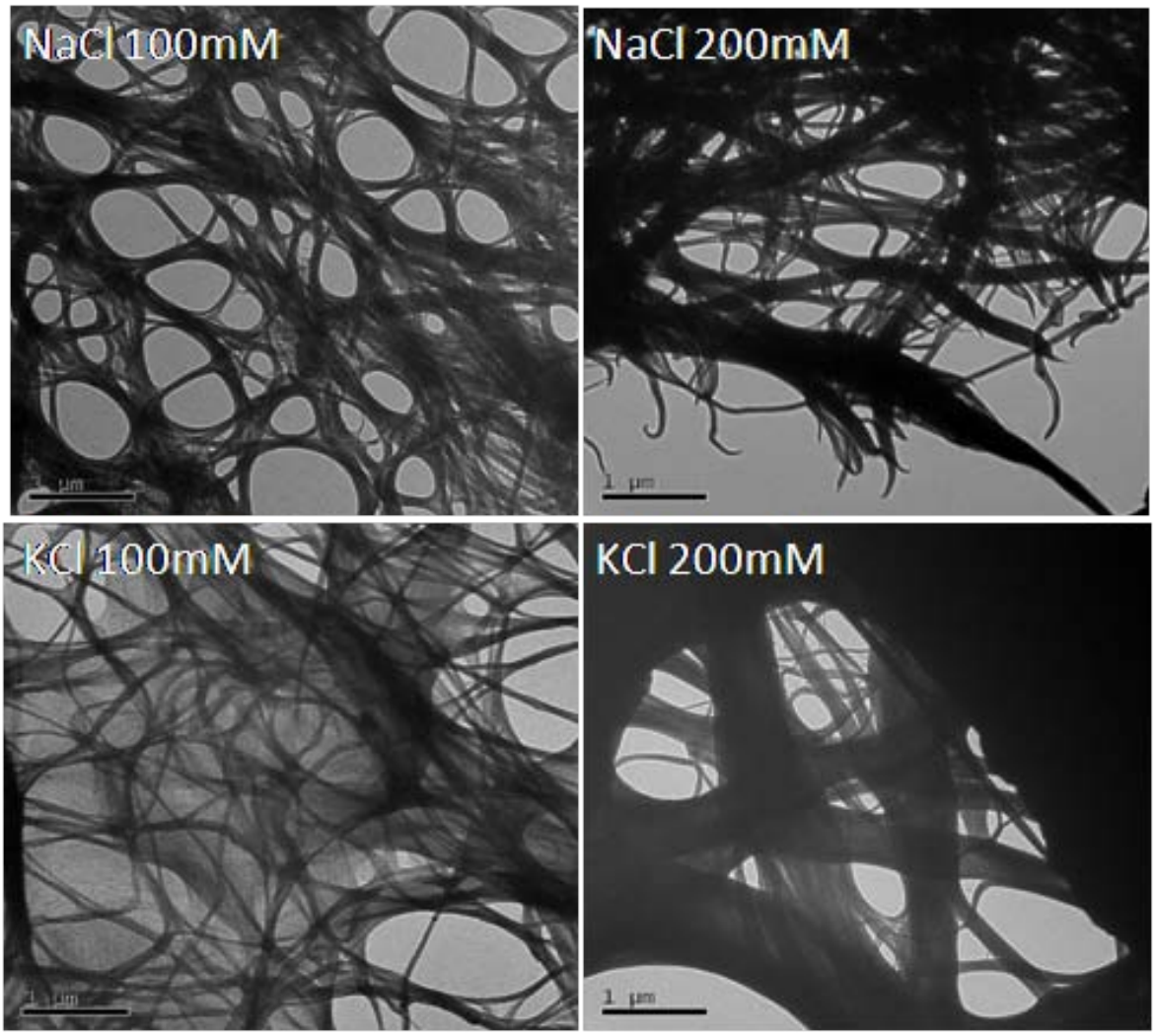

Figure 6-5. TEM images of type I collagen fibrils in mono-valent ions of NaCl and KCl. Scale bar is 1 µm.

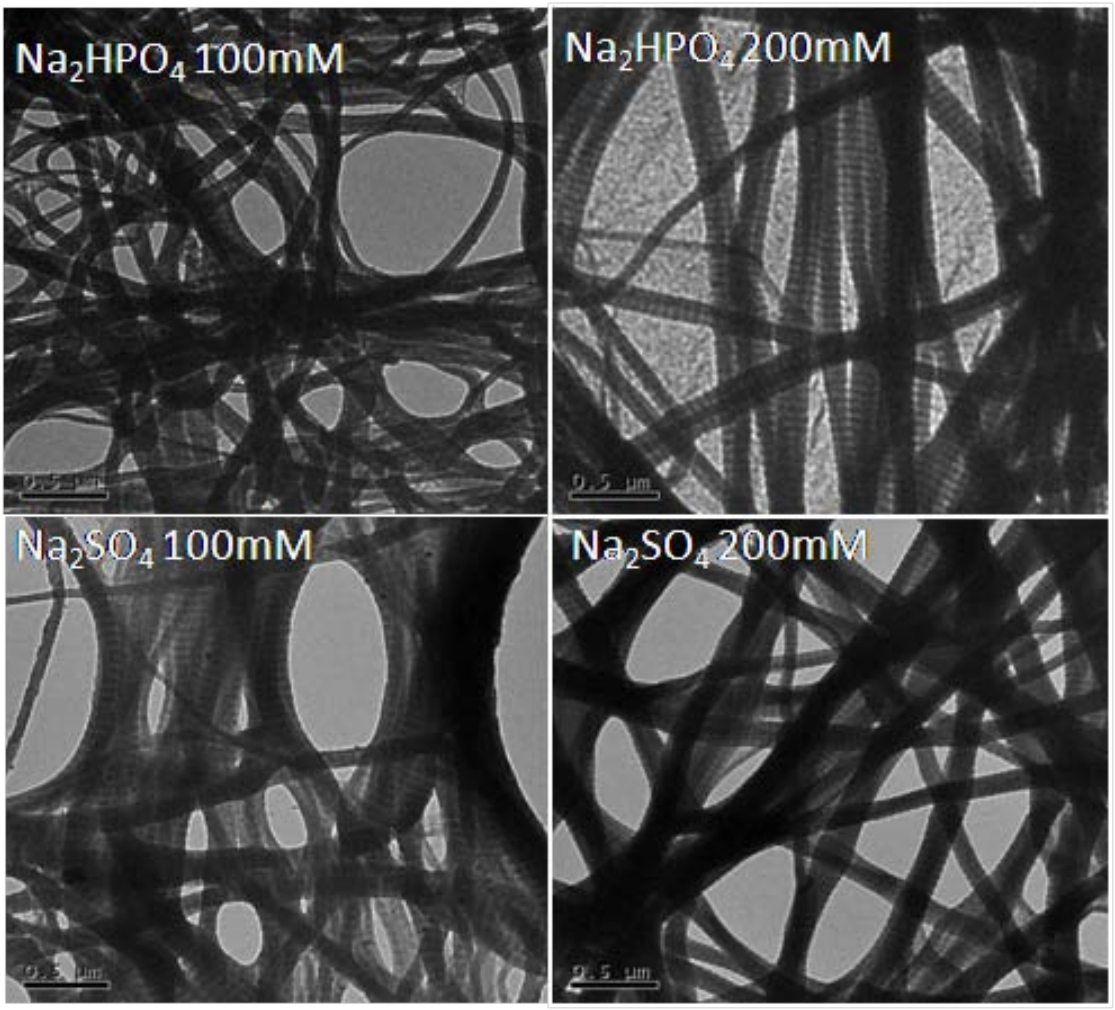

Figure 6-6. TEM images of type I collagen fibrils formed in di-valent cations of Na_2HPO_4 and Na_2SO_4. Scale bar is 500 nm.

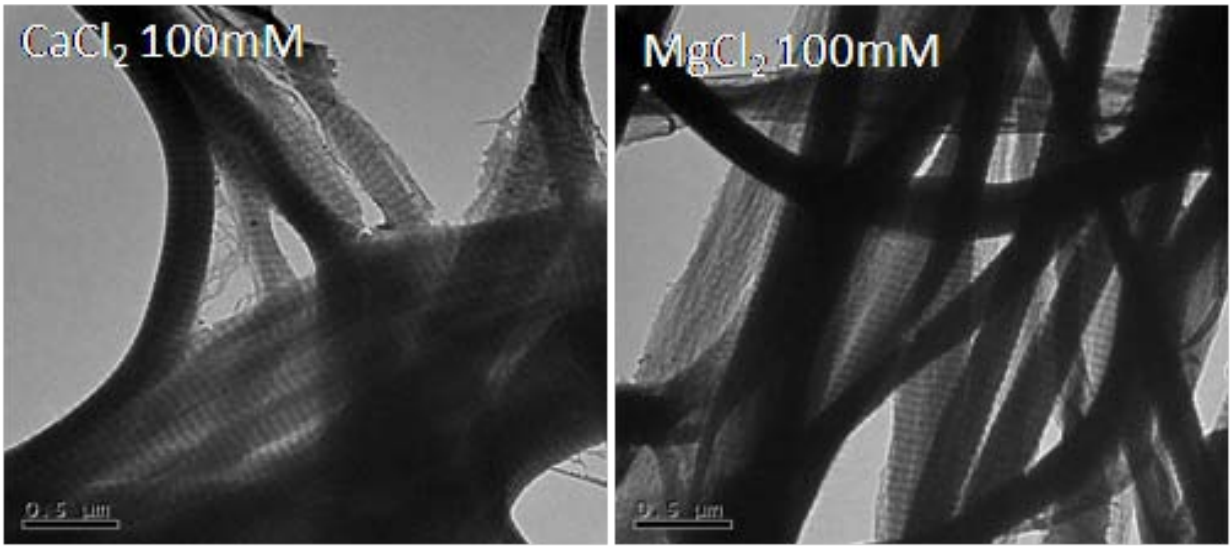

Figure 6-7. TEM images of type I collagen fibrils formed in di-valent cations of $CaCl_2$ and $MgCl_2$Scale bar is 500 nm.

Kinetics of Fibrillogenesis in Salts

The rate of collagen fibrillogenesis is affected by the intermolecular interactions. When collagen molecules are highly positive or negative charged, it is difficult to form the fibrils due to the electrostatic repulsion. When collagen molecules are neutralized, fibrils are easier to be formed. Based on the zeta potential measurement, at pH 7.4, collagen molecules are less charged in Na_2HPO_4 and Na_2SO_4 than in NaCl, $CaCl_2$ and $MgCl_2$. The effects of charge density on rate of fibril formation are observed in Figure 6-8. The order of fibrillogenesis rate is Na_2HPO_4>NaCl>Na_2SO_4>$MgCl_2$>$CaCl_2$ which is consistent with reducing the surface charges of collagen except in the presence of NaCl.

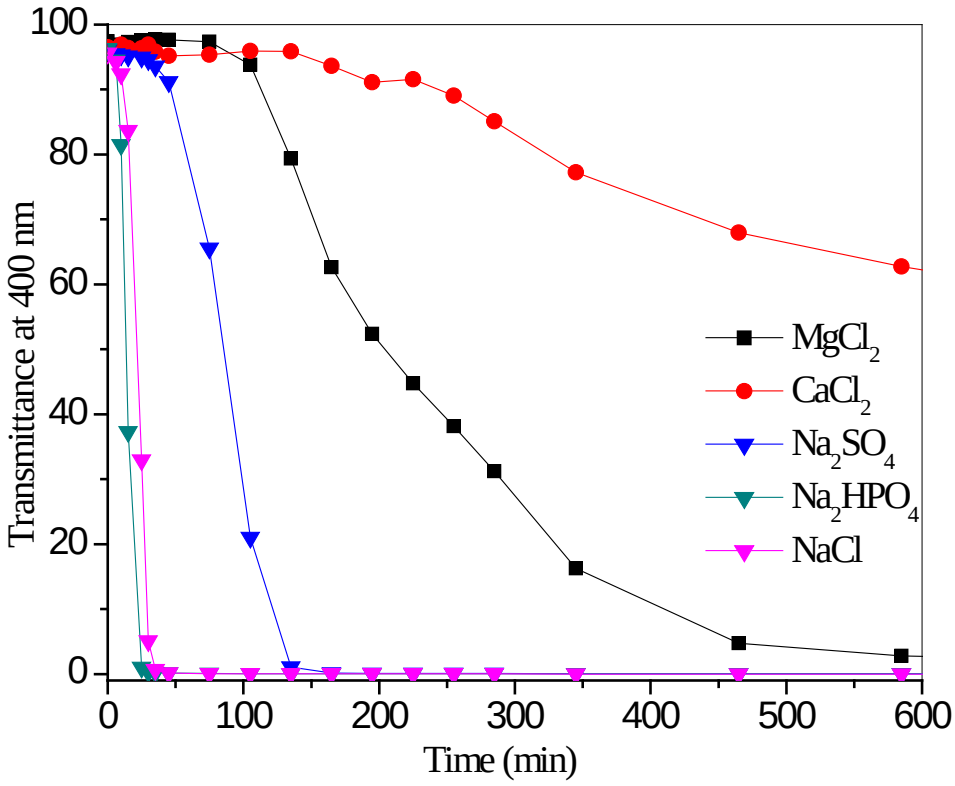

Figure 6-8. Kinetics of collagen gelation in salts determined by turbidity measurements.Ionic Strength 100 mM, pH 7.4, 30°C.

D-periodicity

Collagen exhibits a number of long-range interactions resulting from axial order and possible substructures within the fibrils. The most characteristic long rang order is D-periodicity. The D-periodicity was calculated from TEM images and summarized in Table 6-1. Normal D-periodicities which are around 60 nm was measured in $MgCl_2$, $CaCl_2$ and Na_2HPO_4, but unusual bandings were found in Na_2SO_4 and EDTA.

Table 6-1. D-periodicity of collagen fibrils in presence of different salts

Salts	Ionic Strength (mM)	Banding Length (nm)	Count Number
$CaCl_2$	100	59.4±3.9	89
$MgCl_2$	100	60.3±7.7	85
Na_2HPO_4	200	58.7±4.4	81
Na_2SO_4	200	49.2±3.0	178
EDTA	200	55.7±5.5	316

The D-periodicity of collagen fibrils were also measured by small angle X-ray scattering. The electron density profile of the d-spacing produces a diffraction series of sharp reflections on the small angle scattering image as shown in Figure 6-9. These sharp reflections can be used to determine a change in the d spacing of the collagen molecules as the alteration in electron density along the fibril axis are reflected in changes to the intensity of these peak. The orders of Bragg reflections due to the electron density distribution of the gap and overlap interactions of collagen molecules in the axial direction and the D-periodicity of the fibrils were calculated by the slope of the insert plot using n orders vs. $2\sin\theta/\lambda$. The D-periodicity of fibrils formed in KCl and Na_2HPO_4 is 61 nm which is same as the D-periodicity of natural bone.

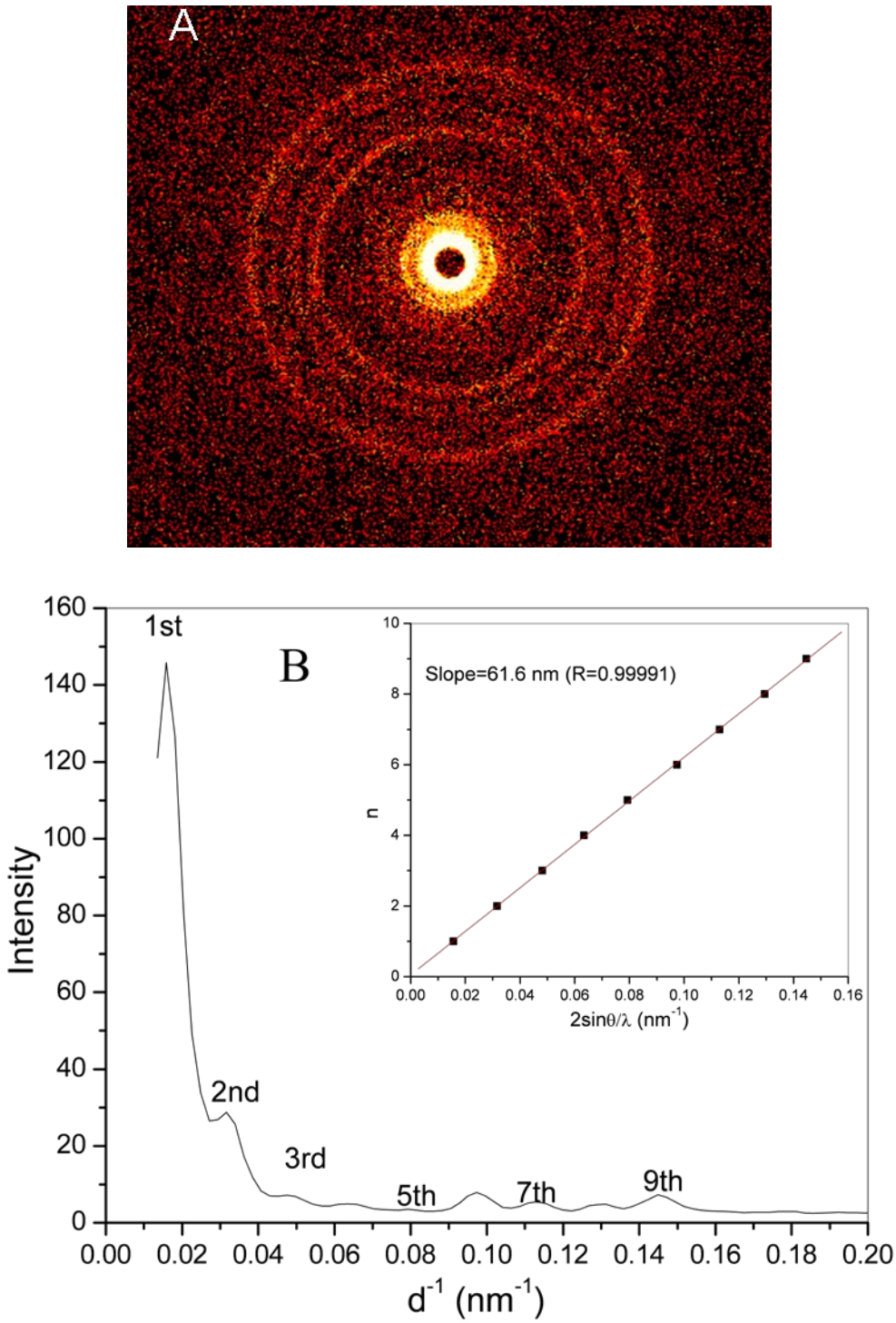

Figure 6-9. Small angle X-ray diffraction measurement of collagen fibrils. A)Small angle X-ray diffraction pattern of collagen fibrils formed in 100 mM KCl. B) A linear intensity profile of the small angle diffraction image of reconstituted collagen fibrils. The orders of Bragg reflections due to the electron density distribution of the gap and overlap interactions of the collagen molecules in the axial direction have been included.

Discussion

Collagen-Ion Complex

Collagen-salt interactions can be divided into two main groups: binding counterions on charged groups which can reduce the effective charge on the collagen; free ions of both charges which act to screen the charge of collagen-ion complex. The binding effects are attributed to the large dipole moment of the peptide group. The amino groups on collagen carry partial negative charges, suggesting anion binding at or near the nitrogen atom. Divalent cations have larger binding affinities to the peptide group than monovalent ions, as indicated by measurements of the retention times of salts on columns containing a stationary phase of polyacrylamide[143]. The binding effects of ions change the surface charge of collagen molecules. Moreover, the shifting of isoelectric point in different salts measured by zeta potential indicates collagen molecules can be overcharged by binding ions. The overcharging phenomenon was found in many other areas of macro-ion electrostatic interaction because of the strong overneutralizing effect of the counterion condensation[150]. For the monovalent salts, they have equal binding affinity on charged groups of collagen molecules and the isoelectric point can not be shifted. However, for the divalent ions, overcharging occurred through the divalent ions binding which reverse the collagen charges.

Stability of Collagen and Fibril Formation

An important phenomenon in our studies is the inhibition of fibril formation at the isoionic point of collagen (pH 9). The formation of collagen fibrils requires the temperature increasing to break the structured water. The hydrophobic attraction and electrostatic attraction overcome hydration to aggregate the collagen molecules. It has been proposed the specific recognition and highest intermolecular interactions occurred in native fibrils driving fibril formation. The instability of collagen in isoionic condition at high temperature is one factor of inhibiting fibril

formation due to the denaturation. Our CD results also confirmed the occurrence of partial denaturation of collagen at high ionic strength. While in pH 9.0, the pH is close to isoionic point of collagen, it is possible that the unfolding of the collagen helix is too fast and prevents fibrillogenesis. However, because of divalent cations, which shift the IEP to base side and make collagen slightly positive charged, the destabilization of collagen is overcome by Fibril formation.

Multivalent Ions Effect on Regulate Banding Pattern

Type I collagen monomers self-assemble into native D-periodic fibrils by a high degree of specific intermolecular interactions. Firstly, the collagen monomers exhibit a high degree of parallel alignment to each other to form microfibrils. Then the microfibrils associate laterally to forming fibrils. When self assembly occurs in the absence of divalent ions, the fibrils are smooth and do not show clear longitudinal periodicity. In the presence of divalent ions, collagen fibrils were formed with periodicity of 62 nm which lies well within the characteristic values of around 64 nm. It is said that the characteristic native periodicity of collagen occurs in the buffer solutions containing potassium[121, 151-154]. Our results indicate that even without potassium, collagen also forms fibrils with native banding pattern. Compared to the salt type, fibril with native banding pattern formed with the divalent ions. It is possible salts with divalent ions induced the like charge attraction during fibrillogenesis through bridging.

Short D-periodicities were found in the presence of Na_2SO_4 and EDTA. We found the short D-periodicities on early stage of fibrillogenesis in PBS. We proposed the misalignment due to the electrostatic interactions between collagen molecules which might also happen in those two salts. The D-periodicity depends on the state of hydration of the fibril and decreases from 67 nm from the hydrated fibril to around 64 nm in air-dried samples, and down to 60 nm after dehydrothermal treatments at 120°C[155, 156]. Short D-periodicities around 57 nm and 62 nm

from air dried collagen fibrils has also been reported from AFM measurement[157]. Since dehydration induces structural disorder and mechanical stresses, it is possible that the collagen fibrils are destabilized and the D-periodicities are decreased after water evaporation.

Usually, the two identical collagen-ion complexes always repel each other, or the magnitude of repulsion is reduced in the electrolytes. It has been know for over a decade, from the simulation and integral equation approaches, the short range correlations between the counterions can lead to attractive corrections to the electrostatic interaction[140]. The occurrence of attractions is usually analyzed in terms of a dimensionless quantity ξ (the Manning parameter), defined by the ratio of the two fundamental lengths in the problem: $\xi=l_B/b$, where $l_B=e^2/4\pi\varepsilon_0\varepsilon k_BT$ is the Bjerrum length (l_B=7.1 A at room temperature in water). According to the Manning criterion[158, 159], because of condensation of the small mobile counterions onto the rod, the effective charge per unit length is only a fraction $1/Z\xi$ (Z is the counterion valency). The fraction $1-1/Z\xi$ of the fixed charges on the rod was neutralized by the counterions that condense on them. An experimental rule for the disappearance of electrostatic repulsion between DNA strands is that the effective charge per unit length should be less that 10% of its bare value. Take the collagen as a rod shape molecule, the electrostatic interaction between collagen molecules is the sum of two terms: The first term is repulsive, and originates from the net charge of each rod, which is nonzero because not all counterions have condensed. The second term is attractive, and originates from charge fluctuations along the rods, due to the free exchange between condensed and free counterions. When the two collagen-ion complexes approach each other during increasing temperature, attractions are induced by hydrophobic attraction. At small distances, the binding ions can undergo dramatic rearrangement that renormalized the effective charge distribution. It is possible that the renormalization of charge distribution of collagen-salt

complexes and subsequently searching a particular target sequence to form the characteristic D-periodic fibrils.

Conclusion

The degree of collagen fibrillogenesis is highly affected by salt type and concentration. Due to the stronger tendency of multivalent ions over monovalents to bind on collagen surface, salts with high binding affinities can screen off the Coulombic repulsion and promote intermolecular interactions. Fibrils with a native banding pattern formed in solutions containing salts with divalent ions. It is thought that these divalent salts could facilitate fibrillogenesis by providing like-charge attraction and forming salt bridges between collagen molecules.

CHAPTER 7
SUMMARY AND FUTURE WORK

Summary

Self-assembly of solubilized collagen into fibrils was first observed about 60 years ago[106]. Under the physiological condition, collagen molecules aggregate spontaneously to form fibrils with the characteristic D-periodic pattern. Subsequent studies indicate that ions, alcohol, and other substances which influence electrostatic, hydrophobic and covalent bonding were able to modify self-assembly behavior. However, the mechanisms by which collagen molecules assembly into fibrils are still not well understood, especially the mechanisms that drive the D-periodic packing of monomers to form native fibril. It has been proposed that specific distribution of charged and hydrophobic amino acids along collagen molecules plays an important role in the molecular packing of collagen[160]. The telopeptides on the collagen also play a critical role in the formation of collagen fibrils[59], but other factors driving collagen assembly into D-periodic fibrils are not known. The aim of this dissertation is to understand the mechanisms of the collagen assembly into D-periodic fibrils, the interactions between the collagen molecules during fibril formation as well as the underlying forces driving the formation of D-periodic pattern. To accomplish these goals, we investigated the kinetics of collagen molecules assemble into fibrils, the temperature, concentration, pH, salts and surfactants effects on controlling the alignment of collagen monomers into fibrils. We employed three kinds of molecular interactions: 1) hydrophobic interactions which were introduced by surfactants of SDS and SDBS; 2) Electrostatic interactions which were controlled by changing the pH of the solution; 3) specific likely charge attractions induced by weak bridges of divalent ions. Morphology studies by electron microscopy suggest that the fundamental mechanism of the

characteristic fibrils is mediated by the electrostatic interactions and salts bridges play an important role on molecular recognition to form D-periodic pattern.

Surfactant Effects

The effects of the presence of ionic surfactants on collagen fibrillogenesis indicated that the rate of collagen fibril formation was accelerated remarkably in the presence of 0.1-0.5 mM sodium dodecylsulfate (SDS) or sodium dodecylbenzenesulfonate (SDBS) while the unfolding of collagen triple helix also occurred when up to 1 mM SDS was added or more than 0.35 mM SDBS was added. The morphology studies from SEM confirmed occurrence of partial unfolding and non-fibrillar collagen gel within fibrils. There is a weak interaction between collagen and SDS at room temperature and stronger binding appeared between collagen and ionic surfactant during collagen dehydration above room temperature. It is possible surfactants bind to collagen which promotes collagen fibril formation.

pH Effects

Collagen self-assembly *in vitro* was conducted in the pH range from 6.0 to 10.5 at 30 °C in order to investigate the electrostatic interactions that occur during fibril formation. A sigmoidal curve was observed in the growth rate of fibrils. Collagen fibril morphologies imaged by transmission electron microscopy (TEM) and scanning electron microscopy (SEM) present bundling of fibrils with a small amount of non-fibrillar collagen. At a low pH of 6.6, collagen molecules form small fibrils with a diameter of 85 nm. In the pH range from 6.9 to 8.0, they form fibrils with diameter of approximately 200 nm, even though the rate of fibrillogenesis accelerates with increasing pH in this range. Zeta potential measurements of soluble collagen indicate that the net surface charge of collagen molecules is not only affected by the pH of medium but also by the presence of added salts. The acceleration of fibrillogenesis rate with increasing pH from 6.6 to 9.2 is consistent with a reduction of surface net charge since the

isoelectric point of soluble collagen is approached. The native D-periodicity of 62 nm was found except at pH 7.1 where collagen molecules form short banding of 50-60 nm in the early stage of fibrillogenesis which might be caused by unusual alignment of collagen molecules in fibrils.

Salts Effects

The behavior of collagen molecules self assembly into fibrils is commonly understood in terms of hydrophobic and electrostatic interactions in the short range by releasing the structured water. As an expectation, the electrostatic interactions are repulsive based on mean field theories, such as the Poisson-Boltzmann theory (PB theory). In our studies, the facilitation of collagen aggregation through reducing surface net charge by adding salts was observed. We also found the competition between unfolding and aggregation of collagen at high pH. The divalent ions binding to the collagen molecules not only change the surface net charge but also facilitate the formation of fibrils with native D-periodic banding pattern. It is possible that the bound divalent ions induce the like-charge attraction during collagen self assembly through coupling and renormalization charge distribution between counter-ion correlation and collagen. We believe these findings can fundamentally help understanding the mechanisms of fibrillgenesis and may initiate new developments of biological self-assembly.

Even though hydrophobic attraction is the major force for collagen aggregation, the formation of native fibrils depends on the appearance of the divalent ions which induce the like-charge attraction and bridging the collagen for fibril formations. As it is know, the self-assembly of molecules has attracted a lot of attention for design and development of new materials. Major mechanism for self-assembly is general the hydrophobic attractions. Our finding of like-charge attraction brings a new sight for developing self-assembly system.

Future Work

The adsorption of collagen at solid surfaces is of importance in a wide variety of applications, including ***in vitro*** cell growth, membrane fouling, protein purification, and biosensor design. Micro-fabrication technology offers the capability to control cell-surface, cell-cell, and cell-medium interactions on a micro- or nanometer scale. Various studies proved that cells are affected by the topography of the surface on which they were seeded. Cells were reported to elongate in the direction of the micrometer-size grooves and migrate as guided by the grooves[161]. Therefore, micro-patterned substrates are expected to better maintain cell morphology, differentiation and functionality over long periods of time. Our studies have indicated that surfactants bind to collagen by hydrophobic interactions. It has also reported adsorption of collagen on the substrate through hydrophobic interactions. One of our future works is to fabricate collagen fibrils on the substrates and control their position by micro-contact patterning. To achieve this goal, experiments are designed as:

1) Design applicable patterns and fabricate the substrates which are suitable for collagen fibril adsorption.

2) Prepare collagen fibril dispersion and print on the substrate.

3) Examine its function on cell attachment and proliferation.

Usually, collagen fibrils are arranged in complex three-dimensional arrays *in vivo*, often in an aligned manner to fulfill certain biomechanical functions such as resisting high tensile stress. Collagen can be found as parallel fiber bundles in tendon and ligaments[162], as concentric waves in bone[163] or as orthogonal lattices in cornea[164]. The spatial organization of collagen fibers *in vivo* is believed to play an important role in directing cell behavior and providing mechanical support. Several approaches have been introduced to reconstitute spatial ordered collagen matrices *in vitro*. Such as exposing collagen solution to a strong magnetic field which

aligns collagen fibrils due to the diamagnetic properties of collagen molecules[165]. Aligned collagen nanofiber matrices have also been produced by electrospinning or use of a mica surface in combination with hydrodynamic flow[166, 167]. We have tried to make the oriented native collagen fibril with concentrated collagen solution. However, the occurrence of non-fibrillar collagen during fibril formation makes it infeasible. Electrospinning method is usually involved in collagen denaturation. We have found that collagen can form native fibrils in divalent ion solution and fibrils can be stabilized after long term storage. Those stabilized fibrils can be dispersed by stirring. Normally, the collagen fibrils formed from gelation are entangled with each other. Strong mechanical agitation causes fibril dissociation. Since we can make the stable and well dispersed fibrils, it is possible that the fibrils can be aligned by hydrodynamic flow to form the 3D matrices.

We found collagen can form the unusual periodicity less than 67 nm. Short periodicities have also been reported but the mechanisms are unclear. Correct longitudinal alignment of collagen monomers in a fibril is important for the mechanical and biological functions of collageneous matrices. Specifically, a precise alignment of monomers facilitates the formation of fibril stabilizing inter-molecular chemical cross-links between specific lysine residues present within telopeptide regions of one monomer and specific lysine residues present with a triple-helical region of interaction monomers. It is worthy of studying the specific factors which cause the short periodicities in order to control the periodicities and help understanding the biological system and collagen synthesis *in vivo*. For this goal, the research is designed as: 1) Produce the collagen fibrillar matrices with shorter periodicity. 2) Examine its mechanical properties. It has been thought native fibrils with D-periodicity are stabilized by inter-molecular chemical cross-links, is it possible that unusual fibrils with short periodicity would be less stable. To study the

mechanical properties, the mechanical strength of single fibril will be measured by AFM. 3) It has been reported that hydrophobic interactions and electrostatic interactions bring a substantial contribution the formation of D-periodicity. Calculating the hydrophobic and electrostatic interactions between collagen molecules in unusual periodicities would be performed.

LIST OF REFERENCES

[1] Friess W. Collagen - biomaterial for drug delivery. Eur J Pharm Biopharm 1998;45(2):113-136.

[2] Burke JF, Yannas IV, Quinby WC, Bondoc CC, Jung WK. Successful Use Of A Physiologically Acceptable Artificial Skin In The Treatment Of Extensive Burn Injury. Annals Of Surgery 1981;194(4):413-428.

[3] Eaglstein WH, Falanga V. Tissue engineering for skin: An update. Journal Of The American Academy Of Dermatology 1998;39(6):1007-1010.

[4] Blair HC, Zaidi M, Schlesinger PH. Mechanisms balancing skeletal matrix synthesis and degradation. Biochem J 2002;364:329-341.

[5] Brekken RA, Sage EH. SPARC, a matricellular protein: at the crossroads of cell-matrix. Matrix Biology 2000;19(7):569-580.

[6] Piez KA, Reddi AH. Extracellular Matrix Biochemistry: New York, 1984.

[7] Kadler K. Extracellular Matrix.1. Fibril-Forming Collagens. Protein Profile 1995;2(5):491-619.

[8] Cunningam W, Frederiksen DW. Methods in Enzymology. New York: Academic Press, 1982.

[9] Hulmes DJS. The collagen superfamily - diverse structures and assemblies. Essays In Biochemistry, Vol 27 1992;27:49-67.

[10] Pachence JM. Collagen-based devices for soft tissue repair. J Biomed Mater Res 1996;33(1):35-40.

[11] Meaney Murray M, Rice K, Wright RJ, Spector M. The effect of selected growth factors on human anterior cruciate ligament cell interactions with a three-dimensional collagen-GAG scaffold. J Orthop Res 2003;21(2):238-44.

[12] Angele P, Kujat R, Nerlich M, Yoo J, Goldberg V, Johnstone B. Engineering of osteochondral tissue with bone marrow mesenchymal progenitor: Cells in a derivatized hyaluronan-gelatin composite sponge. Tissue Engineering 1999;5(6):545-553.

[13] Eaglstein WH, Falanga V. Tissue engineering and the development of Apligraf a human skin equivalent. Adv Wound Care 1998;11(4 Suppl):1-8.

[14] Ananthan.S, Veis A. Molecular Parameters Of Monomeric And Acid-Soluble Collagens - Low Shear Gradient Viscosity And Electric Birefringence. Biopolymers 1972;11(7):1365-1373.

[15] Ramachandran GN. Treatise on Collagen. New York: Academic Press, 1967.

[16] Fraser RDB, Macrae TP, Suzuki E. Chain Conformation In The Collagen Molecule. J Mol Biol 1979;129(3):463-481.

[17] Akeson WH, Amiel D, Mechanic GL, Woo SLY, Harwood FL, Hamer ML. Collagen Cross-Linking Alterations In Joint Contractures - Changes In Reducible Cross-Links In Periarticular Connective-Tissue Collagen After 9 Weeks Of Immobilization. Connect Tissue Res 1977;5(1):15-19.

[18] Yamauchi M, Mechanic G. Crosslinking of collagen. Boca Raton, FL: CRC Press, 1988.

[19] Kuijpers AJ, Engbers GHM, Krijgsveld J, Zaat SAJ, Dankert J, Feijen J. Cross-linking and characterisation of gelatin matrices for biomedical applications. J Biomater Sci-Polym Ed 2000;11(3):225-243.

[20] Khor E. Methods for the treatment of collagenous tissues for bioprostheses. Biomaterials 1997;18(2):95-105.

[21] Hodge AJ. Molecular-Models Illustrating The Possible Distributions Of Holes In Simple Systematically Staggered Arrays Of Type-I Collagen Molecules In Native-Type Fibrils. Connect Tissue Res 1989;21(1-4):467-477.

[22] Veis A, Yuan L. Structure Of Collagen Microfibril - 4-Strand Overlap Model. Biopolymers 1975;14(4):895-900.

[23] Miller A. The molecular packing in collagen fibrils. New York: Plenum Press, 1976.

[24] Currey JD. How well are bones designed to resist fracture? J Bone Miner Res 2003;18(4):591-598.

[25] Landis WJ. Mineral characterization in calcifying tissues: Atomic, molecular and macromolecular perspectives. Connect Tissue Res 1996;35(1-4):1-8.

[26] Landis WJ, Hodgens KJ, Arena J, Song MJ, McEwen BF. Structural relations between collagen and mineral in bone as determined by high voltage electron microscopic tomography. Microscopy Research And Technique 1996;33(2):192-202.

[27] Jaschouz D, Paris O, Roschger P, Hwang HS, Fratzl P. Pole figure analysis of mineral nanoparticle orientation in individual trabecula of human vertebral bone. Journal Of Applied Crystallography 2003;36:494-498.

[28] Yamauchi M. Calcium and phosphorus in Health and Disease. New York: CRC Press, 1996.

[29] Hodge A. J. PJA. Aspects of protein structure. New York: Academic, 1963.

[30] Fratzl P, Fratzlzelman N, Klaushofer K, Vogl G, Koller K. Nucleation And Growth Of Mineral Crystals In Bone Studied By Small-Angle X-Ray-Scattering. Calcif Tissue Int 1991;48(6):407-413.

[31] Fratzl P, Groschner M, Vogl G, Plenk H, Eschberger J, Fratzlzelman N, et al. Mineral Crystals In Calcified Tissues - A Comparative-Study By Saxs. J Bone Miner Res 1992;7(3):329-334.

[32] Cassel JM, Christen.R.G. Volume Change On Formation Of Native Collagen Aggregate. Biopolymers 1967;5(5):431-438.

[33] Wood GC. Formation Of Fibrils From Collagen Solutions.2. Mechanism Of Collagen-Fibril Formation. Biochem J 1960;75:598-605.

[34] Gelman RA, Piez KA. Collagen Fibril Formation Invitro - A Quasi-Elastic Light-Scattering Study Of Early Stages. J Biol Chem 1980;255(17):8098-8102.

[35] Silver FH. A Molecular-Model For Linear And Lateral Growth Of Type-I Collagen Fibrils. Collagen And Related Research 1982;2(3):219-229.

[36] Holmes DF, Capaldi MJ, Chapman JA. Reconstitution Of Collagen Fibrils Invitro - The Assembly Process Depends On The Initiating Procedure. Int J Biol Macromol 1986;8(3):161-166.

[37] Brennan M, Davison PF. Role Of Aldehydes In Collagen Fibrillogenesis Invitro. Biopolymers 1980;19(10):1861-1873.

[38] Haworth RA, Chapman JA. Study Of Growth Of Normal And Iodinated Collagen Fibrils Invitro Using Electron-Microscope Autoradiography. Biopolymers 1977;16(9):1895-1906.

[39] Silver FH. Type-I Collagen Fibrillogenesis Invitro - Additional Evidence For The Assembly Mechanism. J Biol Chem 1981;256(10):4973-4977.

[40] Gross J, Kirk D. Heat Precipitation Of Collagen From Neutral Salt Solutions - Some Rate-Regulating Factors. J Biol Chem 1958;233(2):355-360.

[41] Fratzl P, Fratzlzelman N, Klaushofer K. Collagen Packing And Mineralization - An X-Ray-Scattering Investigation Of Turkey Leg Tendon. Biophys J 1993;64(1):260-266.

[42] Abraham LC, Zuena E, Perez-Ramirez B, Kaplan DL. Guide to collagen characterization for biomaterial studies. Journal Of Biomedical Materials Research Part B-Applied Biomaterials 2008;87B(1):264-285.

[43] Engel J, Bachinger HP. Structure, stability and folding of the collagen triple helix. Collagen. Berlin: Springer-Verlag Berlin, 2005. p. 7-33.

[44] Rho JY, Kuhn-Spearing L, Zioupos P. Mechanical properties and the hierarchical structure of bone. Med Eng Phys 1998;20(2):92-102.

[45] Gross J, Highberger JH, Schmitt FO. Collagen Structures Considered As States Of Aggregation Of A Kinetic Unit - The Tropocollagen Particle. Proc Natl Acad Sci U S A 1954;40(8):679-688.

[46] Highberger JH, Gross J, Schmitt FO. The Interaction Of Mucoprotein With Soluble Collagen - An Electron Microscope Study. Proc Natl Acad Sci U S A 1951;37(5):286-291.

[47] Schmitt FO, Gross J, Highberger JH. A New Particle Type In Certain Connective Tissue Extracts. Proc Natl Acad Sci U S A 1953;39(6):459-470.

[48] Bianchi E, Conio G, Ciferri A. Helix-Coil Transformation For Tropocollagen Solutions And Its Relationship To Transformations Involving Crystalline Form Of Protein. Biopolymers 1966;4(9):957-963.

[49] Wood GC, Keech MK. Formation Of Fibrils From Collagen Solutions.1. Effect Of Experimental Conditions - Kinetic And Electron-Microscope Studies. Biochem J 1960;75:588-598.

[50] Silver FH, Langley KH, Trelstad RL. Type-I Collagen Fibrillogenesis - Initiation Via Reversible Linear And Lateral Growth Steps. Biopolymers 1979;18(10):2523-2535.

[51] Brennan M, Davison PF. Influence Of The Telopeptides On Type-I Collagen Fibrillogenesis. Biopolymers 1981;20(10):2195-2202.

[52] Gelman RA, Williams BR, Piez KA. Collagen Fibril Formation - Evidence For A Multistep Process. J Biol Chem 1979;254(1):180-186.

[53] Delorenzi NJ, Sculsky G, Gatti CA. Effect of monovalent anions on type I collagen fibrillogenesis in vitro. Int J Biol Macromol 1996;19(1):15-20.

[54] Doty P, Edsall JT. Light Scattering In Protein Solutions. AdvProtein Chem 1951;6:35-121.

[55] Doty P, Steiner RF. Light Scattering And Spectrophotometry Of Colloidal Solutions. Journal Of Chemical Physics 1950;18(9):1211-1220.

[56] Silver FH, Birk DE. Kinetic-Analysis Of Collagen Fibrillogenesis.1. Use Of Turbidity - Time Data. Collage Relat Res 1983;3(5):393-405.

[57] Miller EJ, Rhodes RK. Preparation And Characterization Of The Different Types Of Collagen. Methods Enzymol 1982;82:33-64.

[58] Williams BR, Gelman RA, Poppke DC, Piez KA. Collagen Fibril Formation - Optimal Invitro Conditions And Preliminary Kinetic Results. J Biol Chem 1978;253(18):6578-6585.

[59] Veis A. Collagen Fibrillogenesis. Connect Tissue Res 1982;10(1):11-24.

[60] Steinert PM, Idler WW, Zimmerman SB. Self-Assembly Of Bovine Epidermal Keratin Filaments Invitro. J Mol Biol 1976;108(3):547-567.

[61] Hofrichter J, Ross PD, Eaton WA. Supersaturation In Sickle-Cell Hemoglobin Solutions. Proc Natl Acad Sci U S A 1976;73(9):3035-3039.

[62] Cisneros DA, Hung C, Franz CA, Muller DJ. Observing growth steps of collagen self-assembly by time-lapse high-resolution atomic force microscopy. J Struct Biol 2006;154(3):232-245.

[63] Cassel JM. Collagen Aggregation Phenomena. Biopolymers 1966;4(9):989-997.

[64] Cooper A. Thermodynamic Studies Of Assembly In-Vitro Of Native Collagen Fibrils. Biochem J 1970;118(3):355-365.

[65] Hayashi T, Nagai Y. Factors Affecting Interactions Of Collagen Molecules As Observed By In-Vitro Fibril Formation.2. Effects Of Species And Concentration Of Anions. J Biochem (Tokyo) 1973;74(2):253-262.

[66] Steinhar.J, Stocker N, Carroll D, Birdi KS. Nonspecific Large Binding Of Amphiphiles By Proteins. Biochemistry 1974;13(21):4461-4468.

[67] Nozaki Y, Reynolds JA, Tanford C. Interaction Of A Cationic Detergent With Bovine Serum-Albumin And Other Proteins. J Biol Chem 1974;249(14):4452-4459.

[68] Steinhar.J, Krijn J, Leidy JG. Differences Between Bovine And Human Serum Albumins - Binding Isotherms, Optical Rotatory Dispersion, Viscosity, Hydrogen Ion Titration, And Fluorescence Effects. Biochemistry 1971;10(22):4005-4015.

[69] Reynolds JA, Herbert S, Polet H, Steinhar.J. Binding Of Divers Detergent Anions To Bovine Serum Albumin. Biochemistry 1967;6(3):937-947.

[70] Honya M, Mizunuma H. Collagen Fibrillogenesis In-Vitro - Accelerative Effect Of Surfactants On Collagen Fibril Formation. J Biochem (Tokyo) 1974;75(1):113-121.

[71] Hayashi T. Factors Affecting Interactions Of Collagen Molecules As Observed By In-Vitro Fibril Formation.1. Effects Of Small Molecules, Especially Saccharides. J Biochem (Tokyo) 1972;72(3):749-758.

[72] Maldonado F, Almela M, Otero A, Costalopez J. The Binding Of Anionic And Nonionic Surfactants To Collagen Through The Hydrophobic Effect. Journal Of Protein Chemistry 1991;10(2):189-192.

[73] Henriquez M, Lissi E, Abuin E, Ciferri A. Assembly Of Amphiphilic Compounds And Rigid Polymers.1. Interaction Of Sodium Dodecyl-Sulfate With Collagen. Macromolecules 1994;27(23):6834-6840.

[74] Holmberg K. Handbook of applied surface and colloid chemistry. New York: Wiley and Sons, 2002.

[75] Benito I, Garcia MA, Monge C, Saz JM, Marina ML. Spectrophotometric and conductimetric determination of the critical micellar concentration of sodium dodecyl sulfate and cetyltrimethylammonium bromide micellar systems modified by alcohols and salts. Colloids And Surfaces A-Physicochemical And Engineering Aspects 1997;125(2-3):221-224.

[76] Corrin ML, Harkins WD. The Effect Of Salts On The Critical Concentration For The Formation Of Micelles In Colloidal Electrolytes. J Am Chem Soc 1947;69(3):683-688.

[77] Fuguet E, Rafols C, Roses M, Bosch E. Critical micelle concentration of surfactants in aqueous buffered and unbuffered systems. Analytica Chimica Acta 2005;548(1-2):95-100.

[78] Brown RA, Wiseman M, Chuo CB, Cheema U, Nazhat SN. Ultrarapid engineering of biomimetic materials and tissues: Fabrication of nano- and microstructures by plastic compression. Advanced Functional Materials 2005;15(11):1762-1770.

[79] Nezu T, Nishiyama N, Nemoto K, Terada Y. The effect of hydrophilic adhesive monomers on the stability of type I collagen. Biomaterials 2005;26(18):3801-3808.

[80] Honya M. Collagen Fibrillogenesis Invitro - Functional Role Of Nonionic Materials In Collagen Fibril Formation. J Biochem (Tokyo) 1974;75(5):1037-1045.

[81] Miller DD, Lenhart W, Antalek BJ, Williams AJ, Hewitt JM. The Use Of Nmr To Study Sodium Dodecyl-Sulfate Gelatin Interactions. Langmuir 1994;10(1):68-71.

[82] De Cupere VM, Van Wetter J, Rouxhet PG. Nanoscale organization of collagen and mixed collagen-pluronic adsorbed layers. Langmuir 2003;19(17):6957-6967.

[83] Na GC, Phillips LJ, Freire EI. Invitro Collagen Fibril Assembly - Thermodynamic Studies. Biochemistry 1989;28(18):7153-7161.

[84] Tiktopulo EI, Kajava AV. Denaturation of type I collagen fibrils is an endothermic process accompanied by a noticeable change in the partial heat capacity. Biochemistry 1998;37(22):8147-8152.

[85] Miles CA, Ghelashvili M. Polymer-in-a-box mechanism for the thermal stabilization of collagen molecules in fibers. Biophys J 1999;76(6):3243-3252.

[86] Mysels KJ, Princen LH. Light Scattering By Some Lauryl Sulfate Solutions. Journal Of Physical Chemistry 1959;63(10):1696-1700.

[87] Katz EP, Li S. Structure And Function Of Bone Collagen Fibrils. J Mol Biol 1973;80(1):1-15.

[88] Reilly DT, Burstein AH. Review Article - Mechanical-Properties Of Cortical Bone. J Bone Joint Surg-Am Vol 1974;A 56(5):1001-1022.

[89] Landis WJ, Silver FH, Freeman JW. Collagen as a scaffold for biomimetic mineralization of vertebrate tissues. J Mater Chem 2006;16(16):1495-1503.

[90] Olszta MJ, Cheng XG, Jee SS, Kumar R, Kim YY, Kaufman MJ, et al. Bone structure and formation: A new perspective. Mater Sci Eng R-Rep 2007;58(3-5):77-116.

[91] Olszta MJ, Douglas EP, Gower LB. Scanning electron microscopic analysis of the mineralization of type I collagen via a polymer-induced liquid-precursor (PILP) process. Calcif Tissue Int 2003;72(5):583-591.

[92] Song J, Malathong V, Bertozzi CR. Mineralization of synthetic polymer scaffolds: A bottom-up approach for the development of artificial bone. J Am Chem Soc 2005;127(10):3366-3372.

[93] Schmitt F, Hall C, Jakus M. Electron microscope investigations of the structure of collagen. J Cell Comp Physiol 1942;20(1):11-33.

[94] Schmitt FO, Hall CE, Jakus MA. Electron microscope investigations of the structure of collagen. J Cell Comp Physiol 1942;20(1):11-33.

[95] Bear RS. Long x-ray diffraction spacings of collagen. J Am Chem Soc 1942;64:727-727.

[96] Bear RS. Complex formation between starch and organic molecules. J Am Chem Soc 1944;66:2122-2123.

[97] Bensusan HB, Hoyt BL. The Effect Of Various Parameters On The Rate Of Formation Of Fibers From Collagen Solutions. J Am Chem Soc 1958;80(3):719-724.

[98] Cassel JM, Christen.R.G. Volume Change On Formation Of Native Collagen Aggregate. Biopolymers 1967;5(5):431-437.

[99] Hayashi T, Nagai Y. Factors Affecting Interactions Of Collagen Molecules As Observed By Invitro Fibril Formation.3. Non-Helical Regions Of Collagen Molecules. J Biochem (Tokyo) 1974;76(1):177-186.

[100] Helseth DL, Veis A. Collagen Self-Assembly Invitro - Differentiating Specific Telopeptide-Dependent Interactions Using Selective Enzyme Modification And The Addition Of Free Amino Telopeptide. J Biol Chem 1981;256(14):7118-7128.

[101] Cassel JM. Collagen Aggregation Phenomena. Biopolymers 1966;4(9):989-997.

[102] Leikin S, Rau DC, Parsegian VA. Temperature-Favored Assembly Of Collagen Is Driven By Hydrophilic Not Hydrophobic Interactions. Nat Struct Biol 1995;2(3):205-210.

[103] Hofmann H, Fietzek PP, Kuhn K. Role Of Polar And Hydrophobic Interactions For Molecular Packing Of Type-I Collagen - 3-Dimensional Evaluation Of Amino-Acid Sequence. J Mol Biol 1978;125(2):137-165.

[104] Bard JBL, Chapman JA. Diameters Of Collagen Fibrils Grown In-Vitro. Nature-New Biology 1973;246(151):83-84.

[105] Hayes RL, Allen ER. Electron-Microscopic Studies On A Double-Stranded Beaded Filament Of Embryonic Collagen. J Cell Sci 1967;2(3):419-434.

[106] Noda H, Wyckoff RWG. The Electron Microscopy Of Reprecipitated Collagen. Biochim Biophys Acta 1951;7(4):494-506.

[107] Raspanti M, Alessandrini A, Ottani V, Ruggeri A. Direct visualization of collagen-bound proteoglycans by tapping-mode atomic force microscopy. J Struct Biol 1997;119(2):118-122.

[108] Vanamee P, Porter KR. Observations With The Electron Microscope On The Solvation And Reconstitution Of Collagen. J Exp Med 1951;94(3):255-273.

[109] Mertz EL, Leikin S. Interactions of inorganic phosphate and sulfate anions with collagen. Biochemistry 2004;43(47):14901-14912.

[110] Sun YL, Luo ZP, Fertala A, An KN. Direct quantification of the flexibility of type I collagen monomer. Biochem Biophys Res Commun 2002;295(2):382-386.

[111] Fratzl P, Gupta HS, Paschalis EP, Roschger P. Structure and mechanical quality of the collagen-mineral nano-composite in bone. J Mater Chem 2004;14(14):2115-2123.

[112] Glimcher MJ. Molecular Biology Of Mineralized Tissues With Particular Reference To Bone. Rev Mod Phys 1959;31(2):359-393.

[113] Brodsky B, Eikenberry EF, Cassidy K. Unusual Collagen Periodicity In Skin. Biochim Biophys Acta 1980;621(1):162-166.

[114] Stinson RH, Sweeny PR. Skin Collagen Has An Unusual D-Spacing. Biochim Biophys Acta 1980;621(1):158-161.

[115] Hattori S, Adachi E, Ebihara T, Shirai T, Someki I, Irie S. Alkali-treated collagen retained the triple helical conformation and the ligand activity for the cell adhesion via alpha 2 beta 1 integrin. J Biochem (Tokyo) 1999;125(4):676-684.

[116] Jackson DS, Neuberger A. Observations On The Isoionic And Isoelectric Point Of Acid-Processed Gelatin From Insoluble And Citrate-Extracted Collagen. Biochim Biophys Acta 1957;26(3):638-639.

[117] Freudenberg U, Behrens SH, Welzel PB, Muller M, Grimmer M, Salchert K, et al. Electrostatic interactions modulate the conformation of collagen I. Biophys J 2007;92(6):2108-2119.

[118] Goh MC, Paige MF, Gale MA, Yadegari I, Edirisinghe M, Strzelczyk J. Fibril formation in collagen. Physica A 1997;239(1-3):95-102.

[119] Leikina E, Mertts MV, Kuznetsova N, Leikin S. Type I collagen is thermally unstable at body temperature. Proc Natl Acad Sci U S A 2002;99(3):1314-1318.

[120] Feng D, Knight DP. The Effect Of Ph On Fibrillogenesis Of Collagen In The Egg Capsule Of The Dogfish, Scyliorhinus-Canicula. Tissue Cell 1994;26(5):649-659.

[121] Jiang FZ, Horber H, Howard J, Muller DJ. Assembly of collagen into microribbons: effects of pH and electrolytes. J Struct Biol 2004;148(3):268-278.

[122] Ripamonti A, Roveri N, Braga D, Hulmes DJS, Miller A, Timmins PA. Effects Of Ph And Ionic-Strength On The Structure Of Collagen Fibrils. Biopolymers 1980;19(5):965-975.

[123] Katz EP, Li ST. Intermolecular Space Of Reconstituted Collagen Fibrils. J Mol Biol 1973;73(3):351-369.

[124] Weinstock A, King PC, Wuthier RE. Ion-Binding Characteristics Of Reconstituted Collagen. Biochem J 1967;102(3):983-987.

[125] Brodsky B, Eikenberry EF. Characterization Of Fibrous Forms Of Collagen. Methods Enzymol 1982;82:127-174.

[126] Brodsky B, Eikenberry EF, Belbruno KC, Sterling K. Variations In Collagen Fibril Structure In Tendons. Biopolymers 1982;21(5):935-951.

[127] Wu TJ, Huang HH, Lan CW, Lin CH, Hsu FY, Wang YJ. Studies on the microspheres comprised of reconstituted collagen and hydroxyapatite. Biomaterials 2004;25(4):651-658.

[128] Scott JE, Orford CR. Dermatan Sulfate-Rich Proteoglycan Associates With Rat Tail Tendon Collagen At The D-Band In The Gap Region. Biochem J 1981;197(1):213-216.

[129] Gillard GC, Merrilees MJ, Bellbooth PG, Reilly HC, Flint MH. Proteoglycan Content And Axial Periodicity Of Collagen In Tendon. Biochem J 1977;163(1):145-151.

[130] Smith JW, Frame J. Observations On Collagen And Proteinpolysaccharide Complex Of Rabbit Corneal Stroma. J Cell Sci 1969;4(2):421-436.

[131] Tzaphlidou M. Measurement of the axial periodicity of collagen fibrils using an image processing method. Micron 2001;32(3):337-339.

[132] Scott JE, Orford CR, Hughes EW. Proteoglycan-Collagen Arrangements In Developing Rat Tail Tendon - An Electron-Microscopical And Biochemical Investigation. Biochem J 1981;195(3):573-581.

[133] Vanamee P, Porter KR. Observations With The Electron Microscope On The Solvation And Reconstitution Of Collagen. J Exp Med 1951;94(3):255-268.

[134] Vonhippe.Ph, Schleich T. Ion Effects On Solution Structure Of Biological Macromolecules. Accounts Of Chemical Research 1969;2(9):257-263.

[135] Aktas N. The effects of pH, NaCl and CaCl2 on thermal denaturation characteristics of intramuscular connective tissue. Thermochim Acta 2003;407(1-2):105-112.

[136] Usha R, Ramasami T. Effect of pH on dimensional stability of rat tail tendon collagen fiber. J Appl Polym Sci 2000;75(13):1577-1584.

[137] Bianchi E, Conio G, Ciferri A, Puett D, Rajagh L. Role Of Ph Temperature Salt Type And Salt Concentration On Stability Of Crystalline Helical And Randomly Coiled Forms Of Collagen. J Biol Chem 1967;242(7):1361-1369.

[138] Brown EM, Farrell HM, Wildermuth RJ. Influence of neutral salts on the hydrothermal stability of acid-soluble collagen. J Protein Chem 2000;19(2):85-92.

[139] Wong GCL, Lin A, Tang JX, Li YL, Janmey PA, Safinya CR. Regulation of F-actin architecture using simple multivalent ions. Biophys J 2001;80(1):436.

[140] GronbechJensen N, Mashl RJ, Bruinsma RF, Gelbart WM. Counterion-induced attraction between rigid polyelectrolytes. Phys Rev Lett 1997;78(12):2477-2480.

[141] Podgornik R, Rau DC, Parsegian VA. Parametrization Of Direct And Soft Steric-Undulatory Forces Between Dna Double-Helical Polyelectrolytes In Solutions Of Several Different Anions And Cations. Biophys J 1994;66(4):962-971.

[142] Melander W, Horvath C. Salt Effects On Hydrophobic Interactions In Precipitation And Chromatography Of Proteins - Interpretation Of Lyotropic Series. Archives Of Biochemistry And Biophysics 1977;183(1):200-215.

[143] Vonhippe.Ph, Schleich T. Ion Effects On Solution Structure Of Biological Macromolecules. Accounts Of Chemical Research 1969;2(9):257-265.

[144] Robinson DR, Jencks WP. Effect Of Concentrated Salt Solutions On Activity Coefficient Of Acetyltetraglycine Ethyl Ester. J Am Chem Soc 1965;87(11):2470-2479.

[145] Collins KD, Washabaugh MW. The Hofmeister Effect And The Behavior Of Water At Interfaces. Quarterly Reviews Of Biophysics 1985;18(4):323-422.

[146] Nandi PK, Robinson DR. Effects Of Salts On Free-Energy Of Peptide Group. J Am Chem Soc 1972;94(4):1299-1308.

[147] Nandi PK, Robinson DR. Effects Of Salts On Free-Energies Of Nonpolar Groups In Model Peptides. J Am Chem Soc 1972;94(4):1308-1315.

[148] Gjerde DT, Schmuckler G, Fritz JS. Anion Chromatography With Low-Conductivity Eluents.2. Journal Of Chromatography 1980;187(1):35-45.

[149] Rieskautt MM, Ducruix AF. Relative Effectiveness Of Various Ions On The Solubility And Crystal-Growth Of Lysozyme. J Biol Chem 1989;264(2):745-748.

[150] Angelini TE, Liang H, Wriggers W, Wong GCL. Like-charge attraction between polyelectrolytes induced by counterion charge density waves. Proc Natl Acad Sci U S A 2003;100(15):8634-8637.

[151] Agarwal G, Kovac L, Radziejewski C, Samuelsson SJ. Binding of discoidin domain receptor 2 to collagen I: An atomic force microscopy investigation. Biochemistry 2002;41(37):11091-11098.

[152] Paige MF, Rainey JK, Goh MC. Fibrous long spacing collagen ultrastructure elucidated by atomic force microscopy. Biophys J 1998;74(6):3211-3216.

[153] Lin H, Clegg DO, Lal R. Imaging real-time proteolysis of single collagen I molecules with an atomic force microscope. Biochemistry 1999;38(31):9956-9963.

[154] Suzuki Y, Someki I, Adachi E, Irie S, Hattori S. Interaction of collagen molecules from the aspect of fibril formation: Acid-soluble, alkali-treated, and MMP1-digested fragments of type I collagen. J Biochem (Tokyo) 1999;126(1):54-67.

[155] Bella J, Brodsky B, Berman HM. Hydration Structure Of A Collagen Peptide. Structure 1995;3(9):893-906.

[156] Wess TJ, Orgel JP. Changes in collagen structure: drying, dehydrothermal treatment and relation to long term deterioration. Thermochim Acta 2000;365(1-2):119-128.

[157] Habelitz S, Balooch M, Marshall SJ, Balooch G, Marshall GW. In situ atomic force microscopy of partially demineralized human dentin collagen fibrils. J Struct Biol 2002;138(3):227-236.

[158] Stigter D. Evaluation Of The Counterion Condensation Theory Of Polyelectrolytes. Biophys J 1995;69(2):380-388.

[159] Ray J, Manning GS. An Attractive Force Between 2 Rodlike Polyions Mediated By The Sharing Of Condensed Counterions. Langmuir 1994;10(7):2450-2461.

[160] Trus BL, Piez KA. Molecular Packing Of Collagen - 3-Dimensional Analysis Of Electrostatic Interactions. J Mol Biol 1976;108(4):705-732.

[161] Weiss P. Experiments On Cell And Axon Orientation Invitro - The Role Of Colloidal Exudates In Tissue Organization. Journal Of Experimental Zoology 1945;100(3):353-386.

[162] Elliott DH. Structure And Function Of Mammalian Tendon. Biological Reviews Of The Cambridge Philosophical Society 1965;40(3):392-401.

[163] Weiner S, Traub W. Bone-Structure - From Angstroms To Microns. Faseb J 1992;6(3):879-885.

[164] Holmes DF, Gilpin CJ, Baldock C, Ziese U, Koster AJ, Kadler KE. Corneal collagen fibril structure in three dimensions: Structural insights into fibril assembly, mechanical properties, and tissue organization. Proc Natl Acad Sci U S A 2001;98(13):7307-7312.

[165] Torbet J, Malbouyres M, Builles N, Justin V, Roulet M, Damour O, et al. Orthogonal scaffold of magnetically aligned collagen lamellae for corneal stroma reconstruction. Biomaterials 2007;28(29):4268-4276.

[166] Baker BM, Mauck RL. The effect of nanofiber alignment on the maturation of engineered meniscus constructs. Biomaterials 2007;28(11):1967-1977.

[167] Cisneros DA, Friedrichs J, Taubenberger A, Franz CM, Muller DJ. Creating ultrathin nanoscopic collagen matrices for biological and biotechnological applications. Small 2007;3(6):956-963.

BIOGRAPHICAL SKETCH

Yuping Li was born at suburban district of Chengdu, Sichuan province, China in 1978. She had a happy childhood and her parents provided her the nice living environment. She enjoyed playing with friends and the younger brother; learning knowledge. She enjoyed “inventing” new colors with different paints. During her middle school studies, she found she likes analysis and logical thinking. In high school, she chose to study in science and engineering.

In 1997, she enrolled in Zhejiang University to study for a bachelor’s degree in the Department of Polymer Science and Engineering. In August 2001, she entered the graduate school in the same university under the advisors of Liqun Wang and Kehua Tu. During her graduate study, she worked on the synthesis and characterization of temperature responsive graft polymer for target drug delivery. In March 2004, she was awarded the master’s degree from Zhejiang University.

In August 2004, she came to the Department of Materials Science and Engineering at the University of Florida to pursue a Ph. D. degree. She worked under Dr. Elliot P. Douglas to study the mechanism of collagen fibril formation and develop collagen scaffold for bio-mineralization. She received the Doctor of Philosophy in May, 2009.